Natural Product Inhibitors of Hsp90: Potential Leads for Drug Discovery

BY

Michael W. Amolins

B.A., Augustana College, 2007

Submitted to the graduate degree program in Medicinal Chemistry and the Graduate Faculty of The University of Kansas in partial fulfillment of the requirements for the degree of Master's of Science.

Thesis Committee:

_____
Chairperson

_____

_____

Date defended: _____

Page left intentionally blank

The Thesis Committee for Michael W. Amolins certifies
that this is the approved version of the following thesis:

Natural Product Inhibitors of Hsp90: Potential Leads for Drug Discovery

Thesis Committee:

_____
Chairperson

_____

_____

Date approved: _____

Abstract

Molecular chaperones, such as the 90 kDa heat-shock protein (Hsp90), regulate many key cellular processes and as a result have emerged as promising targets for drug discovery. For example, Hsp90 is responsible for folding nascent polypeptides associated with each of the six hallmarks of cancer, a feature that renders inhibition of Hsp90 unique in its ability to simultaneously disrupt multiple signaling cascades and selectively induce apoptosis in malignant cells. Likewise, cells utilize heat-shock proteins (Hsps) for the dissolution of protein aggregates associated with neurodegenerative diseases such as Alzheimer's, Huntington's, and Parkinson's disease, as well as spinal and bulbar muscular atrophy (SBMA).

Studies have shown that Hsp90 inhibitors are not only potent as anti-cancer and neuroprotective agents, but are also well tolerated by patients. It is not surprising, therefore, that medicinal chemists have become interested in discovering new scaffolds that exhibit Hsp90 modulatory activity. Given the inherent diversity and vast array of scaffolds that allow for protein interaction, natural products have become a key component in Hsp90 drug discovery research. This thesis represents a discussion of the advancements made by medicinal and natural product chemists in the area of Hsp90 therapeutics, as well as the development of a novel Hsp90 inhibitory scaffold of natural product origin.

Through utilization of a recently reported firefly luciferase assay, our group was able to conduct a high–throughput screen that resulted in the

identification of several Hsp90 inhibitors that contained a 1,4-naphthoquinone scaffold. From this, a library of naphthoquinones was synthesized, exhibiting anti-proliferative activities from 1.3 μM to >100 μM. To further probe structure–activity relationships, a comparative molecular field analysis was performed, and a second generation of 1,4-naphthoquinones was developed, all of which exhibited anti-proliferative activities between ~1–2 μM.

Although this activity was promising, concerns arose regarding the nature of the scaffold itself. It is well documented that many quinone-based scaffolds exert non-selective cytotoxicity through formation of covalent bonds via Michael reaction chemistry or catalytic reduction of reactive oxygen species as a result of their redox activity. To circumvent this concern, the core scaffold was changed from a 1,4-naphthoquinone core to a structurally similar flavone core. This process was completed through utilization of the molecular modeling program AutoDock to determine the mode of binding, and was confirmed through Western Blot analyses. The resulting compounds exhibited anti-proliferative activities between 9–100 μM, and displayed a unique set of biological properties previously unknown via Hsp90 inhibition, making determination of their mechanism of action difficult.

Acknowledgments

In the Robert Frost poem, “The Road Not Taken,” we learn of two paths diverging into a wood. The first, a simple hiking trail: flat, worn, and free of obstacles – this, of course, is the road taken by almost everyone. The second, although equal in beauty, is grassy and overgrown – we know this to be the demanding path, difficult and overlooked. In the poem, Frost decides to take the road less traveled, and says this made all the difference.

I have referenced this poem, in brief, because I believe that all too often in life, we take the path laid out in front of us simply because it’s there – it’s what we are “supposed to do.” It seems rare that someone has the courage to leave the beaten trail and pursue something that might make them truly happy, for fear of difficulty, change, or ill impression. I’d like to think that this thesis defines one of those moments – my road less traveled. And of course, in bringing this chapter of my life to a close, there are a number of people I would like to thank.

First and foremost, I would like to thank my parents, Doug and Betty, and my brother, Anthony. Their love and support has never faltered, and in that, have taught me the invaluable lesson that life is not about prestige and recognition, but rather about loving the experiences you are privileged to be a part of and loving the people you experience them with. For that, this thesis is dedicated to them.

I would like to thank my advisor, Dr. Brian S. J. Blagg, for giving me the freedom and flexibility to be creative with my work, and at the same time pushing me to expand my productivity and knowledge beyond what I thought possible.

I would also like to thank the Blagg lab members, all of which have played a part in my development as a scientist. In particular, I'd like to thank Dr. Jared R. Mays, Laura Peterson, and Adam Duerfeldt for their contributions to my work and education.

I would like to acknowledge the members of the Medicinal Chemistry and Chemistry Departments for their instruction in and out of the classroom. In particular, I'd like to thank Dr. Thomas E. Prisinzano and Dr. Helena Malinakova for their time in serving on my thesis committee, and Dr. Gerald Lushington for assisting with the molecular modeling experiments described herein.

Finally, I would like to thank the Madison and Lila Self Fellowship for not only funding me throughout my graduate career, but also for offering me an opportunity to advance my education and professional development beyond the field of chemistry.

Table of Contents

List of Figures

List of Schemes

List of Tables

List of Abbreviations

17-AAG	17-Allylamino-17-demethoxygeldanamycin
17-DMAG	17-dimethylaminoethylamino-17-demethoxygeldanamycin
3D-QSAR	Three-dimensional quantitative structure activity relationship
AhR	Aryl hydrocarbon receptor
Ala	Alanine
AR	Androgen receptor
ATP	Adenosine triphosphate
BAG	Bcl2-associated athanogene
***c*-MET**	Hepatocyte growth factor receptor (HGFR)
CoMFA	Comparative molecular field analysis
DMEM	Dulbecco's modified Eagle's medium
DMSO	Dimethylsulfoxide
EGCG	Epigallocatechin-3-gallate
ErbB2	Human epidermal growth factor receptor 2 (Her2/neu)
EtOAc	Ethyl acetate
EtOH	Ethanol
FBS	Fetal bovine serum
GDA	Geldanamycin
GHKL	DNA gyrase, heat shock protein 90, histidine kinase, Mut-L (ATPase/kinase superfamily)
GRP94	Glucose-regulated protein of 94 kDa
HIP	Hsp70 interacting protein
HOP	Hsp70-Hsp90 organizing protein

HPLC	High performance liquid chromatography
HRMS	High resolution mass spectrometry
HSF-1	Heat shock factor 1
Hsp	Heat shock protein
HTS	High–throughput screen
IC_{50}	The concentration of compound necessary to inhibit cellular growth by 50%
IR	Infrared
JNK	*c*-jun *N*-terminal kinase
Leu	Leucine
MCF-7	Human breast adenocarcinoma cell line
MPTP	1-Methyl-4-phenyl-1,2,3,6-tetrahydropyridine
Mut-L	Mismatch repair protein L
NMR	Nuclear magnetic resonance
ONC	Optimum number of coefficients
PLS	Partial least squares
RDC	Radicicol
SAR	Structure–activity relationships
SBMA	Spinal and bulbar muscular atrophy
SkBr3	Human mammory gland adenocarcinoma cell line
THF	Tetrahydrofuran
TLC	Thin layer chromatography
TPR	Tetratricopeptide repeat
TRAP-1	Hsp75/tumor necrosis factor receptor associated protein

Chapter I: Introduction and Background

I. An Introduction to Heat Shock Protein 90

In recent years, molecular chaperones such as the 90 kDa heat-shock protein (Hsp90) have surfaced as promising targets for drug discovery.[1-7] Their role in the folding and maturation of various client proteins, as well as the renaturation of misfolded proteins,[8-11] makes them potential targets for many diseases ranging from the disruption of multiple signaling pathways associated with cancer[1,2,4,6,12-17] to the clearance of protein aggregates in neurodegenerative diseases.[4,5,18-23] In fact, cytotoxic inhibitors of Hsp90 are the only cancer chemotherapeutic agents known to impact all six hallmarks of cancer simultaneously.[6] As defined by Hanahan and Weinberg, this includes 1) self-sufficiency in growth signals, 2) insensitivity to antigrowth signals, 3) evasion of apoptosis, 4) limitless replicative potential, 5) sustained angiogenesis, and 6) tissue invasion/metastasis.[24] Disruption of the Hsp90 protein folding machinery by non-cytotoxic agents promotes dissociation of heat shock factor 1 (HSF-1), which induces the expression of Hsp90 and facilitates the disaggregation of proteins associated with several neurodegenerative diseases.[21,25]

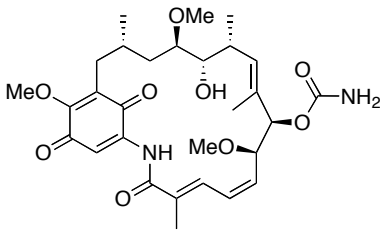

Figure 1. Structure of geldanamycin (GDA).

Geldanamycin (GDA), a natural product isolated from the bacteria *Streptomyces hygroscopicus* (Figure 1), was the first identified Hsp90 inhibitor. Although it showed significant anti-proliferative activity against many cancer cell lines, its dose-limiting toxicity prevented successful completion of clinical trials. Since that time, a variety of natural product inhibitors of Hsp90 have emerged. Among these are herbimycin, radicicol, novobiocin, coumermycin A1, clorobiocin, epigallocatechin-3-gallate (EGCG), taxol, pochonin, derrubone, curcumin, gedunin, and celastrol.

Properties of Hsp90

Heat-shock proteins (HSPs) act as molecular chaperones, guiding nascent polypeptides through the process of folding and maturation into three-dimensional structures.[26,27] Chaperones are also responsible for refolding denatured proteins that result from cellular stresses such as nutrient deprivation, abnormal temperature or pH, malignancy, and exposure to various toxins and drugs.[4,28] Heat-shock response is conserved across all species, from prokaryotes to

eukaryotes, and provides a mechanism for the maintenance of intercellular processes, including protection against protein aggregation in the cytosol.[29,30]

Hsp90, the most prominent of the heat-shock proteins, makes up 1–2% of all cellular protein[8] and exists in four isoforms: Hsp90α, Hsp90β, glucose-regulated protein (GRP94), and Hsp75/tumor necrosis factor receptor associated protein 1 (TRAP-1). Hsp90α and Hsp90β can be found in the cytosol, and are the inducible and constitutive forms, respectively. GRP94 resides in the endoplasmic reticulum, while TRAP-1 is located in the mitochondrial matrix.[31,32] To date, Hsp90 has been found to interact with over 200 client proteins, as well as ~50 co-chaperones, making it a cornerstone in the cellular protein-folding machinery and an emerging target for the treatment of various disease states.[33,34]

Structure

Since the first reported crystal structure by Prodromou and co-workers in 1996,[35] it has been determined that Hsp90 is comprised of three distinct structural domains: a 10 kDa *C*-terminus, 55 kDa middle domain, and a 25 kDa *N*-terminus.[36,37] In its biologically active form, Hsp90 exists as a homodimer bound in a quaternary helix bundle formed by overlapping and antiparallel pairs of helices from each of the *C*-terminal domains.[38-41] *C*-Terminus crystal structures of bacterial HtpG[42] and eukaryotic Hsp90[43] were solved in 2004 and 2006, respectively. Although rumors of its existence have surfaced from industry, a co-crystal structure of the *C*-terminus bound to an inhibitor has not been published.

Csermely and co-workers first reported this binding site in 1998,[44] and in 2000 Neckers and co-workers were able to show that inhibition of Hsp90 at the *C*-terminus interrupts activity in a non-ATP competitive fashion.[45,46] This discovery has been highly influential in the development of *C*-terminal Hsp90 inhibitors, and further highlights the necessity of attaining a co-crystal structure to further understand this process.

The 55 kDa middle domain of Hsp90 is the most variable region across species, but nonetheless is intimately involved in the binding and maturation of client proteins.[9,38] The 25 kDa *N*-terminal domain is similar in structure to DNA gyrase B, histidine kinase, and MutL – together forming the GHKL (ATPase/kinase) superfamily.[47] This structural homology was determined through domain-specific human[48] and yeast[49] crystal structures and eventually led to elucidation of the ATP-binding site at the *N*-terminus. A co-crystal structure with ADP bound in a bent conformation, characteristic of the GHKL superfamily, was reported soon after.[50] These structures have played a critical role in the design of new and more efficacious Hsp90 inhibitors.[51]

The Hsp90 Protein Folding Mechanism

Under normal physiological conditions, HSF-1 is tightly bound to and regulated by Hsp90 in its inactive state (**2a**, Figure 2). Upon activation, Hsp90 releases HSF-1, allowing translocation to the nucleus and induction of HSPs by binding to the heat shock response element.[52] These newly formed molecular

chaperones are then responsible for governing the folding and maturation of nascent and denatured polypeptides into biologically active structures. It should be noted that the following description of this process has been simplified for the purposes of this thesis. A gamut of proteins have been linked to this folding mechanism, but only key interactions are highlighted herein.

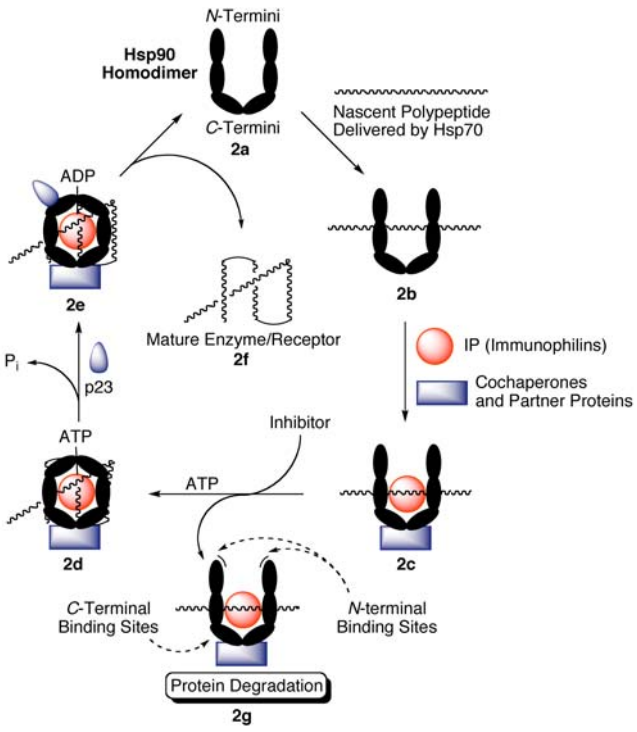

Figure 2. The Hsp90 protein folding mechanism.

Hsp70 binds nascent polypeptides emerging from the ribosome in an ATP and Hsp40-dependent fashion. This complex is stabilized by Hsp70 interacting protein (HIP), and can be dissociated by Bcl2-associated athanogene (BAG).

Hsp70-Hsp90 organizing protein (HOP) contains tetratricopeptide repeats (TPRs) recognized by both molecular chaperones, and recruitment by the Hsp70 complex facilitates transfer of the client protein to the Hsp90 homodimer (**2b**, Figure 2).[53-55] Next, several co-chaperones, partner porteins, and immunophilins, shown in Table 1, can bind Hsp90 (**2c**, Figure 2), forming a stabilized heteroprotein complex capable of binding ATP at the *N*-terminus.[56-58] Upon ATP-mediated dimerization of the *N*-terminii, the activated Hsp90 multiprotein complex takes on a closed "clamped" conformation, engulfing the bound client protein (**2d**, Figure 2).[59,60] Recruitment of p23 facilitates ATP hydrolysis (**2e**, Figure 2) and further stabilizes Hsp90,[61,62] allowing for maturation and subsequent release of the client protein (**2f**, Figure 2).[63]

Table 1. Co-chaperones, partner proteins, and immunophilins involved in the Hsp90 folding mechanism.

Co-chaperones	Partner Proteins	Immunophilins
Hsp40	HOP	FKBP51
Hsp70	Tom70	FKBP52
Cdc37	PP5	Cyclophilin-40
Aha	ARA9	UNC-45
p23	CNS1	
CHIP	Dpit47	
	Tpr2	
	SGT1	
	CRN	
	WISp39	
	NASP	
	TAH1	
	Rar1	

Inhibition of Hsp90 prior to ATP-mediated dimerization (**2g**, Figure 2) can effectively destabilize the heteroprotein complex. ATP hydrolysis provides the energy necessary for the conformational changes that facilitate folding, maturation, and release of the client protein. By preventing the dimerization process, the Hsp90 complex is disabled, and the client becomes a substrate for ubiquinylation and subsequent proteasomal degradation.[64,65] In a similar fashion, inhibition of Hsp90 can also prevent the renaturation of misfolded client proteins. Application of this concept has proven very useful in the renaturation of heat denatured firefly luciferase. A representative example by Yonehara[66] has demonstrated that inhibition of Hsp90 reduces luciferase activity, and a 2007 publication by Galam and co-workers used this information to establish a high-throughput screening assay to identify both *N*- and *C*-terminal inhibitors of Hsp90 based on the renaturation of heat denatured firefly luciferase.[67]

A Selective Target for Cancer Treatment

Cancer is often referred to as a multifaceted class of diseases,[68] dependent upon satisfaction of each of the six hallmarks as defined by Hanahan and Weinberg.[24] Although many cancer chemotherapeutics have successfully targeted proteins associated with multiple hallmarks, none have been able to simultaneously affect all six. Of the numerous client proteins dependent upon Hsp90 for folding and maturation, many are deemed essential for malignant progression. Over the last ten years, Hsp90 client proteins have been linked to all

six hallmarks of cancer (Table 2),[6,14] making Hsp90 inhibition an exciting new chemotherapeutic target. Whitesell and Lindquist reviewed this concept in 2005,[13] and several studies and clinical trials have verified Hsp90 as a viable cancer target.[69-71]

Table 2. The six hallmarks of cancer.

Hallmark	Hsp90 Client Proteins
Self-sufficiency in growth signals	Raf-1, AKT, Her-2, MEK, Bcr-Abl, FLT-3, EGFR, IGF-1R, FGFR, KDR
Insensitivity to antigrowth signals	Wee 1, Myt 1, CDK4, CDK6, Plk
Evasion of apoptosis	RIP, AKT, mutant p53, c-MET, Apaf-1, Survivin
Limitless replicative potential	Telomerase (h-TERT)
Sustained angiogenesis	FAK, AKT, HIF-1α, VEGFR, FLT-3
Tissue invasion/metastasis	c-MET, MMP

Inhibitors of Hsp90 have shown as high as a 200-fold differential selectivity toward malignant versus normal cells. Several mechanisms have been suggested to explain this high selectivity. First, Hsp90 is significantly overexpressed in malignant cells to compensate for their dependency on Hsp90 client proteins, including Her2 (ErbB2), c-Met (HGFR), Raf-1, and Akt.[72-77] The increased concentration of Hsp90 in tumor cells inherently results in greater drug accumulation. A second mechanism, introduced by Conforma Therapeutics in 2003, proposes that the Hsp90 heteroprotein complex (**2c**, Figure 2) exhibits a higher affinity for *N*-terminal inhibitors than the inactive homodimer (**2a**, Figure 2). In cancer cells, Hsp90 exists predominantly in a heteroprotein complex due to

the abundance of mutated, denatured, and naturally expressed proteins. In contrast, the primary form of Hsp90 in normal cells is the inactive homodimer, which explains why *N*-terminal inhibitors accumulate with the high-affinity Hsp90 complex found in tumor cells.[2,78,79] Finally, a 2006 report by Duvvuri and co-workers[80] suggests a physiochemical explanation for selectivity. Under normal physiological conditions, lysosomal pH is around 4–5. Hsp90 inhibitors, like many chemotherapeutic agents, often contain basic nitrogens, and in a process known as pH partitioning[81] become protonated as the ammonium salt within the lysosome, trapping them in the organelle and preventing interaction with Hsp90, which resides in the cytosol. Conversely, the lysosomal pH in cancerous cells is essentially neutral, favoring an unprotonated amine[82,83] and suggesting that the equilibrium drug concentration between lysosome and cytosol favors cytosolic interaction with tumor-derived Hsp90 (Figure 3).

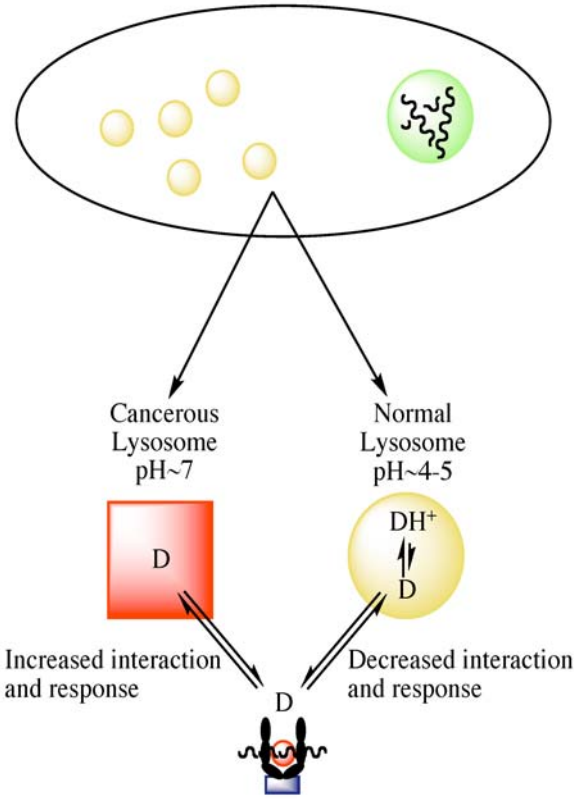

Figure 3. The effects of lysosomal pH on cellular drug distribution.

Neurodegenerative Applications

Neurodegeneratvie disorders such as Alzheimer's, Parkinson's, Huntington's, and spinal and bulbar muscular atrophy (SBMA), are in part characterized by the accumulation of misfolded protein aggregates. Under normal circumstances, this buildup can be prevented through resolubilization and rematuration of proteins by molecular chaperones. However, when suffering from

these pathological conditions, aggregation exceeds the capacity of normal chaperone function, and can result in neuronal death.[84]

Inhibition of Hsp90 stimulates the release of HSF-1, which in turn translocates to the nucleus, and promotes transcription of HSP mRNA, leading to increased synthesis of HSPs.[21,25] Increased levels of Hsp70 and Hsp90 have shown to be inversely proportional to β-amyloid and tau aggregation, and directly proportional to the binding of tau to microtubules, suggesting that non-cytotoxic inhibition of Hsp90 could serve as a neuroprotective approach for the treatment of Alzheimer's disease through dissolution of protein aggregates.[22] Recent studies by Shen and co-workers have affirmed this hypothesis by demonstrating the protective effects of GDA *in vivo* against 1-methyl-4-phenyl-1,2,3,6-tetrahydropyridine (MPTP)-induced dopaminergic toxicity associated with the formation of Lewy bodies (α-synuclein aggregation) in a Parkinson's disease model through inhibition of Hsp90.[19] A similar study by Waza showed that 17-allylamino-17-demethoxygeldanamycin (17-AAG, Figure 4), a more efficacious analogue of GDA, can diminish the effects of SBMA by inhibiting Hsp90, thus promoting degradation of mutant androgen receptor (AR) resulting from expansion of trinucleotide CAG repeats in the AR gene.[20] Ansar and co-workers have produced a select number of non-toxic Hsp90 inhibitors that further highlight this concept through neuronal protection against Aβ-induced toxicity.[85]

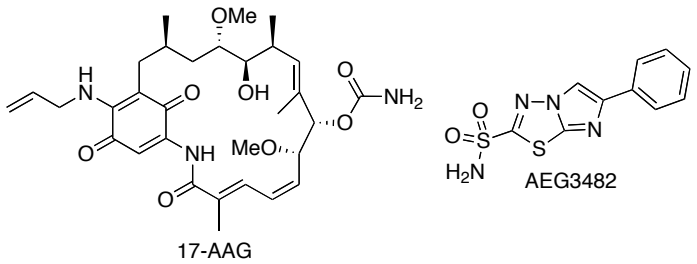

Figure 4. Structures of 17-AAG and AEG3482.

Finally, Huntington's, Parkinson's, and Alzheimer's disease attribute neuronal apoptosis to activation of the c-*jun N*-terminal kinase (JNK) signaling pathway. Hsp70 can attenuate this cascade by binding JNK, disrupting substrate interactions necessary for the initiation of apoptosis. In 2006, Gallo and co-workers demonstrated that the imidazothiadiazole sulfonamide AEG3482 (Figure 4) inhibits Hsp90, causing the release of HSF-1 and inducing HSP transcription. This in turn provides neuroprotection through Hsp70 inhibition of the JNK signal transduction pathway.[5] Studies are underway to further refine the potential significance of modulating the Hsp90 protein folding machinery in a manner that can alleviate the accumulation of protein aggregates while providing a large therapeutic window that exhibits low cytotoxicity.[85]

II. Natural Product Inhibitors of Hsp90

Clinical trials have shown that Hsp90 inhibitors are not only potent as anti-cancer agents, but are also well tolerated by patients. In fact, the toxicities

and side effects discovered thus far have not resulted from Hsp90 inhibition, but rather from hepatotoxicity, gastrointestinal irritation, and constitutional symptoms.[86,87] It is not surprising, therefore, that medicinal chemists have become interested in discovering new scaffolds that exhibit Hsp90 modulatory activity for the treatment of cancer and neurodegenerative diseases. Given the inherent diversity and vast array of scaffolds that allow for protein interaction, natural products have become a key component in Hsp90 discovery research.[88]

Geldanamycin and Herbimycin

Geldanamycin and herbimycin (Figure 5) are naturally occurring benzoquinone ansamycin antibiotics that can be isolated through fermentation of *Streptomyces hygroscopicus*.[89,90] The first total synthesis of herbimycin was reported by Nakata and co-workers in 1991.[91] However, the total synthesis of GDA was not available until 2002, when Andrus and co-workers reported a procedure that afforded the product as a 1:10 mixture with (–)-*o*-quinogeldanamycin in low yield.[92] This result was due primarily to problematic oxidation of the trimethoxy precursor to the paraquinone. Andrus improved upon this methodology,[93] and a subsequent 20 step total synthesis (2% overall yield) was achieved by Panek and Qin in 2008.[94]

The antitumor properties of GDA were first reported in 1986, and were initially attributed to its ability to inhibit v-Src phosphorylation in whole cells via Src tyrosine kinase.[95,96] However a direct link between v-Src and GDA was never

identified, as they were unable to directly inhibit the purified recombinant protein.[97] This suggested there might be a non-explicit interaction between the kinase and GDA. In 1994, Whitesell and Neckers proved this relationship as a downstream effect of GDA's ability to specifically bind and antagonize Hsp90, a chaperone for v-Src.[98,99] Using affinity purification, immobilized GDA affixed to agarose beads was incubated with reticulocyte lysate, resulting in the identification of Hsp90. Further investigation proved that GDA specifically inhibited the Src/Hsp90 heteroprotein complex, facilitating degradation of the client protein. This observation was consistent with all prior work linking GDA to Src tyrosine kinase modulation.

Initial reports by Roe and co-workers reported that GDA acted as a polypeptide mimic, interacting with Hsp90 at a highly conserved, 15 Å polypeptide substrate binding pocket involved in protein folding and maturation.[48,50] However, Roe's co-crystallization of Hsp90 with GDA later revealed that it was actually binding to a previously unidentified ATP-binding pocket.[100] This seminal work opened the door for structure–activity relationship (SAR) studies that have since led to the development of several analogues.

Although respectable IC_{50} values have been reported for GDA and herbimycin against various cancer cell lines, their poor solubility and hepatotoxicity in animals has prevented them from successfully completing clinical trials as anti-cancer agents.[101] SAR studies have shown that modifications

to the carbamate group of GDA can substantially decrease the potency of derivatives, as it serves to mimic the exocylic amino and imino nitrogens of adenine. A similar loss in activity can be observed upon reduction of the 2–3 double bond, as the target–specific conformation of the macrocycle is compromised.[88,100] Modification of the 17-methoxy substituent appears to be the most effective option, as it projects away from the ATP binding pocket and exhibits a minimal affect on Hsp90 affinity.[50,102] Substituting an electron donating group for the 17-methoxy group decreases toxicity by stabilizing the quinone moiety and retarding formation of the semiquinone, which is capable of reacting with molecular oxygen and producing superoxide radicals.[103,104]

The synthetic analogue, 17-AAG (Figure 5), produced by Schulte and Neckers, displayed a 100-fold increase in differential selectivity at doses similar to GDA, as well as decreased hepatotoxicity.[105] Although 17-AAG proved to be more potent than GDA, solubility issues and its moderately persistent toxicity proved to be a factor in clinical development.[106] Additional work has produced 17-(dimethylaminoethylamino)-17-demethoxygeldanamycin (17-DMAG, Figure 5), which displays lower toxicity, higher potency, and improved bioavailability with respect to 17-AAG.[106,107] 17-DMAG has entered phase I clinical trials and has demonstrated sensitization of therapeutically-resistant cancer stem cells to chemotherapy.[108]

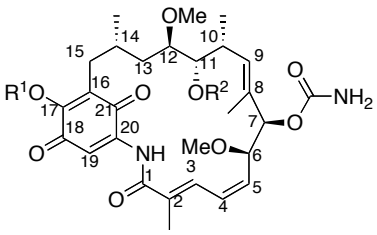

Geldanamycin $R^1 = OCH_3$, $R^2 = H$
17-AAG $R^1 = NHCHCH_2$, $R^2 = H$
17-DMAG $R^1 = NH(CH_2)_2N(CH_3)_2$, $R^2 = H$
Herbimycin $R^1 = H$, $R^2 = CH_3$

Figure 5. Structures of geldanamycin, herbimycin, and structural analogues 17-AAG and 17-DMAG.

Since the development of 17-AAG, several analogues of GDA have exhibited improved antitumor properties, as well as demonstrated neuroprotective activity. These include bioengineered compounds developed through site-directed mutagenesis of the polyketide synthase gene cluster,[109] semi-synthesized analogues resulting from biosynthetically generated metabolites,[110] as well as several compounds arising from traditional synthetic techniques.[111,112] The biologically modified synthetic approaches have offered alternative pathways to GDA analogues that were previously hindered by the lack of an efficient total synthesis. Traditional synthetic work, while effective, has been limited to alteration at the 17-position and the quinone moiety itself.

Radicicol and Pochonin

To date, radicicol (RDC, Figure 6) is the most potent natural product inhibitor of Hsp90, manifesting an IC_{50} value of 23 nM.[100] Its mechanism of action is similar to that of GDA, in that it binds to the *N*-terminal ATP binding

pocket of Hsp90. However, it does not manifest selectivity for the activated heteroprotein complex versus the homodimeric form, as is the case for GDA. This can be attributed to the more rigid structure of RDC.[100,113] RDC, isolated from *Diheterospora chlamydosporia*, has proven to have many downstream oncogenic effects through Hsp90 inhibition, including activity against 17-AAG resistant retinoblastoma cells.[114] However, no activity has been demonstrated *in vivo*, as RDC is rapidly metabolized to inactive structures due to the electrophilicity of the epoxide ring and α,β,γ,δ-unsaturated ketone.[115]

Several analogues of RDC have been synthesized that minimize *in vivo* metabolism by decreasing its electrophilic nature.[116-121] These compounds display nanomolar activity *in vivo*. For example, synthesis of radicicol 6-oxime derivatives, such as KF25706 (Figure 6), has produced several compounds that demonstrate potent antiproliferative activity. Furthermore, the oxime stereochemistry has shown to be critical, as higher potency is observed with the *E*-isomer.[116,117,122] Other studies have determined that Hsp90 inhibitory activity is dependent on the RDC scaffold being restrained to a bent conformation. This can be assisted by an sp^2-hybridized C6 or a β-oriented oxygen close in proximity to C10 and C12.[123] However, the best resource for synthetic SAR studies has been the total synthesis of RDC and analogues by Danishefsky and co-workers.[124] This route offers a notably straightforward synthesis, providing several opportunities for diversification. By replacing the electrophilic allylic epoxide with a

cyclopropyl group (c-RDC, Figure 6), these researchers were able to reintroduce activity comparable to GDA *in vivo*.

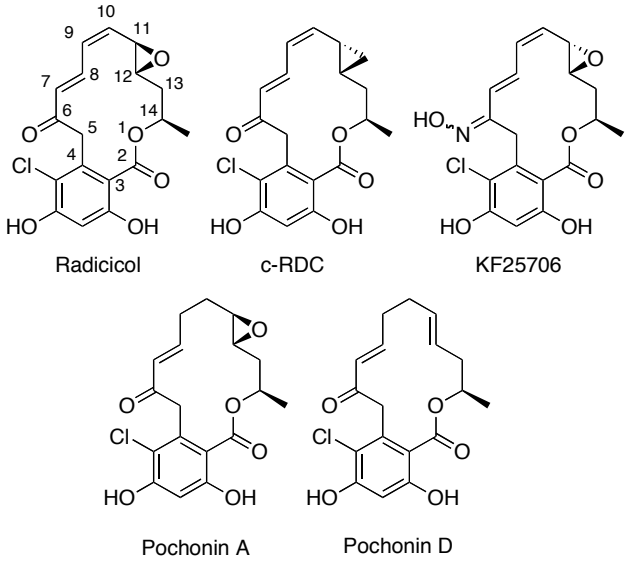

Figure 6. Structures of radicicol, c-RDC, KF25706 and pochonin A & D.

Isolation of the structurally similar pochonin family of natural products from *Pochonia chlamydosporia* has also shown promise in Hsp90 inhibition, particularly with pochonin A and pochonin D.[125,126] Pochonin A and D have been shown to directly inhibit Hsp90.[126] Pochonins A–F, while themselves displaying cytotoxicity in the micromolar range,[125] provide an opportunity for conformational diversity that is not as easily achieved with radicicol.[127] As a result, several syntheses have now been reported.[127,128]

Chimeric Analogues of Geldanamycin and Radicicol

SAR studies have shown that GDA activity is dependent upon the structural integrity of the quinone ring as well as the stereochemistry of the carbamate. Similarly, RDC activity is dependent on the resorcinol ring, and to a lesser extent, the epoxide.[129] In addition, the amide functionality in GDA appears to impart high differential selectively towards the Hsp90 heteroprotein complex.[130]

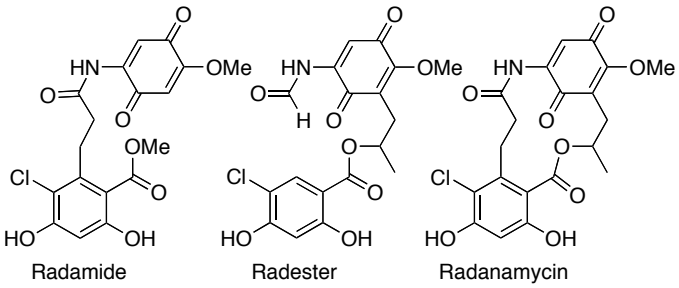

Figure 7. Structure of the chimeric analogues of geldanamycin and radicicol.

Seminal work by Shen and co-workers utilized this knowledge to compose a new class of chimeric analogues, combining the pro-inhibitory properties of GDA and RDC to form radamide, radester, and radanamycin.[131-134] Each chimera improved upon Hsp90 inhibitory activity with respect to the parent compounds (IC_{50} = 42 μM, 7.1μM, and 1.2 μM against MCF-7 breast cancer cells, respectively), and was synthesized in a minimal number of steps that would allow for diversification of this potential drug class. Early studies by this group identified the

hydroquinone species to be more active than the corresponding quinone, which was later confirmed with GDA by several other research laboratories.[134]

Novobiocin, Coumermycin A1, and Clorobiocin

The coumermycin family of antibiotics (Figure 8), isolated from *Streptomyces spheroids*, have long been used clinically for antimicrobial purposes.[135,136] Mechanistically, they bind to the ATP binding pocket of DNA gyrase, another member of the GHKL superfamily,[47] thus preventing ATP hydrolysis.[137,138] Novobiocin in particular has been shown to display anti-cancer properties, and has been used in the clinic for many years.[139] Ground breaking work by Neckers and co-workers demonstrated that this activity could be ascribed to novobiocin's Hsp90 inhibitory activity. Using affinity chromatography, Neckers determined that novobiocin could competitively displace immobilized GDA bound to Hsp90, however GDA could not displace immobilized novobiocin when the reciprical experiment was performed. Further studies revealed that novobiocin bound to a previously unrecognized *C*-terminal binding pocket, and induced degradation of Hsp90-dependent client proteins.[45,46] These studies laid the groundwork for a vast library of novobiocin and coumermycin analogues that have since been prepared.[85,140-143]

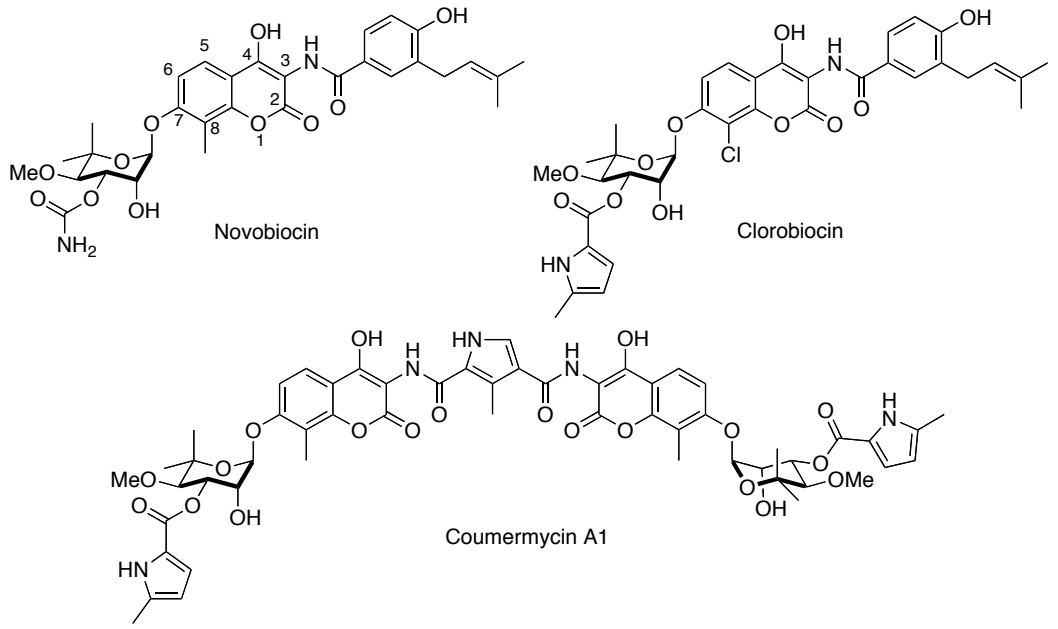

Figure 8. The coumermycin family of antibiotics.

SAR studies in our lab have revealed many significant features that can control the activity manifested by these novobiocin analogues. Synthesis of A4 in 2005, along with DHN1 and DHN2 in 2006 (Figure 9), highlighted key structural differences necessary for distinguishing between inhibition of DNA gyrase and Hsp90.[139,140] The 4-hydroxyl and 3'-carbamate of novobiocin are critical for DNA gyrase activity. Removing the 4-hydroxyl moiety and hydrolysis the carbamate provided a 500-fold increase in selectivity for Hsp90. A methyl group at the C8 position also moderately increased activity. As of 2006, A4 was not only the most potent novobiocin analogue to date, but interestingly displayed no growth inhibitory activity. This feature was exploited in its development as a

neuroprotective agent in 2007 when Ansar and co-workers demonstrated that A4 could provide

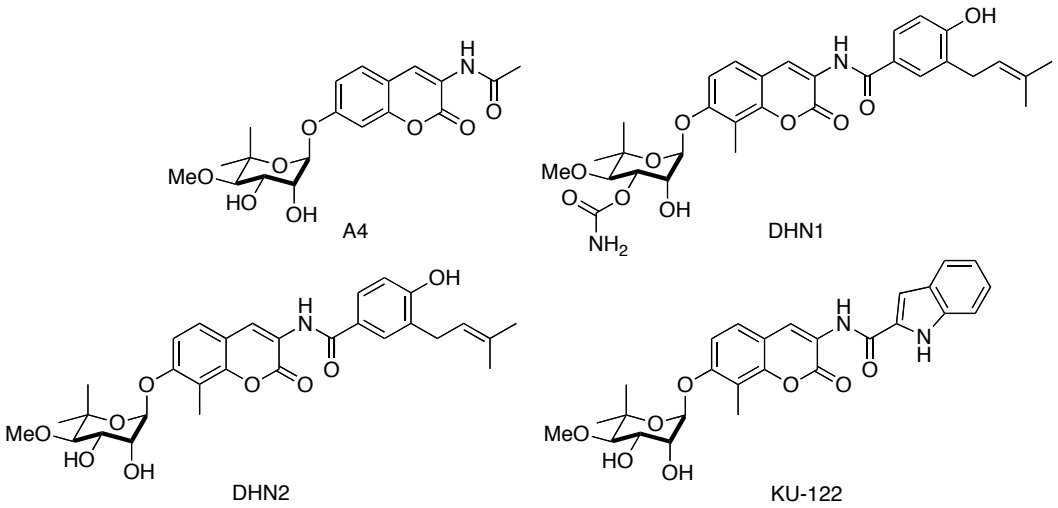

Figure 9. Structures of novobiocin analogues.

significant protection against Aβ-induced toxicity of neurons at non-cytotoxic concentrations.[85] Subsequent SAR studies concluded that the benzamide functionality of novobiocin was necessary for cytotoxicity.[143,144] It was also found that the addition of a *p*-hydrogen bond acceptor and an *m*-aryl side chain were most effective in increasing anti-proliferative activity. Further derivitization resulting in heterocyclic analogues of the benzamide side chain revealed the most potent novobiocin analogue to date, KU-122. Installation of a 2-indole moiety in lieu of the native benzene ring resulted in a significant increase in anti-proliferative properties (IC_{50} = 0.37 μM in SKBr3 breast cancer cells, 0.17 μM in

HCT-116 colon cancer cells). This variation in activity can be credited to the hydrogen bond donating capability and the rigid 2,3-olefin on the indole ring. These novobiocin analogues are unique in that rational modification of these compounds can provide molecules that selectively treat bacterial infections, cancer, or neurodegenerative diseases. Multiple projects are currently underway to further elucidate these properties and to create more potent inhibitors of Hsp90.[145]

EGCG

Epigallocatechin-3-gallate (EGCG, Figure 10) is a naturally occuring polyphenol extract from *Camellia sinensis*, found in green tea. Although green tea has been marketed in Eastern medicine for years as an anticancer agent, it wasn't until 2003 that Palermo and co-workers ascribed this feature to inhibition of Aryl Hydrocarbon Receptor (AhR) activity.[146] Shortly thereafter, affinity studies concluded that EGCG did not bind directly to AhR, but instead antagonized Hsp90. Affinity purification studies concluded that EGCG, like novobiocin, binds to the *C*-terminus of Hsp90.[147,148]

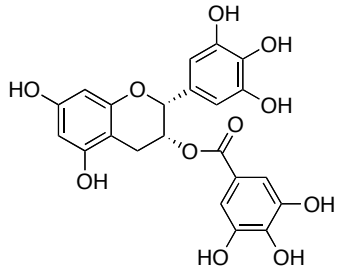

Figure 10. Structure of EGCG.

More recent studies have discussed EGCG's potential as a neuroprotective agent.[149] Although Weinreb and co-workers attribute this property to EGCG's ability to chelate iron in areas of the brain associated with Parkinson's and Alzheimer's disease, one cannot overlook the vastly growing array of Hsp90 inhibitors known to display neuroprotective qualities.

Taxol

Taxol's (Figure 11) biological activity as an anticancer agent has been attributed to its stabilization of microtubles and prevention of mitosis, and has been used clinically for over twenty years.[150] Through the activation of kinases and transcription factors, it has also been shown to elicit cell signaling in a manner indistinguishable from bacterial lipopolysaccharide (LPS).[151,152]

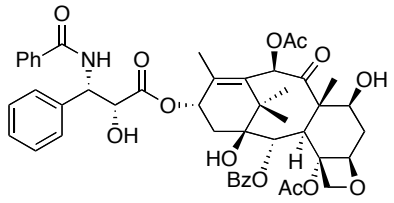

Figure 11. Structure of taxol.

Its isolation from the Pacific yew tree, *Taxus brevifolia L.*, by Monroe Wall, and his subsequent discovery of its anticancer properties, stands as one of the most significant findings in the history of natural product research.[153,154] What is interesting, however, is that in recent years Rosen and co-workers have been able

to show through affinity purification studies that taxol binds Hsp90, resulting in a stimulatory response.[155-157] This response not only sensitizes malignant tumors to taxol, but could even prove useful in the future development of neuroprotective agents. The site to which taxol binds Hsp90 has not yet been elucidated.

Derrubone

Derrubone (Figure 12) is a prenylated isoflavone that was isolated from the Indian tree, *Derris robusta*, in 1969.[158] A total synthesis was reported three years later by Jain and Jain that consisted of 14 steps.[159] This feat was matched by Hossain and co-workers in 2006, and then improved upon by Hastings in 2007, reducing its preparation to 8 linear steps.[160,161] Through utilization of the HTS luciferase assay discussed earlier,[67] Hadden and co-workers identified derrubone as a *C*-terminal inhibitor of Hsp90, yielding an IC_{50} value of 11.9 μM against human MCF-7 breast cancer cells.[162]

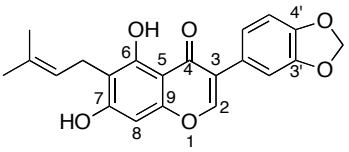

Figure 12. Structure of derrubone.

SAR studies by Hastings and Hadden have identified key features of derrubone that allow for optimal interaction with Hsp90, and several potent analogues have been synthesized.[160] First, the C3 aromatic ring substituent is

essential for activity. Addition of an electron-withdrawing group at the C4′ position can further increase anti-proliferative activity, whereas substitution at C3′ results in complete loss of activity. Second, replacing the prenyl substituent with a more polar functionality results in decreased activity, whereas replacing it with a non-polar functionality gives comparable activity to the prenyl group. A slight increase in activity was observed when the C6 substituent was translocated to the C8 position. Overall, this study produced analogues with IC_{50} values in the low micromolar range, and further development of the derrubone library is currently underway.

Curcumin

Turmeric has been utilized for centuries in Ayurvedic medicine as a topical treatment for wounds, inflammation, and tumors.[163] The active component was identified as curcumin (Figure 13), and its isolation from the rhizome of *Curcuma longa L. (Zingiberaceae)* over two centuries ago eventually allowed for structural identification and testing against various diseases.[164]

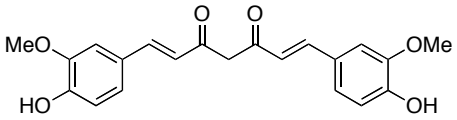

Figure 13. Structure of curcumin.

Properties exhibited by curcumin include anti-inflammatory, anti-oxidant, anti-viral, cutaneous wound healing, hypocholesterolemic effects in diabetic patients,

anti-angiogenic, and stimulatory response to stress-induced biological activity.[165,166] Curcumin has demonstrated neuroprotective activity against Aβ aggregation in Alzheimer's models,[167] and several studies have shown that curcumin manifests anti-proliferative activity against various cancers, including leukemia, colon, liver, breast, and prostate cancers.[165,168-170] However, the truly unique feature of this molecule is its lack of toxicity. Large quantities of curcumin can be consumed without toxicity, suggesting this molecule may serve as a valuable scaffold for therapeutic development. Three phase I clinical trials have demonstrated tolerances as high as 12 g per day, although this is in part due to its poor bioavailability.[171,172] These distinctive properties make curcumin a valuable lead compound for drug development, and it remains the focus of several clinical trials.[173]

Recent studies in the Blagg laboratory have shown that curcumin exhibits its diverse range of activities through modulation of Hsp90. It was determined that a number of previously identified protein targets of curcumin were client proteins of Hsp90, and a subsequent binding study and Western Blot analysis confirmed that this correlation in activity was likely a result of Hsp90 inhibition. A major concern, however, was the potential that this activity was due to covalent modification of the molecular chaperone through its Michael acceptor properties, and not reversible binding to one of its terminii. To test this hypothesis, a number of analogues were synthesized that converted the electron-deficient α,β-

unsaturated 1,3-diketone moiety into one of two electron rich heterocycles: an isoxazole, which directly mimicked the 1,3-diketone central to curcumin's core, or a pyrazole, which mimicked the hydrogen-bonding network of the corresponding enol.[174] A number of analogues were synthesized, and it was determined that Michael acceptor properties were not critical to the retention of curcumin's inhibitory activity. Furthermore, it was determined that the pyrazole analogues were slightly more potent than the corresponding isoxazole analogues, emphasizing the importance of the hydrogen-bonding network curcumin exhibits in its enol form. Studies are currently underway to further elucidate the interaction between this natural product and Hsp90.

Gedunin and Celastrol

In recent years, gedunin (Figure 14), a tetranotriterpenoid isolated from the Indian neem tree *Azadirachta Indica*,[175] and structurally related celastrol (Figure 15), a quinone methide triterpene from *Celastraceae* family of plants, have become compounds of interest due to their anti-proliferative and neuroprotective properties.[176-178] More recent studies identified these natural products as Hsp90 inhibitors.[3,179,180] Using a connectivity map, Lamb and co-workers were able to find high correlation scores between gedunin, celastrol, GDA, 17-AAG, and 17-DMAG, suggesting these natural products exhibited their activity through Hsp90 modulation. A subsequent paper confirmed this hypothesis, however a mechanism of action was not fully revealed. In a

fluorescence polarization assay, gedunin and celastrol failed to displace GDA, indicating that the natural products were not binding competitively to the *N*-terminal ATP-binding site. Zhang and co-workers have reported that celastrol may disrupt Hsp90 function by blocking interactions between the molecular chaperone and the co-chaperone, Cdc37, preventing formation of the Hsp90 heteroprotein complex responsible for the maturation of Hsp90-dependent kinases[176]. Based on structural similarities between gedunin and celastrol, it is likely that gedunin utilizes a similar mechanism of action for Hsp90 inhibition.

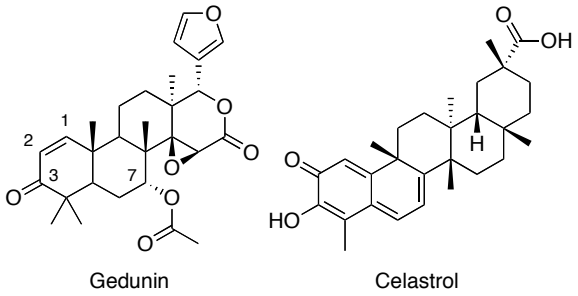

Figure 14. Structures of gedunin and celastrol.

In an attempt to elucidate structure–activity relationships between the molecular chaperone and natural products, a semi-synthetic library has been synthesized.[181] Although the analogues made thus far have not proven to be more effective than gedunin in anti-proliferation assays, Brandt and co-workers have identified key structural features necessary for activity.[182] Steric bulk applied at the C7 position has a pronounced effect on anti-proliferative activity, as inhibitory

activity is diminished in response to an increase in size. Although it appears as though the electronic nature of the substituent is not imperative, the presence of a hydrogen bond acceptor can slightly improve upon anti-proliferative properties. C7 substituents also exhibit an influence on the overall conformation of the molecule, and mediate the binding of other substituents. The olefin of the α,β-unsaturated ketone is also essential for activity. One can assume this is due to the electrophilic nature of this moiety, however modifications to and reduction of the ketone itself have proven otherwise. Hydrogen bond accepting properties at the C3 substituent, as well as the rigidity of the 1,2-olefin are responsible for retention of activity. Studies are currently underway to further clarify gedunin's structure–activity relationship with Hsp90.

III. Summary

Natural products have long withstood the test of time for their contributions to medicinal chemistry. The development of new and interesting scaffolds, as well as small molecules that exhibit targeted selectivity, have been dependent on the isolation and modification of complex structures from Mother Nature. As Hsp90 continues to emerge as a promising target for the treatment of cancer, neurodegenerative diseases, and other disease states, the construction of viable inhibitors with drug-like properties becomes increasingly more important. The structures presented in this introduction have provided a summary of past

achievements by natural product chemists and their recent impact on future applications. The remainder of this thesis will focus on a specific project involving the development of Hsp90 inhibitors based on the 1,4-naphthoquinone and flavone scaffolds, both of which are prevalent in natural products.

IV. References

(1) Shimamura, T.; Shapiro, G. I. *J. Thor. Oncol.* **2008**, *3*, S152–S159.

(2) Bishop, S. C.; Burlison, J. A.; Blagg, B. S. J. *Curr. Canc. Drug Targ.* **2007**, *7*, 369–388.

(3) Powers, M. V.; Workman, P. *FEBS Lett.* **2007**, *581*, 3758–3769.

(4) Chaudhury, S.; Welch, T. R.; Blagg, B. S. J. *ChemMedChem* **2006**, *1*, 1331–1340.

(5) Gallo, K. A. *J. Chem. Biol.* **2006**, *13*, 115–116.

(6) Zhang, H.; Burrows, F. *J. Mol. Med.* **2004**, *82*, 488–499.

(7) Sreedhar, A. S.; Söti, C.; Csermely, P. *Biochim. Biophys. Acta* **2004**, *1697*, 233–242.

(8) Pratt, W. B.; Toft, D. O. *Exp. Biol. Med.* **2003**, *228*, 111–133.

(9) Meyer, P.; Prodromou, C.; Hu, B.; Vaughan, C.; Roe, S. M.; Panaretou, B.; Piper, P. W.; Pearl, L. H. *Molecular Cell* **2003**, *11*, 647–658.

(10) Chiosis, G. *Expert Opin. Ther. Targets* **2006**, *10*, 37–50.

(11) Chiosis, G.; Vilenchik, M.; Kim, J.; Solit, D. *Drug Discovery Today* **2004**, *9*, 881–888.

(12) Csermely, P.; Schnaider, T.; Soiti, C.; Prohaszka, Z.; Nardi, G. *Pharmacol. Ther.* **1998**, *79*, 129–168.

(13) Whitesell, L.; Lindquist, S. L. *Nat. Rev. Cancer* **2005**, *5*, 761–772.

(14) Adams, J.; Elliot, P. J. *Oncogene* **2000**, *19*, 6687–6692.

(15) Yufu, Y.; Nishimura, J.; Nawata, H. *Leuk. Res.* **1992**, *16*, 597–605.

(16) Franzen, B.; Linder, S.; Alaiya, A. A.; Eriksson, E.; Fujioka, K.; Bergman, A. C. *Electrophoresis* **1997**, *18*, 582–587.

(17) Luparello, C.; Noel, A.; Pucci-Minafra, I. *DNA Cell Biol.* **1997**, *16*, 1231–1236.

(18) Zou, J.; Guo, Y.; Guettouche, T.; Smith, D. F.; Voellmy, R. *Cell* **1998**, *94*, 471–480.

(19) Shen, H. Y.; He, J. C.; Wang, Y.; Huang, Q. Y.; Chen, J. F. *J. Biol. Chem.* **2005**, *280*, 39962–39969.

(20) Waza, M.; Adachi, H.; Katsuno, M.; Minamiyama, M.; Sang, C.; Tanaka, F.; Inukai, A.; Doyu, M.; Sobue, G. *Nat. Med.* **2005**, *11*, 1088–1095.

(21) Kim, H. R.; Kang, H. S.; Kim, H. D. *IUBMB Life* **1999**, *48*, 429–433.

(22) Dou, F.; Netzer, W. J.; Tanemura, K.; Li, F.; Hartl, F. U.; Takashima, A.; Gouras, G. K. *Proc. Natl. Acad. Sci. USA* **2003**, *100*, 721–726.

(23) Dickey, C. A.; Erikson, J.; Kamal, A.; Burrows, F.; Kasibhatla, S.; Eckman, C. B.; Hutton, M.; Petrucelli, L. *Curr. Alzheimer Res.* **2005**, *2*, 231–238.

(24) Hanahan, D.; Weinberg, A. *Cell* **2000**, *100*, 57–70.

(25) Workman, P.; de Billy, E. *Nature Med.* **2007**, *13*, 1415–1417.

(26) Pearl, L. H.; Prodromou, C.; Workman, P. *Biochem. J.* **2008**, *410*, 439–453.

(27) Söti, C.; Nagy, E.; Giricz, Z.; Vigh, L.; Csermely, P.; Ferdinandy, P. *Brit. J. Pharmacol.* **2005**, *146*, 769–780.

(28) Welch, W. J.; Feramisco, J. R. *J. Biol. Chem.* **1982**, *257*, 14949–14959.

(29) Lindquist, S.; Craig, S. E. *Annu. Rev. Genet.* **1988**, *22*.

(30) Frydman, J. *Annu. Rev. Biochem.* **2001**, *70*, 603–649.

(31) Blagg, B. S. J.; Kerr, T. D. *Med. Res. Rev.* **2006**, *26*, 310–338.

(32) Wright, L.; Barril, X.; Dymock, B.; Sheridan, L.; Surgenor, A.; Beswick, M.; Drysdale, M.; Collier, A.; Massey, A.; Davies, N.; Fink, A.; Fromont, C.; Aherne, W.; Boxall, K.; Sharp, S.; Workman, P.; Hubbard, R. E. *Chem. Biol.* **2004**, *11*, 775–785.

(33) Toft, D. O. *Trends Endocrinol. Metab.* **1998**, *9*, 238–243.

(34) Picard, D. Hsp90 Interactors. *www.picard.ch/downloads/Hsp90interactors.pdf* (accessed Jul, 2008).

(35) Prodromou, C.; Piper, P. W.; Pearl, L. H. *Proteins: Struct. Funct. Genet.* **1996**, *25*, 517–522.

(36) Nemoto, T. N.; Sato, N.; Iwanari, H.; Yamashita, H.; Takagi, T. *J. Biol. Chem.* **1997**, *272*, 26179–26187.

(37) Young, J. C.; Schneider, C.; Hartl, F. U. *FEBS Lett.* **1997**, *418*, 139–143.

(38) Huai, Q.; Wang, H.; Liu, Y.; Kim, H. Y.; Toft, D.; Ke, H. *Structure* **2005**, *13*, 579–590.

(39) Prodromou, C.; Panaretou, B.; Chohan, S.; Siligardi, G.; O'Brien, R.; Ladbury, J. E.; Roe, S. M.; Piper, P. W.; Pearl, L. H. *EMBO* **2000**, *19*.

(40) Pearl, L. H.; Prodromou, C. *Annu. Rev. Biochem.* **2006**, *75*, 271–294.

(41) Terasawa, K.; Minami, M.; Minami, Y. *J. Biochem.* **2005**, *137*, 443–447.

(42) Harris, S. F.; Shiau, A. K.; Agard, D. A. *Structure* **2004**, *12*, 1087–1097.

(43) Ali, M. U.; Roe, S. M.; Vaughan, C. K.; Meyer, P.; Panaretou, B.; Piper, P. W.; Prodromou, C.; Pearl, L. H. *Nature* **2006**, *440*, 1013–1017.

(44) Söti, C.; Radics, L.; Yahara, I.; Csermely, P. *Eur. J. Biochem.* **1998**, *255*, 611–617.

(45) Marcu, M. G.; Schulte, T. W.; Neckers, L. *J. Natl. Canc. Inst.* **2000**, *92*, 242–248.

(46) Marcu, M. G.; Chadli, A.; Bouhouche, I.; Catelli, M.; Neckers, L. M. *J. Biol. Chem.* **2000**, *275*, 37181–37186.

(47) Dutta, R.; Inouye, M. *Trends Biochem. Sci.* **2000**, *25*, 24–28.

(48) Stebbins, C. E.; Russo, A. A.; Schneider, C.; Rosen, N.; Hartl, F. U.; Pavletich, N. P. *Cell* **1997**, *89*, 239–250.

(49) Prodromou, C.; Roe, S. M.; Piper, P. W.; Pearl, L. H. *Nat. Struct. Biol.* **1997**, *4*, 477–482.

(50) Prodromou, C.; Roe, S. M.; O'Brien, R.; Ladbury, J. E.; Piper, P. W.; Pearl, L. H. *Cell* **1997**, *90*, 65–75.

(51) Janin, Y. L. *J. Med. Chem.* **2005**, *48*, 7503–7512.

(52) Hu, Y.; Mivechi, N. F. *J. Biol. Chem.* **2003**, *278*, 17299–17306.

(53) Rutherford, S. L.; Lindquist, S. *Nature* **1998**, *396*, 336–342.

(54) Carrello, A.; Ingley, E.; Minchin, R. F.; Tsai, A.; Ratajczak, T. *J. Biol. Chem.* **1999**, *274*, 2682–2689.

(55) Knight, C. A. *Science* **2002**, *296*, 2348–2349.

(56) Kosano, H.; Stensgard, B.; Charlesworth, M. C.; McMahon, N.; Toft, D. *J. Biol. Chem.* **1998**, *273*, 32973–32979.

(57) Prodromou, C.; Siligardi, G.; O'Brien, R.; Woolfson, D. N.; Regan, L.; Panaretou, B.; Ladbury, J. E.; Piper, P. W.; Pearl, L. H. *EMBO* **1999**, *18*, 754–762.

(58) Forsythe, H. L.; Jarvis, J. L.; Turner, J. W.; Elmore, L. W.; Holt, S. E. *J. Biol. Chem.* **2001**, *276*, 15571–15574.

(59) Chen, S.; Sullivan, W. P.; Toft, D. O.; Smith, D. F. *Cell Stress Chaperones* **1998**, *3*, 118–129.

(60) Ratajczak, T.; Carrello, A. *J. Biol. Chem.* **1996**, *271*, 2961–2965.

(61) Obermann, W. M. J.; Sondermann, H.; Russo, A. A.; Pavletich, N.; Hartl, F. U. *J. Cell Biol.* **1998**, *143*, 901–910.

(62) Panaretou, B.; Prodromou, C.; Roe, S. M.; O'Brien, R.; Ladbury, J. E.; Piper, P. W.; Pearl, L. H. *EMBO* **1998**, *17*, 4829–4836.

(63) Chadli, A.; Bouhouche, I.; Sullivan, W. P.; Stensgard, B.; McMahon, N.; Catelli, M.; Toft, D. O. *Proc. Natl. Acad. Sci. USA* **2000**, *97*, 12524–12529.

(64) Wu, L. X.; Xu, J. H.; Zhang, K. Z.; Lin, Q.; Huang, X. W.; Wen, C. X.; Chen, Y. Z. *Leukemia* **2008**, *22*, 1402–1409.

(65) Eleuteri, A. M.; Cuccioloni, M.; Bellesi, J.; Lupidi, G.; Fioretti, E.; Angeletti, M. *Proteins: Struc. Funct. Genet.* **2002**, *48*, 169–177.

(66) Yonehara, M.; Minami, Y.; Kawata, Y.; Nagai, J.; Yahara, I. *J. Biol. Chem.* **1996**, *271*, 2641–2645.

(67) Galam, L.; Hadden, M. K.; Ma, Z.; Ye, Q.; Yun, B.; Blagg, B. S. J.; Matts, R. L. *Bioorg. Med. Chem.* **2007**, *15*, 1939–1946.

(68) Hondermarck, H.; Tastet, C.; Yazidi-Belkoura, I. E.; Toillon, R.; Le Bourhis, X. *J. Prot. Res.* **2008**, *7*, 1403–1411.

(69) Biamonte, M. A.; Shi, J.; Hurst, D.; Hong, K.; Boehm, M. F.; Kasibhatla, S. R. *J. Org. Chem.* **2005**, *70*, 717–720.

(70) Martin, C. J.; Gaisser, S.; Challis, I. R.; Carletti, I.; Wilkinson, B.; Gregory, M.; Prodromou, C.; Roe, S. M.; Pearl, L. H.; Boyd, S. M.; Zhang, M. Q. *J. Med. Chem.* **2008**, *51*, 2853–2857.

(71) Cortajarena, A. L.; Yi, F.; Regan, L. *ACS Chem. Biol.* **2008**, *3*, 161–166.

(72) Chiosis, G.; Huezo, H.; Rosen, N.; Mimnaugh, E.; Whitesell, L.; Neckers, L. *Mol. Cancer Ther.* **2003**, *2*, 123–129.

(73) Xu, W.; Neckers, L. *Clin. Cancer Res.* **2007**, *13*, 1625–1629.

(74) Jolly, C.; Morimoto, R. I. *J. Natl. Cancer Inst.* **2000**, *92*, 1564–1572.

(75) Neckers, L. *Trends Mol. Med.* **2002**, *8*, S55–S61.

(76) Chiosis, G.; Timaul, M. N.; Lucas, B.; Munster, P. N.; Zheng, F. F.; Sepp-Lorenzino, L.; Rosen, N. *Chem. Biol.* **2001**, *8*, 289–299.

(77) Schnur, R. C.; Corman, M. L.; Gallaschun, R. J.; Cooper, B. A.; Dee, M. F.; Doty, J. L.; Muzzi, M. L.; DiOrio, C. I.; Barbacci, E. G.; Miller, P. E.; Pollack, V. A.; Savage, D. M.; Sloan, D. E.; Pustilnik, L. R.; Moyer, J. D.; Moyer, M. P. *J. Med. Chem.* **1995**, *38*, 3813–3820.

(78) Kamal, A.; Thao, L.; Sensintaffar, J.; Zhang, L.; Boehm, M. F.; Fritz, L. C.; Burrows, F. *Nature* **2003**, *425*, 407–410.

(79) Le Brazidec, J.; Kamal, A.; Busch, D.; Thao, L.; Zhang, L.; Timony, G.; Grecko, R.; Trent, K.; Lough, R.; Salazar, T.; Khan, S.; Burrows, F.; Boehm, M. F. *J. Med. Chem.* **2004**, *47*, 3865–3873.

(80) Duvvuri, M.; Konkar, S.; Hong, K. H.; Blagg, B. S. J.; Krise, J. *ACS Chem. Biol.* **2006**, *1*, 309–315.

(81) de Duve, C.; de Barsy, T.; Poole, B.; Trouet, A.; Tulkens, P.; Van Hoof, F. *Biochem. Pharmacol.* **1974**, *23*, 2495–2531.

(82) Altan, N.; Chen, Y.; Schindler, M.; Simon, S. M. *J. Exp. Med.* **1998**, *187*, 1583–1598.

(83) Kokkonen, N.; Rivinoja, A.; Kauppila, A.; Suokas, M.; Kellokumpu, I.; Kellokumpu, S. *J. Biol. Chem.* **2004**, *279*, 39982–39988.

(84) Muchowski, P. J.; Wacker, J. L. *Nature Rev. Neuro.* **2005**, *6*, 11–22.

(85) Ansar, S.; Burlison, J. A.; Hadden, M. K.; Yu, X. M.; Desino, K. E.; Bean, J.; Neckers, L.; Audus, K. L.; Michaelis, M. L.; Blagg, B. S. J. *Bioorg. Med. Chem. Lett.* **2007**, *17*, 1984–1990.

(86) Sausville, E. A. *Curr. Cancer Drug Targets* **2003**, *3*, 377–383.

(87) Banerji, U. *Proc. Am. Assoc. Cancer Res.* **2003**, *44*, 677.

(88) Driggers, E. M.; Hale, S. P.; Lee, J.; Terrett, N. K. *Nature Rev. Drug Disc.* **2008**, *7*, 608–624.

(89) DeBoer, C.; Meulman, P. A.; Wnuk, R. J.; Peterson, D. H. *J. Antibiot. (Tokyo)* **1970**, *23*, 442–447.

(90) Omura, S.; Iwai, Y.; Takahashi, Y.; Sadakane, N.; Nakagawa, A. *J. Antibiot.* **1979**, *32*, 255–261.

(91) Nakata, M.; Osumi, T.; Ueno, A.; Kimura, T.; Tamai, T.; Tatsuta, K. *Tetrahedron Lett.* **1991**, *32*, 6015–6018.

(92) Andrus, M. B.; Hicken, E. J.; Meredith, E. L.; Simmons, B. L.; Cannon, J. F. *Org. Lett.* **2003**, *5*, 3859–3862.

(93) Andrus, M. B.; Hicken, E. J.; Meredith, E. L.; Simmons, B. L.; Cannon, J. F. *Org. Lett.* **2003**, *5*, 3859–3862.

(94) Qin, H.; Panek, J. S. *Org. Lett.* **2008**, *10*, 2477–2479.

(95) Uehara, Y.; Hori, M.; Takeuchi, T.; Umezawa, H. *Mol. Cell. Biol.* **1986**, *6*, 2198–2206.

(96) Jove, R.; Hanafusa, H. *Ann. Rev. Cell Biol.* **1987**, *3*, 31–56.

(97) Whitesell, L.; Shifrin, S. D.; Schwab, G.; Neckers, L. M. *Cancer Res.* **1992**, *52*, 1721–1728.

(98) Whitesell, L.; Mimnaugh, E. G.; De Costa, B.; Myers, C. E.; Neckers, L. M. *Proc. Natl. Acad. Sci. USA* **1994**, *91*, 8323–8328.

(99) Neckers, L.; Schulte, T. W.; Mimnaugh, E. G. *Invest. New Drugs* **1999**, *17*, 361–373.

(100) Roe, S. M.; Prodromou, C.; O'Brien, R.; Ladbury, J. E.; Piper, P. W.; Pearl, L. H. *J. Med. Chem.* **1999**, *42*, 260–266.

(101) Supko, J. G.; Hickman, R. L.; Grever, M. R.; Malspeis, L. *Cancer Chemother. Pharmacol.* **1995**, *36*, 305–315.

(102) An, W. G.; Schnur, R. C.; Neckers, L.; Blagosklonny, M. V. *Cancer Chemother. Pharmacol.* **1997**, *40*, 60–64.

(103) Dikalov, S.; Rumyantseva, G. V.; Piskunov, A. V.; Weiner, L. M. *Biochemistry* **1992**, *31*, 8947–8953.

(104) Dikalov, S.; Landmesser, U.; Harrison, D. G. *J. Biol. Chem.* **2002**, *277*, 25480–25485.

(105) Schulte, T. W.; Neckers, L. M. *Cancer Chemother. Pharmacol.* **1998**, *42*, 273–279.

(106) Jez, J. M.; Chen, C.; Rastelli, G.; Stroud, R. M.; Santi, D. V. *Chem. Biol.* **2003**, *10*, 361–368.

(107) Egorin, M. J.; Lagattuta, T. F.; Hamburger, D. R.; Covey, J. M.; White, K. D.; Musser, S. M.; Eiseman, J. L. *Cancer Chemother. Pharmacol.* **2002**, *49*, 7–19.

(108) Wright, M. H.; Calcagno, A. M.; Salcido, C. D.; Carlson, M. D.; Ambudkar, S. V.; Varticovski, L. *Breast Cancer Res.* **2008**, *10*, R10.

(109) Patel, K.; Piagentini, M.; Rascher, A.; Tian, Z.; Buchanan, G. O.; Regentin, R.; Hu, Z.; Hutchinson, C. R.; McDaniel, R. *Chem. Biol.* **2004**, *11*, 1625–1633.

(110) Lee, K.; Ryu, J. S.; Jin, Y.; Kim, W.; Kaur, N.; Chung, S. J.; Jeon, Y.; Park, J.; Bang, J. S.; Lee, H. S.; Kim, T. Y.; Lee, J. J.; Hong, Y. *Org. Biomol. Chem.* **2008**, *6*, 340–348.

(111) Tadtong, S.; Meksurlyen, D.; Tanasupawat, S.; Isobe, M.; Suwanborirux, K. *Bioorg. Med. Chem. Lett.* **2007**, *17*, 2939–2943.

(112) Maroney, A. C.; Marugan, J. J.; Mezzasalma, T. M.; Barnakov, A. N.; Garrabrant, T. A.; Weaner, L. E.; Jones, W. J.; Barnakova, L. A.; Koblish, H. K.; Todd, M. J.; Masucci, J. A.; Deckman, I. C.; Galemmo Jr., R. A.; Johnson, D. L. *Biochemistry* **2006**, *45*, 5678–5686.

(113) Cutler, H. G.; Arrendale, R. F.; Springer, J. P.; Cole, P. D.; Roberts, R. G.; Hanlin, R. T. *Agric. Biol. Chem.* **1987**, *51*, 3331–3338.

(114) Yamamoto, K.; Garbaccio, R. M.; Stachel, S. J.; Solit, D. B.; Chiosis, G.; Rosen, N.; Danishefsky, S. J. *Angew. Chem. Int. Ed.* **2003**, *42*, 371–376.

(115) Geng, X.; Yang, Z.; Danishefsky, S. J. *Synlett* **2004**, *8*, 1325–1333.

(116) Soga, S.; Neckers, L. M.; Schulte, T. W.; Shiotsu, Y.; Akasaka, K.; Narumi, H.; Agatsuma, T.; Ikuina, Y.; Murakata, C.; Tamaoki, T.; Akinaga, S. *Cancer Res.* **1999**, *59*, 2931–2938.

(117) Agatsuma, T.; Ogawa, H.; Akasaka, K.; Asai, A.; Yamashita, Y.; Mizukami, T.; Akinaga, S.; Saitoh, Y. *Bioorg. Med. Chem.* **2002**, *10*, 3445–3454.

(118) Ikuina, Y.; Amishiro, N.; Miyata, M.; Narumi, H.; Ogawa, H.; Akiyama, T.; Shiotsu, Y.; Akinaga, S.; Murakata, C. *J. Med. Chem.* **2003**, *46*, 2534–2541.

(119) Kitamura, Y.; Nara, S.; Nakagawa, A.; Nakatsu, R.; Nakashima, T.; Soga, S.; Kajita, S.; Shiotsu, Y.; Kanda, Y. Japan Patent WO2005063222, 2005.

(120) Drysdale, M. J.; Dymock, B. W.; Barril-Alonso, X. England Patent WO2005034950, 2005.

(121) Dymock, B. W.; Drysdale, M. J.; Fromont, C.; Jordan, A. England Patent WO2005021552, 2005.

(122) Soga, S.; Sharma, S. V.; Shiotsu, Y.; Shimizu, M.; Tahara, H.; Yamaguchi, K.; Ikuina, Y.; Murakata, C.; Tamaoki, T.; Kurebayashi, J.; Schulte, T. W.; Neckers, L. M.; Akinaga, S. *Cancer Chemother. Pharmacol.* **2001**, *48*, 435–445.

(123) Turbyville, T. J.; Wijeratne, E. M. K.; Liu, M. X.; Burns, A. M.; Seliga, C. J.; Luevano, L. A.; David, C. L.; Faeth, S. H.; Whitesell, L.; Gunatilaka, A. A. L. *J. Nat. Prod.* **2006**, *69*, 178–184.

(124) Yang, Z.; Geng, X.; Solit, D.; Pratilas, C. A.; Rosen, N.; Danishefsky, S. J. *J. Am. Chem. Soc.* **2004**, *126*, 7881–7889.

(125) Hellwig, V.; Mayer-Bartschmid, A.; Müller, H.; Greif, G.; Kleymann, G.; Zitzmann, W.; Tichy, H.; Stadler, M. *J. Nat. Prod.* **2003**, *66*, 829–837.

(126) Moulin, E.; Zoete, V.; Barluenga, S.; Karplus, M.; Winssinger, N. *J. Am. Chem. Soc.* **2005**, *127*, 6999–7004.

(127) Barluenga, S.; Moulin, E.; Lopez, P.; Winssinger, N. *Chem. Eur. J.* **2005**, *11*, 4935–4952.

(128) Moulin, E.; Barluenga, S.; Winssinger, N. *Org. Lett.* **2005**, *7*, 5637–5639.

(129) Schulte, T. W.; Akinaga, S.; Soga, S.; Sullivan, W.; Stensgard, B.; Toft, D.; Neckers, L. M. *Cell Stress Chaperones* **1998**, *3*, 100–108.

(130) Logan, I. R.; Gaughan, L.; McCracken, S. R. C.; Sapountzi, V.; Leung, H. Y.; Robson, C. N. *Mol. Cell Biol.* **2006**, *26*, 6502–6510.

(131) Clevenger, R. C.; Blagg, B. S. J. *Org. Lett.* **2004**, *2004*, 4459–4462.

(132) Shen, G.; Blagg, B. S. J. *Org. Lett.* **2005**, *7*.

(133) Wang, M.; Shen, G.; Blagg, B. S. J. *Bioorg. Med. Chem. Lett.* **2006**, *16*, 2459–2462.

(134) Hadden, M. K.; Lubbers, D. J.; Blagg, B. S. J. *Curr. Top. Med. Chem.* **2006**, *6*, 1173–1182.

(135) Hooper, D. C.; Wolfson, J. S.; McHugh, G. L.; Winters, M. B.; Swartz, M. N. *Antimicrob. Agents Chemother.* **1982**, *22*, 662–671.

(136) Tanitame, A.; Oyamada, Y.; Ofuji, K.; Fujimoto, M.; Suzuki, K.; Ueda, T.; Terauchi, H.; Kawasaki, M.; Nagai, K.; Wachi, M.; Yamagishi, J. *Bioorg. Med. Chem.* **2004**, *12*, 5515–5524.

(137) Laurin, P.; Ferroud, D.; Schio, L.; Klich, M.; Dupuis-Hamelin, C.; Mauvais, P.; Lassaigne, P.; Bonnefoy, A.; Musicki, B. *Bioorg. Med. Chem. Lett.* **1999**, *9*, 2875–2880.

(138) Ali, J. A.; Jackson, A. P.; Howells, A. J.; Maxwell, A. *Biochemistry* **1993**, *32*, 2717–2724.

(139) Burlison, J. A.; Neckers, L.; Smith, A. B.; Maxwell, A.; Blagg, B. S. J. *J. Am. Chem. Soc.* **2006**, *128*, 15529–15536.

(140) Yu, X. M.; Shen, G.; Neckers, L.; Blake, H.; Holzbeierlein, J.; Cronk, B.; Blagg, B. S. J. *J. Am. Chem. Soc.* **2005**, *127*, 12778–12779.

(141) Burlison, J. A.; Blagg, B. S. J. *Org. Lett.* **2006**, *8*, 4855–4858.

(142) Huang, Y.; Blagg, B. S. J. *J. Org. Chem.* **2007**, *72*, 3609–3613.

(143) Burlison, J. A.; Avila, C.; Vielhauer, G.; Lubbers, D. J.; Holzbeierlein, J.; Blagg, B. S. J. *J. Org. Chem.* **2008**, *73*, 2130–2137.

(144) Donnelly, A.; Blagg, B. S. J. *Curr. Med. Chem.* **2008**, *15*, 2702–2717.

(145) Donnelly, A. C.; Mays, J. R.; Burlison, J. A.; Nelson, J. T.; Vielhauer, G.; Holzbeierlein, J.; Blagg, B. S. J. *J. Org. Chem.* **2008**, *73(22)*, 8901–8920.

(146) Palermo, C. M.; Hernando, J. I. M.; Dertinger, S. D.; Kende, A. S.; Gasiewicz, T. A. *Chem. Res. Toxicol.* **2003**, *16*, 865–872.

(147) Palermo, C. M.; Westlake, C. A.; Gasiewicz, T. A. *Biochemistry* **2005**, *44*, 5041–5052.

(148) Beltz, L. A.; Bayer, D. K.; Moss, A. L.; Simet, I. M. *Anti-Cancer Agents in Med. Chem.* **2006**, *6*, 389–406.

(149) Weinreb, O.; Amit, T.; Youdim, M. B. H. *Free Rad. Biol. Med.* **2007**, *43*, 546–556.

(150) Schiff, P. B.; Horwitz, S. B. *Proc. Natl. Acad. Sci. USA* **1980**, *77*, 1561–1565.

(151) Ding, A. H.; Porteu, F.; Sanchez, E.; Nathan, C. F. *Science* **1990**, *248*, 370–372.

(152) Byrd, C. A.; Bornmann, W.; Erdjument-Bromage, H.; Tempst, P.; Pavletich, N.; Rosen, N.; Nathan, C. F.; Ding, A. *Proc. Natl. Acad. Sci. USA* **1999**, *96*, 5645–5650.

(153) Wani, M. C.; Taylor, H. L.; Wall, M. E.; Coggon, P.; McPhail, A. T. *J. Am. Chem. Soc.* **1971**, *93*, 2325–2327.

(154) Kingston, D. G. I. *Pharmac. Ther.* **1991**, *52*, 1–34.

(155) Basso, A. D.; Solit, D.; Chiosis, G.; Giri, B.; Tsichlis, P.; Rosen, N. *J. Biol. Chem.* **2002**, *277*, 39858–39866.

(156) Solit, D. B.; Basso, A. D.; Olshen, A. B.; Scher, H. I.; Rosen, N. *Cancer. Res.* **2003**, *63*, 2139–2144.

(157) Sawai, A.; Chandarlapaty, S.; Greulich, H.; Gonen, M.; Ye, Q.; Arteaga, C. L.; Sellers, W.; Rosen, N.; Solit, D. *Cancer Res.* **2008**, *68*, 589–596.

(158) East, A. J.; Ollis, W. D.; Wheeler, R. E. *J. Chem. Soc.* **1969**, *C*, 365–373.

(159) Jain, A. C.; Jain, S. M. *Tetrahedron* **1972**, *28*, 5063–5067.

(160) Hastings, J. M.; Hadden, M. K.; Blagg, B. S. J. *J. Org. Chem.* **2008**, *73*, 369–373.

(161) Hossain, M. M.; Kawamura, Y.; Yamashita, K.; Tsukayama, M. *Tetrahedron* **2006**, *62*, 8625–8635.

(162) Hadden, M. K.; Galam, L.; Gestwicki, J. E.; Matts, R. L.; Blagg, B. S. J. *J. Nat. Prod.* **2007**, *70*, 2014–2018.

(163) Sharma, R. A.; Gescher, A. J.; Steward, W. P. *Eur. J. Cancer* **2005**, *41*, 1955–1968-1955.

(164) Aggarwal, B. B.; Sundaram, C.; Malani, N.; Ichikawa, H. *Adv. Exp. Med. Biol.* **2007**, *595*, 1–75.

(165) Goel, A.; Kunnumakkara, A. B.; Aggarwal, B. B. *Biochem. Pharmacol.* **2008**, *75*, 787–809.

(166) Joe, B.; Vijaykumar, M.; Lokesh, B. R. *Crit. Rev. Food Sci. Nutr.* **2004**, *44*, 97–111.

(167) Park, S.; Kim, D. S. H. L. *J. Nat. Prod.* **2002**, *65*, 1227–1231.

(168) Wahlstrom, B.; Blennow, G. *Acta. Pharmacol. Toxicol.* **1978**, *43*, 83–87.

(169) Ammon, H. P. T.; Wahl, M. A. *Planta Med.* **1991**, *57*, 1–7.

(170) Rashmi, R.; Santhosh Kumar, T. R.; Karunagaran, D. *FEBS Lett* **2003**, *538*, 19–24.

(171) Cheng, A.; Hsu, C.; Lin, J.; Hsu, M.; Ho, Y.; Shen, T.; Ko, J.; Lin, J.; Lin, B.; Wu, M.; Yu, H.; Jee, S.; Chen, G.; Chen, T.; Chen, C.; Lai, M.; Pu, Y.; Pan, M.; Wang, Y.; Tsai, C.; Hsieh, C. *Anticancer Res.* **2001**, *21*, 2895–2900.

(172) Shoba, G.; Joy, D.; Joseph, T.; Majeed, M.; Rajendran, R.; Srinivas, P. S. *Planta Med.* **1998**, *64*, 353–356.

(173) Strimpakos, A. S.; Sharma, R. A. *Antiox. and Redox. Sig.* **2008**, *10*, 511–546.

(174) Amolins, M. W.; Peterson, L. B.; Blagg, B. S. J. *Bioorg. Med. Chem.* **2009**, *17*, 360–367

.

(175) Khalid, S. A.; Duddeck, H.; Gonzalez-Sierra, M. *J. Nat. Prod.* **1989**, *52*, 922–927.

(176) Zhang, T.; Hamza, A.; Cao, X.; Wang, B.; Yu, S.; Zhan, C.; Sun, D. *Mol. Canc. Ther.* **2008**, *7*, 162–170.

(177) Westerheide, S. D.; Bosman, J. D.; Mbadugha, B. N. A.; Kawahara, T. L. A.; Matsumoto, G.; Kim, S.; Gu, W.; Devlin, J. P.; Silverman, R. B.; Morimoto, R. I. *J. Biol. Chem.* **2004**, *279*, 56053–56060.

(178) Uddin, S. J.; Nahar, L.; Shilpi, J. A.; Shoeb, M.; Borkowski, T.; Gibbons, S.; Middleton, M.; Byres, M.; Sarker, S. *Phytother. Res.* **2007**, *21*, 757–761.

(179) Hieronymus, H.; Lamb, J.; Ross, K. N.; Peng, X. P.; Clement, C.; Rodina, A.; Nieto, M.; Du, J.; Stegmaier, K.; Raj, S. M.; Maloney, K. N.; Clardy, J.; Hahn, W. C.; Chiosis, G.; Golub, T. R. *Cancer Cell* **2006**, *10*, 321–330.

(180) Lamb, J.; Crawford, E. D.; Peck, D.; Modell, J. W.; Blat, I. C.; Wrobel, M. J.; Lerner, J.; Brunet, J.; Subramanian, A.; Ross, K. N.; Reich, M.; Hieronymus, H.; Wei, G.; Armstrong, S. A.; Haggarty, S. J.; Clemons, P. A.; Wei, R.; Carr, S. A.; Lander, E. S.; Golub, T. R. *Science* **2006**, *313*, 1929–1935.

(181) Vinson-Hieronymous, H.; Golub, T. R.; Lamb, J.; Stegmaier, K. United States Patent WO2007117466, 2007.

(182) Brandt, G. E. L.; Schmidt, M. D.; Prisinzano, T. E.; Blagg, B. S. J. *J. Med. Chem.* **2008**, *51*, 6495–6502.

Chapter II: *In Silico* Development of a Novel Hsp90 Inhibition Scaffold

I. Introduction

Previously, the synthesis and biological evaluation of several compounds based on the 1,4-naphthoquinone scaffold were described.[1] A high-throughput screen of natural products, using the aforementioned firefly luciferase assay,[2] identified three naphthoquinone analogues that inhibited the renaturation of heat denatured luciferase at concentrations of ~20 μM (Table 1).

Table 1. *In vitro* results of HTS hits with the 1,4-naphthoquinone scaffold.

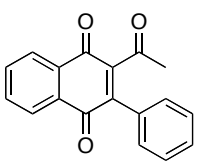

HTS1

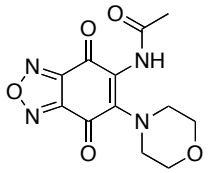

HTS2

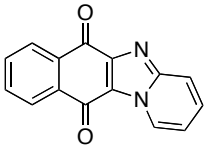

HTS3

Compound	Luciferase Assay[a]	Anti-Proliferation[a]		Her2 ELISA[a]
		MCF-7	SKBr3	
HTS1	0.25	0.21 ± 0.02	0.82 ± 0.02	3.3 ± 1
HTS2	0.38	19 ± 4	2.9 ± 0.5	1.2 ± 0.2
HTS3	0.02	0.83 ± 0.13	0.87 ± 0.23	1.2 ± 0.3

[a]Data presented as IC_{50} concentrations in μM ± standard deviation.

Upon further evaluation, these hits exhibited significant anti-proliferative activity against MCF-7 (ERα+ human breast cancer) and SKBr3 (ERα-, Her2 over-expressing human breast cancer) cell lines, and induced degradation of Her2, a

known Hsp90-dependent client protein. These core structures provided a starting point for evaluation of structure–activity relationships (SAR). In total, 31 compounds were synthesized and evaluated, and exhibited IC_{50} values ranging from 1.3 μM to >100 μM against MCF-7 breast cancer cells (Table 2). These results suggested that further evaluation would be necessary before potent analogues containing the 1,4-naphthoquinone scaffold could be identified as Hsp90 inhibitors.

Table 2. *In vivo* results of initial 1,4-naphthoquinone library.

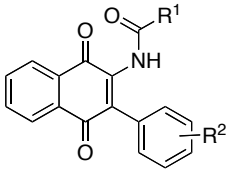

Scaffold A

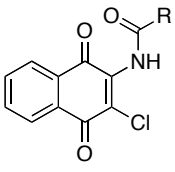

Scaffold B

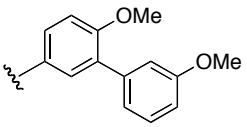

Biphenyl

Compound	Scaffold	R^1	R^2	MCF-7[a]
1a	A	CH_3	H	1.6 ± 0.5
1b	A	CH_3	2-OMe	2.2 ± 0.7
1c	A	CH_3	3-OMe	2.7 ± 0.7
1d	A	CH_3	4-OMe	2.2 ± 0.3
1e	A	CH_3	2-Cl	3.0 ± 0.3
1f	A	CH_3	3-Cl	1.3 ± 0.5
1g	A	CH_3	4-Cl	1.4 ± 0.2
1h	A	CH_3	Benzo[*b*,*d*]furan	2.4 ± 0.3
1i	A	CH_3	4-OPh	2.5 ± 0.2
2a	A	Ph	H	2.1 ± 0.4
2b	A	Ph	2-OMe	2.2 ± 0.1
2c	A	Ph	3-OMe	1.4 ± 0.1

2d	A	Ph	4-OMe	1.4 ± 0.02
2e	A	Ph	2-Cl	1.8 ± 0.1
2f	A	Ph	3-Cl	4.8 ± 2.0
2g	A	Ph	4-Cl	2.6 ± 0.1
2h	A	Ph	Benzo[*b,d*]furan	6.0 ± 0.1
2i	A	Ph	4-OPh	23 ± 1.9
3	B	CH_3	–	1.7 ± 0.1
4	B	Ph	–	1.8 ± 0.3
5	A	Biphenyl	4-OMe	>100
6	B	Biphenyl	–	3.0 ± 0.4
7a	A	2-Cl-Phenyl	4-OMe	2.2 ± 0.1
7b	A	3-Cl-Phenyl	4-OMe	3.4 ± 1.5
7c	A	4-Cl-Phenyl	4-OMe	3.3 ± 1.2
7d	A	2-OMe-Phenyl	4-OMe	2.1 ± 0.1
7e	A	3-OMe-Phenyl	4-OMe	1.8 ± 0.1
7f	A	4-OMe-Phenyl	4-OMe	1.5 ± 0.3
7g	A	1-Naphthyl	4-OMe	2.2 ± 0.3
7h	A	2-Naphthyl	4-OMe	6.8 ± 0.6
7i	A	Cyclohexyl	4-OMe	1.9 ± 0.6

[a]Data presented as IC_{50} concentrations in μM ± standard deviation.

Prior to our studies, it was unknown how 1,4-naphthoquinones bind Hsp90, and given the shortage of Hsp90 co-crystal structures, particularly the lack of any *C*-terminal inhibitor co-crystal structure, comparative molecular field analysis (CoMFA) became a suitable method for further refinement of this scaffold.[3] Three-dimensional quantitative structure–activity relationship (3D-QSAR) studies, such as CoMFA, have played a decisive role in *in silico* drug design, although a number of limitations have been associated with this

technique.[4-6] For example, only non-covalent interactions with the binding pocket are evaluated during analysis, and thus covalent modifications are not considered. However, given the scope of our study, this approach was deemed optimal. In this chapter, the development of two CoMFA models based on the previously reported structures, as well as the design, synthesis, and biological evaluation of a second generation of novel naphthoquinone compounds is described. In particular, these models were used to probe two key structural features. First, it was necessary to determine the preferred *cis*- or *trans*- conformation of the amide side chain. Second, optimization of substituent effects within the aryl side chain was desired.

In a second part of this study, it was our objective to utilize the information compiled from the CoMFA model and biological evaluation of the prepared compounds to determine the mode of binding for a 1,4-naphthoquinone scaffold to Hsp90. A number of *N*- and *C*-terminal inhibitors of Hsp90 have been previously identified, and each class of compounds exhibits a unique set of characteristic activities that allows for mechanistic elucidation via Western Blot analyses[3,7] (Figure 1).

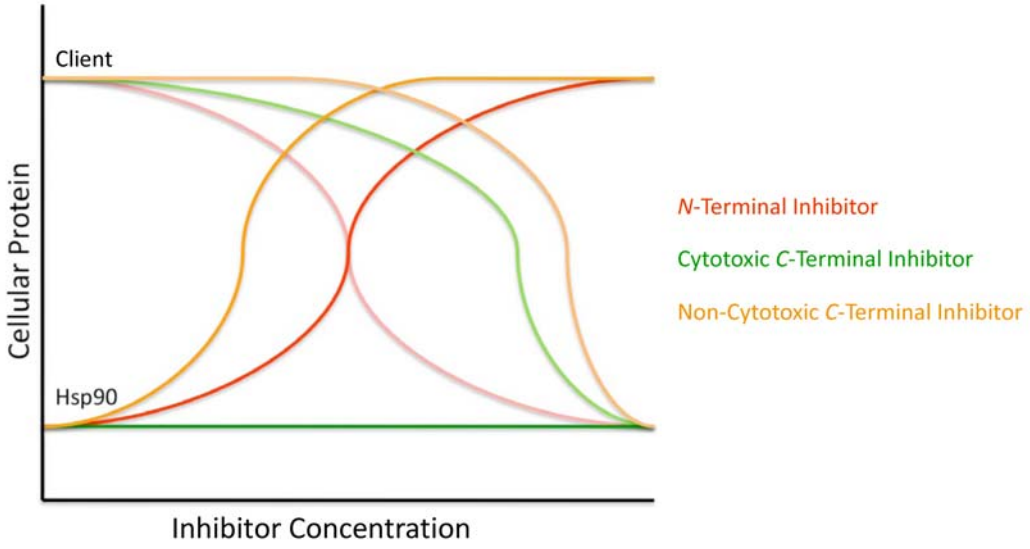

Figure 1. Protein lysate profile after exposure to various Hsp90 inhibitors.

For example, *N*-terminal inhibitors not only cause Hsp90 client protein degradation,[8,9] but they also induce concentration-dependent upregulation of Hsp70 and Hsp90 at the anti-proliferative IC_{50} concentration.[10,11] As described in chapter one, this property has been identified as problematic in clinical trials for the treatment of diseases such as cancer, where upregulation of the molecular chaperone can result in dosing and scheduling complications. Upregulation of heat shock proteins has also been identified as a physiological response to *non-cytotoxic C*-terminal inhibition, however in this case client protein degradation is not observed within a 1000-fold increase in inhibitor concentration. This has proven beneficial for the potential treatment of neurodegenerative diseases, wherein the increased levels of molecular chaperones can assist in the dissolution

of protein aggregates.[11-15] In contrast, *cytotoxic C*-terminal inhibitors do not cause upregulation of Hsp70 and Hsp90, but do induce the degradation of Hsp90-dependent client proteins, thereby offering a dosing regime that can be particularly beneficial for the treatment of cancer.[16,17]

With this knowledge in hand, it therefore became critical to not only determine where these novel Hsp90 inhibitors bind, but also the physiological response exhibited by the scaffold. In terms of SAR, it is well known that many quinone-based structures exert non-selective cytotoxicity through formation of covalent bonds via Michael additions or catalytic reduction of reactive oxygen species as a result of their redox activity.[18] In this case, having an understanding of the naphthoquinone mode of binding would provide an additional route for the development of analogues with increased potency, as well as the potential for removing the problematic quinone moiety without jeopardizing activity, mode of binding, or physiological properties of each compound. In this study, the naphthoquinone mode of binding was predicted by making use of the modeling program, AutoDock, and was confirmed through Western Blot analyses. AutoDock has been shown to outperform other common docking programs based on its descriptive algorithms and scoring function for several target proteins.[19] Developments in molecular docking over the past several years, such as with the program AutoDock, have provided a useful and complementary tool for estimating the binding energy of lead compounds, as well as for visualization of

predicted interactions with residues in the binding pocket. From this information, the rational design of a library of flavone compounds, a scaffold novel to Hsp90 inhibition, was pursued. These accounts, as well as the concluding observations, are discussed herein.

II. Results and Discussion

3D-QSAR/CoMFA Models and 1,4-Naphthoquinone Analogue Design

The 31 compounds made by Hadden and co-workers[1] were computationally aligned to produce two CoMFA models, each of which was generated based on one of two amide conformations, *cis*- or *trans*-, known to be energetically favorable for this scaffold. Compounds whose inclusion in the model resulted in a 3D-QSAR cross-validated correlation score (q^2, leave-one-out technique) of less than 0.500 were considered outliers, and removed from the data set. In the *cis*-amide model, compounds **HTS1**, **2h**, **2i**, and **5** were removed, whereas compounds **HTS2**, **1e**, and **7i** were removed from the *trans*-amide model. Outliers were later used to validate the predictive ability of each model.

3D-QSAR models were derived by utilizing the modeling program SYBYL through a partial least squares (PLS) regression, wherein the predicted IC_{50} (pIC_{50}) value was the dependent variable, and the calculated CoMFA parameters were the independent variables. In the *cis*-amide model (Figure 2), a q^2 of 0.629 was observed with an optimum number of coefficients (ONC) totaling

four. The *trans*-amide model yielded similar values of 0.671 and four, respectively.

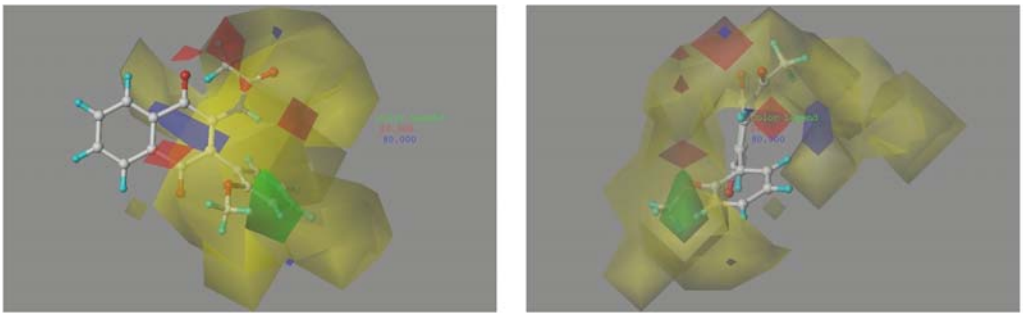

(a) (b)

Figure 2. *cis*-Amide CoMFA model.

These parameters were reinforced with a five-group non-cross-validation technique, in which the resulting correlation scores (r^2) were 0.629 for the *cis*-model and 0.603 for the *trans*- model. Both models were derived from the electrostatic and hydrophobic properties of each data set. The field contributions for each model averaged ~30% electrostatic and ~70% hydrophobic. Additional statistical parameters, including the predictive ability for each model, are summarized in Table 3.

Table 3. Statistical data for 3D-QSAR CoMFA Models

Parameters	*cis*-Amide	*trans*-Amide
$q^{2\,a}$	0.629	0.671
ONC[b]	4	4
SEE_{tr}[c]	0.103	0.103
r^2_{pred}[d]	0.865	0.954
F[e]	38.556	130.128
Outliers[f]	4	3
Field Contribution		
Electrostatic	0.357	0.257
Hydrophobic	0.643	0.743

[a]Leave-one-out cross-validated correlation coefficient
[b]Optimum number of components
[c]Standard error of estimate for the training set
[d]Predicted correlation coefficient for the test set
[e]Ratio of r^2 to 1-r^2
[f]Number of compounds whose inclusion results in a q^2 less than 0.500

From the 3D-QSAR experiments, a number of novel 1,4-naphthoquinones were modeled, and pIC_{50} values obtained for each set of amide conformers. A major limitation of CoMFA is that it tolerates only very focused structural changes. For this reason, the SAR study was focused on the aryl side chain previously reported by Hadden and co-workers, as it appeared to be the most synthetically relevant substituent falling within the parameters of the 3D-QSAR models. It also allowed for a more accurate prediction of *cis*- and *trans*- amide pIC_{50} values, which was reinforced by using an acetamide side chain in all cases to allow for further structural consistency and optimal potency. The majority of

compounds appeared to benefit from electron-donating substituents in the *ortho*- and *para*- position of the aryl side chain, although electron withdrawing substituents and *meta*-substituted aryl side chains occasionally proved beneficial. Furthermore, multi-substituted aryl side chains had not been previously investigated, and were therefore included in this study in an attempt to take advantage of multiple interactions with the binding pocket. From the resulting analysis, a select number of compounds were carried forward for synthesis and biological evaluation.

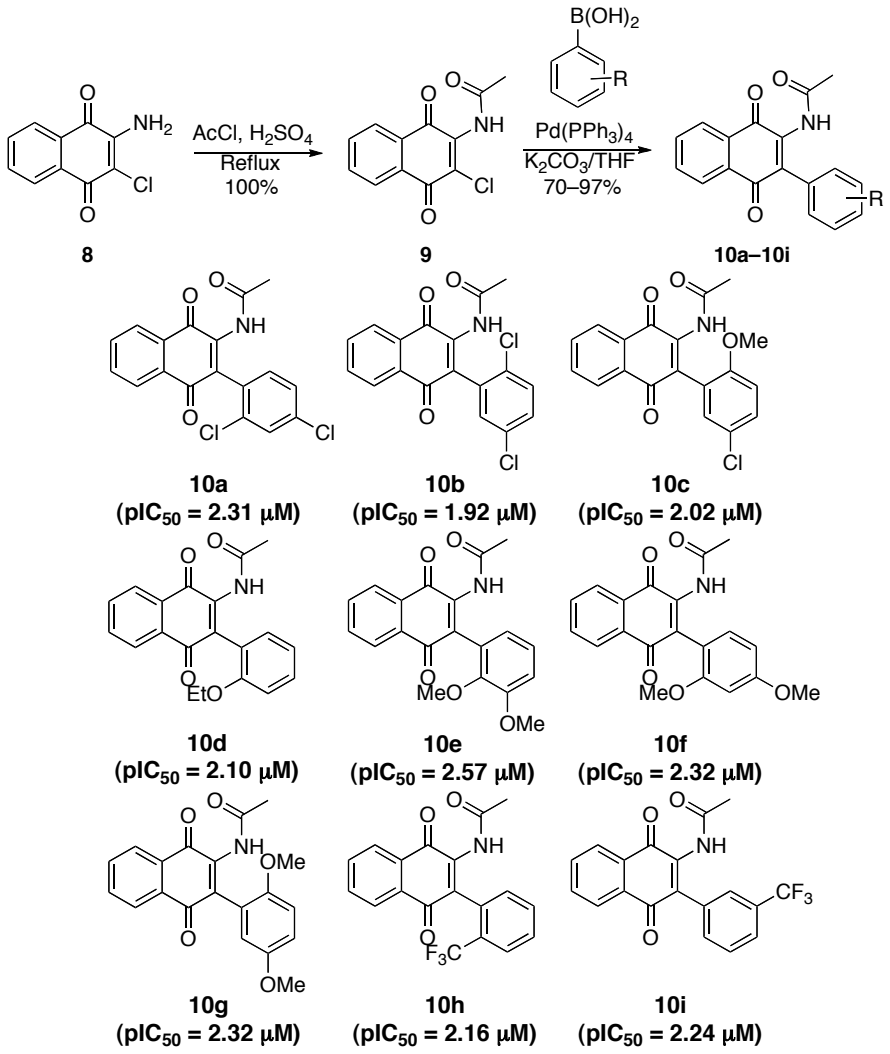

Scheme 1. Synthesis of 1,4-naphthoquinone analogues.

1,4-Naphthoquinone Analogue Synthesis

Chemistry previously optimized by our group was expanded upon to prepare a novel library of 1,4-naphthoquinones (Scheme 1). In step 1, the reduced nucleophilicity of the amino group in commercially available 2-amino-3-chloro-

1,4-naphthoquinone **8** required stringent conditions for acetylation. After several failed attempts with traditional peptide coupling techniques, it was found that the acetylated naphthoquinone **9** could only be afforded after stirring at reflux in acetyl chloride with catalytic sulfuric acid for three hours.

Compounds **10a–10i** were formed through a traditional Suzuki coupling reaction between **9** and the appropriate aryl boronic acid. Stirring these components at reflux in the presence of a catalytic amount of tetrakis(triphenylphosphine)palladium(0) and aqueous sodium bicarbonate in THF resulted in the desired products in moderate to excellent yields (51–97%).

Evaluation of Novel 1,4-Naphthoquinones

Table 4. Anti-proliferative activities of naphthoquinone analogues[a,b].

Compound	IC_{50} (SKBr3)	IC_{50} (MCF-7)	pIC_{50} (MCF-7, *cis*-amide)	pIC_{50} (MCF-7, *trans*-amide)
10a	3.8 ± 0.8	2.2 ± 0.4	2.309	1.944
10b	2.76 ± 0.04	2.01 ± 0.04	1.915	2.170
10c	2.51 ± 0.01	2.2 ± 0.1	2.019	1.717
10d	3.1 ± 0.4	2.2 ± 0.5	2.103	1.852
10e	5.5 ± 0.2	3.3 ± 0.3	2.570	2.673
10f	5.1 ± 0.5	2.9 ± 0.4	2.318	1.908
10g	3.0 ± 0.2	2.3 ± 0.2	2.320	2.477
10h	4.4 ± 0.3	2.4 ± 0.3	2.164	1.759
10i	3.8 ± 0.9	2.1 ± 0.1	2.238	2.669
	Correlation Scores (R^2):		0.612	0.069

[a]All values are in units of μM, and represent ± standard deviation for two separate experiments performed in triplicate.

[b]pIC_{50} is defined as the predicted IC_{50} in units of μM.

The data shown in Table 4 correspond to the growth inhibitory activities of 1,4-naphthoquinone analogues **10a–10i** against SKBr3 and MCF-7 breast cancer cell lines, as well as the predicted IC_{50} values against MCF-7 cells from each of the CoMFA models (*cis*- and *trans*- amide). Compounds **10b** and **10i** represent the most potent analogues, however a very flat SAR was observed for the entire library, which manifested low micromolar activities against both cell lines. Upon analysis of the anti-proliferation data, it was evident that installation of a multi-substituted aryl side chain, or a carefully selected mono-substituted aryl side chain, allowed for improved interaction in the binding pocket. In each case, an increase in activity compared to the previous library was observed. It also appeared that both hydrogen and halogen bonding interactions were possible, as moderate activity was observed when each type of substituent was introduced. In a broad sense, it appeared that improvement in activity was primarily due to proper control of steric constraints, as a number of small substituents were tolerated. It had been shown via the CoMFA model that steric bulk on the amide and aryl side chain resulted in a significant loss in activity. Furthermore, correlation scores (R^2) between the experimentally determined IC_{50} data and the pIC_{50} values indicated that a *trans*-amide conformation was most likely favored in the binding pocket. A correlation score of 0.612 was determined for the *trans* model, whereas a score of 0.069 was reported for the *cis* model, indicating preference for the former.

Computational and Western Blot Analysis Toward Further Analogue Development

Although moderate potency had been established with the second generation of naphthoquinones, it was clear that further development of the scaffold would be necessary in order to produce activities in the nanomolar concentration range. Optimization of the eastern portion of the molecule appeared complete, and thus focus was turned to the western half for the remainder of the project. It was also desired at this point to remove the liabilites associated with the quinone moiety, while attempting to maintain a physiological profile similar to the 1,4-naphthoquinone scaffold. In order to accomplish this effectively, it was necessary to first determine the mode of binding for this class of compounds. This was achieved through computational analysis, utilizing the AutoDock program, and confirmed through Western Blot analyses.

A recent paper by Park and co-workers described a novel class of *N*-terminal Hsp90 inhibitors isolated through structure-based virtual screening.[20] These quinazolinones bear a striking resemblance to our first two libraries of compounds (Figure 3), and thus became an intellectual lead for development of a hypothesis regarding 1,4-naphthoquinone binding and inhibition.

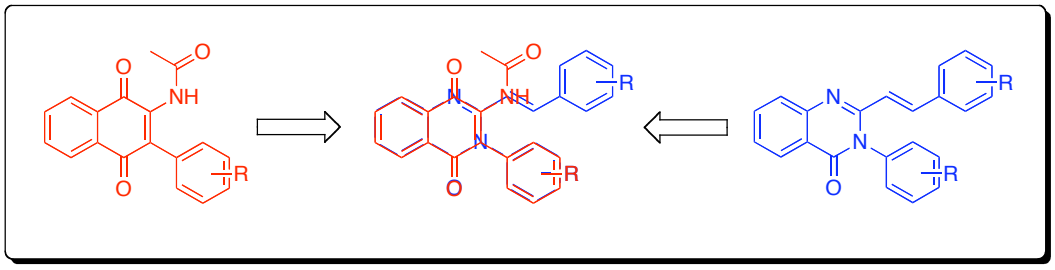

Figure 3. Overlay of the 1,4-naphthoquinone nad quinazolinone scaffolds.

The AutoDock program was used to simulate binding of compound **10d** to the *N*-terminal of Hsp90, using the same parameters and scoring function as those described in the paper by Park and co-workers. From the analysis, the lowest-scoring molecular solvation free energy conformation was determined (-13.16 kcal/mol, Figure 4a). An overlay of the two compounds indicated a correlative mode of binding (Figure 4b), justifying biological evaluation through Western Blot analyses.

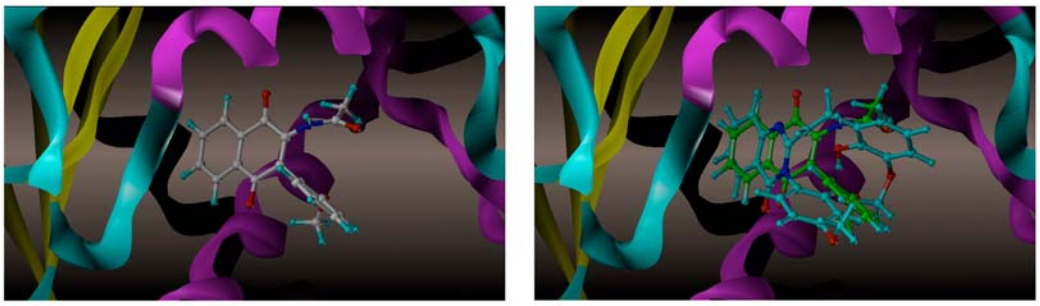

Figure 4. (a) Docking of **10d** in the ATP-binding pocket of Hsp90. (b) Overlay of **10d** and a quinazolinone in the ATP-binding pocket of Hsp90.

As discussed previously, each class of Hsp90 inhibitors renders a unique physiological profile, differentiable through Western Blot Analyses. In this case, compounds **10c** and **10d** each induced concentration-dependent upregulation of Hsp90, as well as concentration-dependent degradation of Her2, a known client protein of Hsp90 (Figure 5). This trend is a clear hallmark of *N*-terminal Hsp90 inhibition.

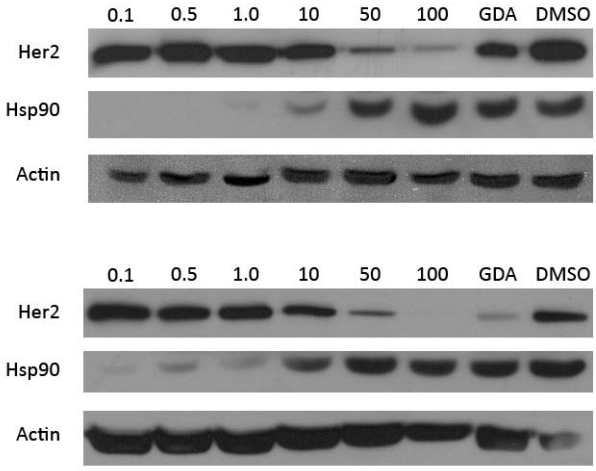

Figure 5. Western Blot analysis of protein lysates following exposure to **10c** (top) and **10d** (bottom) in MCF-7 cells (μM). Geldanamycin (500 nM) was used as a positive control.

Design of Flavone Analogues

Once a mode of binding had been established for the 1,4-naphthoquinone scaffold, it was necessary to return to the docking model for further analysis. Specific residue interactions were assigned by using SYBYL 7.0 to calculate the intermolecular distance between the ligand **10d** and specific amino acid residues

in the *N*-terminal crystal structure. Intermolecular distances of less than 3.5 Å were considered significant for potential hydrogen or halogen bonding, and Figure 6 represents a schematic drawing of proposed interactions between **10d** and the Hsp90 *N*-terminal ATP-binding site.

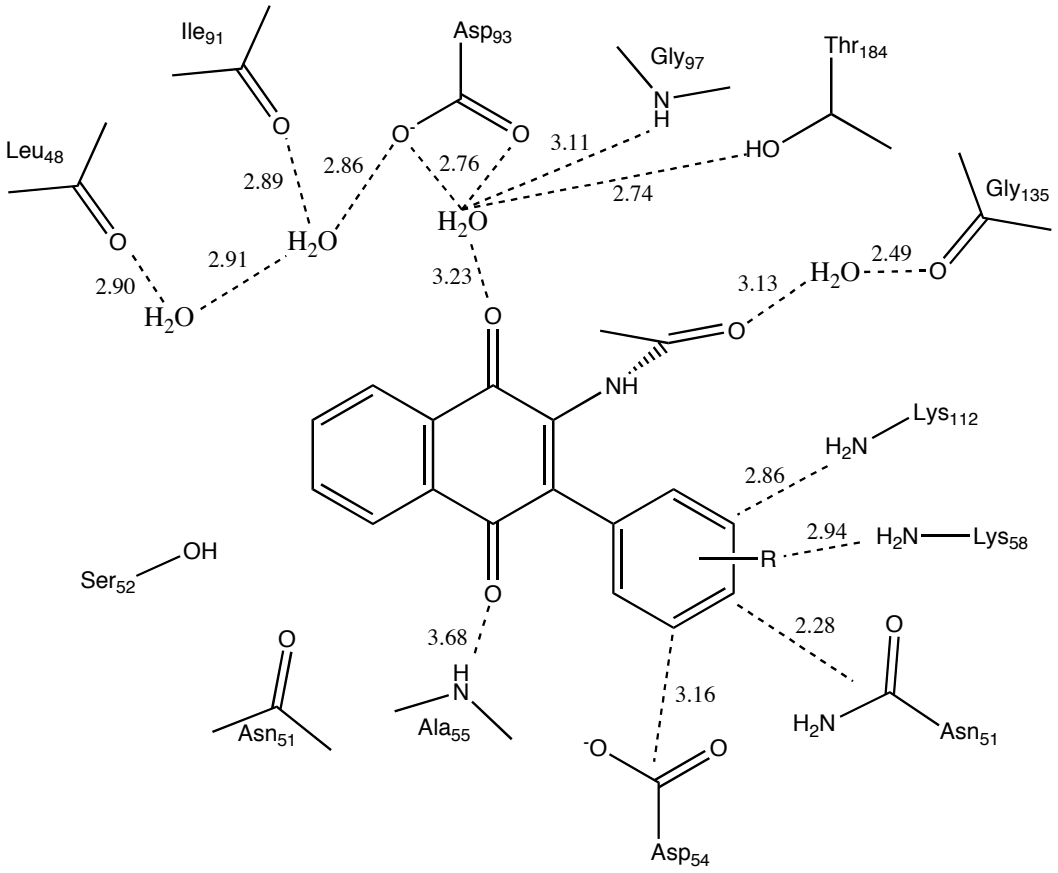

Figure 6. Proposed interactions between **10d** and the ATP-binding site of Hsp90. Hydrogen bonds are shown as dotted lines with distances given in angstroms.

Based on this analysis, key interactions appeared to exist between the C1 carbonyl and the intricate hydrogen-bonding network centered about Asp93. It should be noted that water molecules involved in this network are highly conserved in all

known co-crystal structures with *N*-terminal inhibitors, such as radicicol and geldanamycin, and are considered critical for binding.[21,22] Hydrogen-bonding interactions between the C4 carbonyl and Ala55, and between the acetamide side chain and Gly135 via a water molecule also seemed plausible. The most interesting feature to note, however, was the unusual abundance of active residues surrounding the aryl side chain at C3. A number of amino acids in this region were close enough in proximity to **10d** that a potential hydrogen or halogen bonding interaction could take place. This was in agreement with the SAR trend observed in our previous two libraries, and served as the starting point for the design of the next set of analogues.

In order to remove the quinone moiety, while maintaining the integrity of the interactions described above, a 3-acetamido-6-hydroxyflavone core was selected for analogue development. After inserting this scaffold into the previously constructed schematic, one could see that all key interactions, with the exception of that between the C4 carbonyl of the 1,4-naphthoquinone and Ala55, were conserved (Figure 7). However, with the vinylogous ester replacement, allowance of this interaction was still possible, albeit less likely, due to greater intermolecular distance.

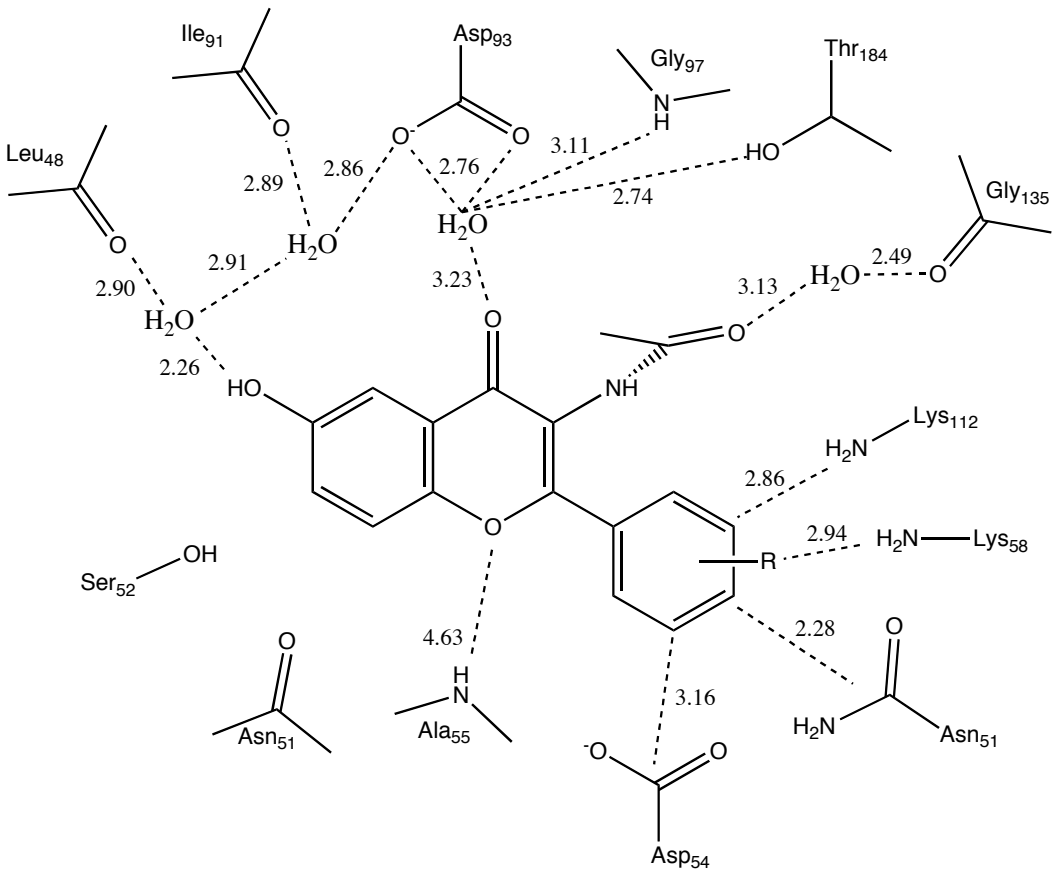

Figure 7. Proposed interactions between the newly constructed flavone scaffold and the ATP-binding site of Hsp90. Hydrogen bonds are shown as dotted lines with distances given in angstroms.

Three dimensional analysis via AutoDock indicated that installation of a phenol at the C6 position would allow for additional hydrogen bonding interactions with Leu49 via a conserved water molecule, thereby utilizing the conserved network surrounding Asp93 and potentially increasing binding affinity. With respect to the aryl side chain, extensive investigation of SAR had been established for the 1,4-naphthoquinone analogues, and six of those substitution patterns were selected for

comparison with the flavone library. This included analogues corresponding to compounds **10a**, **10c**, **10d**, **10h**, and **10i**, as well as an unsubstituted aryl ring. Due to synthetic barriers, which will be discussed in the next section, a 2′-methoxy substituent was placed in lieu of a 2′-ethoxy substituent to create an analogue corresponding to **10d**.

Synthesis of Flavone Analogues.

Flavones **17a**–**17f** were prepared through a traditional approach, beginning with esterification of 2-hydroxy-5-methoxymethoxyacetophenone **11** and the appropriate benzoyl chloride to give compounds **12a–12d** in good yield (Scheme 2). Subsequent base-mediated isomerization via a Baker–Venkataraman rearrangement afforded the corresponding 1,3-diketones, **13a–13d**.[23,24]

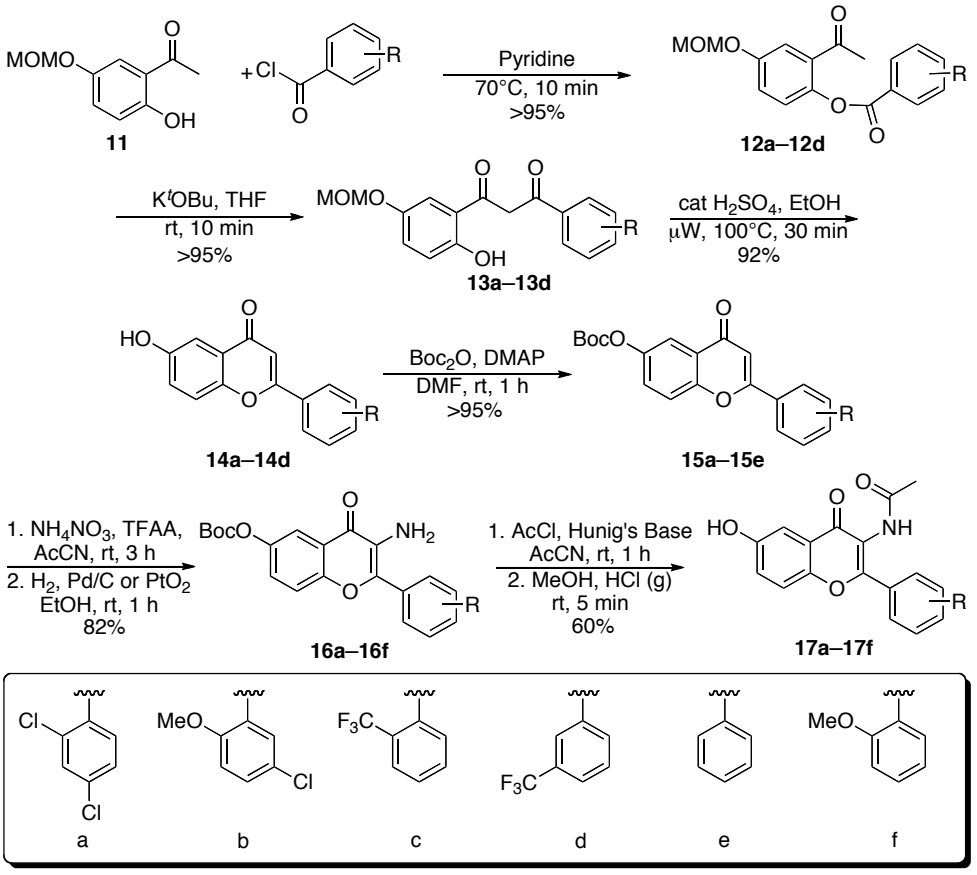

Scheme 2. Synthesis of flavone analogues.

Microwave-assisted cyclization yielded flavones **14a–14d**, which were then Boc-protected to give compounds **15a–15d**.[25] Commercially available 6-hydroxyflavone was also submitted to Boc-protection to give compound **15e**.

Initial attempts toward installation of the acetamide side chain involved a 3-bromo flavone intermediate that was prepared via bromination of compounds **15a–15e** using N-bromosuccinimide as a source of electrophilic bromine. The Boc protecting group installed in the preceding step allowed for selective

electrophilic addition, generating products in moderate yield. This approach was quickly rescinded, however, when it was determined that the α-bromo intermediate was completely inactive towards rudimentary S_N^2Ar chemistry, as well as traditional coupling techniques, such as Ullman[26] or Buchwald–Hartwig[27] conditions. This was likely due to poor electrophilicity at the C3 carbon, as it was positioned alpha to the carbonyl of a vinylogous ester. To overcome this obstacle, selective α-nitration of the Boc-protected flavones **15a–15e** was performed under mild conditions, enlisting trifluoroacetic acid anhydride and ammonium nitrate to afford the intermediate Boc-protected 3-nitroflavones. Reduction of the nitro group using 10% wt/wt Pd/C under a hydrogen atmosphere afforded anilines **16a** and **16c–16d**. It was determined that reduction of the α-nitrated 2′-methoxy-5′-chloro-flavone intermediate under the given conditions resulted in undesired dehalogenation, and thus, milder conditions utilizing a PtO_2 catalyst were necessary to acquire compound **16b**.[28] Serendipitously, the latter technique provided a route to α-aminated 2′-alkoxy flavones that were previously unattainable using the presented approach, due to their *ortho*- and *para*-directed activation of the aryl side chain during nitration. This observation was therefore exploited to synthesize compound **16f** in moderate yield. In the final step, N-acetylation followed by Boc deprotection afforded the final products, **17a–17f**.

Evaluation of Flavone Analogues

Table 5. Growth inhibitory activities of flavone analogues[a].

Compound	IC_{50} (SKBr3)	IC_{50} (MCF-7)
17a	9.8 ± 0.6	9.4 ± 0.3
17b	16 ± 1	19 ± 2
17c	38 ± 4	24 ± 1
17d	45 ± 4	>100
17e	>100	>100
17f	>100	>100

[a]All values are in units of μM, and represent ± standard error for two separate experiments performed in triplicate

The data shown in Table 5 represent growth inhibitory activities of flavone analogues **17a–17f** against SKBr3 and MCF-7 breast cancer cell lines. Upon inspection, it became immediately apparent that the activities of the flavone analogues were not as desirable as those of the 1,4-naphthoquinones. However, the data did provide intricate SAR. In this case, the most active component of the library was compound **17a**, which contained a 2′,4′-dichlorophenyl side chain and exhibited a 9 μM IC_{50} concentration against both cell lines. Moderate to low activity in both cell lines was also observed for compounds **17b** and **17c**, as well as compound **17d** (SKBr3 cells only). Although this library was small, the data suggests that halogen bonding is associated with the binding interactions, as each of the active compounds **17a**–**17d** possess halogen-containing substituents. This is reinforced through comparison of compounds **17b** and **17f**, wherein complete loss in activity was observed upon removal of the 5′-chloro substituent, and also

through compound **17e**, wherein lack of aryl substitution resulted in a complete loss of activity.

Initially, it was perceived that this activity was associated with the electron-withdrawing properties of the aryl substituents in compounds **17a**–**17f**. However, one would expect that the trifluoromethyl-substituted compounds would display a higher binding affinity, and thus improved activity versus the corresponding chloro-substituted species, which was not observed. If the hypothesis is correct, then *para*- and *ortho*- halogen substitution is favored over *meta*-, as observed when comparing compound **17a** to **17b** and compound **17c** to **17d**. Furthermore, as fluorine is not usually associated with halogen bonding, it is more likely that the trifluoromethyl group is actually involved in hydrogen-bonding interactions.[29]

Western Blot analyses confirmed that compounds **17a** and **17b** induced a concentration-dependent heat shock response that reciprocated their cytotoxicity profile (Figure 8). As previously discussed, this is a property associated with anti-proliferative *N*-terminal inhibition of Hsp90. However, to our surprise the corresponding concentration-dependent degradation of client proteins was not observed. Typically, a lysate profile of this nature is associated with neuroprotective inhibitors of Hsp90. However, whereas the nueroprotective inhibitors are non-toxic, this scaffold clearly exhibits toxicity, and as such suggests a physiological profile previously unidentified for Hsp90 modulators.

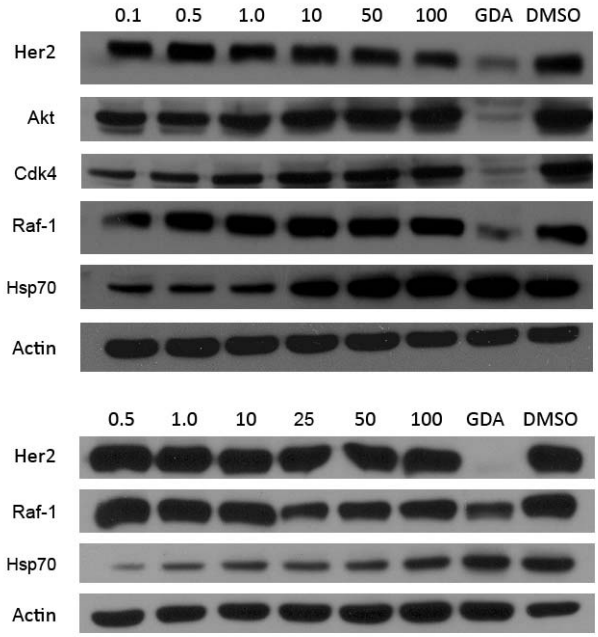

Figure 8. Western Blot analysis of protein lysates following exposure to **17a** (top) and **17b** (bottom) in MCF-7 cells.

In light of this observation, it is unclear how these compounds induce Hsp expression and cell death without induction of client protein degredation. As a result, further biological investigation will be required to elucidate the mechanism of action manifested by these compounds.

III. Conclusions

As Hsp90 continues to emerge as a promising target for the treatment of cancer, neurodegenerative diseases, and other disease states, the construction of viable inhibitors with drug-like properties will become increasingly more

important. Using traditional chemical, biological, and computational techniques, two novel scaffolds were developed, and their mode of action probed. Where it was apparent that the 1,4-naphthoquinone scaffold inhibits Hsp90 via the *N*-terminus, the corresponding flavone scaffold exhibits a unique set of biological properties, making determination of its mechanism of action unclear at present. Additional studies will be needed to further understand the attributes possessed by the scaffolds, and perhaps, the intricate mechanism of Hsp90 modulation.

IV. Experimental Section

General Methods

Unless otherwise indicated, all reagents were purchased from commercial suppliers and were used without further purification. All stir bars and glassware were flame-dried, and glassware was flushed with argon immediately prior to use. The ^{1}H and ^{13}C NMR spectra were recorded at 500 and 125 MHz, respectively, on a Bruker DRX 500 using the indicated solvents, δ in ppm, and *J* (Hz) assignments of resonance coupling. Column chromatography was performed with silica gel (40–63 μm particle size) from Sorbent Technologies (Atlanta, GA). Analytical HPLC was carried out on an Agilent 1100 series capillary HPLC system with diode array detection at 209 nm (naphthoquinones) or 254 nm (flavones) on a Phenomenex Luna C18 column (10 x 250 mm, 5 μm) with isocratic elution in 60% acetonitrile and 40% H_2O at a flow rate of 5.0 mL/min.

CoMFA Models and *in silico* Analysis (AutoDock)

A training set of 31 compounds was compiled from a paper by Hadden and co-workers.[1] The biological data (IC_{50} values: drug concentration in μM) were obtained through methods described below, and converted into pIC_{50} ($-\log IC_{50}$) values. This data was used as an independent variable in the CoMFA analyses. Molecular structures were built using SYBYL 7.0 on a Silicon Graphics 02 workstation under the IRIX Release 6.5 operating system, and energy minimizations were performed using the Tripos force field utilizing a distance-dependent dielectric function. After minimization, manual manipulation of the amide bond, followed by minimization with limited convergence criterion (NB cutoff set to 1.0 Å), was performed to provide both a *cis* and *trans* amide library.

Atomic charges were calculated using Gasteiger-Marsili methodology. Molecular alignment of each amide library was performed using the database alignment feature of SYBYL 7.0, using the Hadden compound **1a** and the core naphthoquinone scaffold as a reference. CoMFA models were constructed based on electrostatic and hydrophobic field energies calculated through SYBYL (default settings) and the Tripos force field. All grid point calculations were completed using an sp^3 hybridized carbon atom with a +1.0 charge and a van der Waals radius of 1.52 Å as a probe.

3D-QSAR models were derived with SYBYL through a partial least squares regression, where pIC_{50} was the dependent variable, and the calculated

CoMFA parameters were the independent variables. These models were confirmed through a leave one out cross-validation technique, where specific compounds were either removed or region-focused to offer the highest possible q^2 value. Non-cross-validation was used to reinforce this, sighting r^2 for accuracy. Upon validation, each model was used to predict pIC_{50} values in the development of the naphthoquinones described in this paper.

The AutoDock program was used to simulate binding of compound **10d** to the *N*-terminal of Hsp90. The coordinates in the co-crystal structure of Hsp90 and a benzenesulfonamide inhibitor (PBD: 2BZ5) were used for the receptor molecule, while the energy-minimized structure generated from the previous CoMFA study was selected for **10d**. During the simulation, the default AutoDock scoring function was used,[19] incorporating van der Waals, hydrogen bonding, and electrostatic interactions, as well as torsional and ligand desolvation factors. From the resulting analysis, the lowest-scoring molecular solvation free energy conformation was selected for each ligand. Protein-ligand hydrogen bonding interactions were determined through a 3D analysis of the model, wherein intermolecular distances of less than 3.5 Å were considered significant for potential hydrogen bonding interactions. Overlay of the protein-ligand complex and CoMFA was achieved by introducing both models of compound **10d** into the same molecular area, and using the Match algorithm associated with SYBYL 7.0.

Analogue Synthesis

***N*-(3-Chloro-1,4-dioxo-1,4-dihydronaphthalen-2-yl)acetamide (9)**. 2-Amino-3-chloro-1,4-naphthoquinone (**8**, 5.000 g, 24.08 mmol) was dissolved in acetyl chloride (150 mL) and stirred at rt. A catalytic amount of concentrated sulfuric acid (625 μL) was added at rt. The solution heated to reflux and stirred for 3 h. The solvent was removed, and the residue was partitioned between EtOAc (200 mL) and H_2O (200 mL). The organic layer was washed with saturated aqueous sodium chloride (2 x 200 mL), dried (Na_2SO_4), filtered, and concentrated in vacuo. The residue was purified by column chromatography (SiO_2, 20:3 hexanes:EtOAc, then 20:9 hexanes:EtOAc) to afford **9** (1.25 g, 18%) as a yellow amorphous solid: ^{1}H NMR (DMSO-d_6, 500 MHz) δ 8.06 (m, 1H), 8.02 (m, 1H), 7.89 (m, 2H), 2.13 (s, 3H); ^{13}C NMR (DMSO-d_6, 125 MHz) δ 178.8, 177.6, 168.0, 141.3, 134.55, 134.52, 131.0, 130.8, 126.7, 126.6 (2C); IR (film) ν_{max} 3310, 3250, 2359, 2341, 1711, 1693, 1661, 1609, 1587, 1479, 1456, 1427, 1375, 1327, 1312, 1294, 1254, 1223, 1198, 1169, 1126, 1051, 1038, 1022, 986, 964 cm^{-1}; HRMS(ES$^+$) *m/z*: [M+H] calcd for $C_{12}H_8NO_3Cl$ 250.0271; found 250.0275.

***N*-(3-(2,4-Dichlorophenyl)-1,4-dioxo-1,4-dihydronaphthalen-2-yl)acetamide (10a)**. A solution of **9** (20.0 mg, 0.068 mmol) and tetrakis(triphenylphosphine)palladium(0) (6 mol%, 4.75 mg, 4.11 μmol) in THF:2M K_2CO_3 (10:1, 4.4 mL) stirred at rt for 30 min. 2,4-Dichlorophenyl boronic acid (39.19 mg, 0.21 mmol) was added and the solution stirred for 30 min

at rt, then heated to reflux 15 hr. The solution was cooled, filtered through celite, and diluted with EtOAc (50 mL). The organic layer was washed with H_2O (50 mL) and saturated aqueous sodium chloride (50 mL), dried (Na_2SO_4), filtered, and concentrated. The residue was purified by column chromatography (SiO_2, 20:1 hexanes:EtOAc) to afford **10a** (14.8 mg, 60%) as a yellow amorphous solid: ^{1}H NMR ($CDCl_3$, 500 MHz) δ 8.16 (m, 2H), 7.98 (bs, N-H), 7.79 (m, 2H), 7.48 (d, *J* = 2.1 Hz, 1H), 7.31 (dd, *J* = 8.3, 2.1 Hz, 1H), 7.19 (d, *J* = 8.3 Hz, 1H), 2.07 (s, 3H); ^{13}C NMR ($CDCl_3$, 125 MHz) δ 182.2, 181.9, 166.5, 138.3, 134.9, 134.0, 133.7, 132.2, 131.6, 130.9, 130.2, 129.4, 127.2, 126.7, 126.5 24.1; IR (film) ν_{max} 3292, 1701, 1668, 1618, 1587, 1555, 1491, 1472, 1425, 1369, 1329, 1294, 1236, 1205, 1188, 1159, 1144, 1101, 1059, 1041, 1013, 987, 974, 943 cm^{-1}; HRMS(ES^+) *m/z*: [M+H] calcd for $C_{18}H_{11}NO_3Cl_2$ 360.0194; found 360.0182.

***N*-(3-(2,5-Dichlorophenyl)-1,4-dioxo-1,4-dihydronaphthalen-2-yl)acetamide (10b)**. A solution of **9** (20.0 mg, 0.068 mmol) and tetrakis(triphenylphosphine)palladium(0) (4 mol%, 3.17 mg, 2.74 μmol) in THF:2M K_2CO_3 (10:1, 4.4 mL) stirred at rt for 30 min. 2,5-Dichlorophenyl boronic acid (32.66 mg, 0.17 mmol) was added and the solution stirred for 30 min at rt, then heated to reflux for 15 hr. The solution was cooled, filtered through celite, and diluted with EtOAc (50 mL). The organic layer was washed with H_2O (50 mL) and saturated aqueous sodium chloride (50 mL), dried (Na_2SO_4), filtered, and concentrated. The residue was purified by column chromatography (SiO_2,

20:1 hexanes:EtOAc) to afford **10b** (12.6 mg, 51%) as a yellow amorphous solid: ^{1}H NMR ($CDCl_3$, 500 MHz) δ 8.17 (m, 2H), 8.00 (bs, N-H), 7.79 (m, 2H), 7.41 (d, *J* = 8.6 Hz, 1H), 7.29 (dd, *J* = 8.6, 2.5 Hz, 1H), 7.21 (d, *J* = 2.5 Hz, 1H), 2.08 (s, 3H); ^{13}C NMR ($CDCl_3$, 125 MHz) δ 181.90, 181.88, 166.5, 138.2, 135.1, 134.8, 133.7, 132.2, 132.1, 132.0, 130.5, 130.4, 130.1, 130.0, 127.2, 126.6 (2C), 24.2; IR (film) ν_{max} 3290, 2922, 2851, 1668, 1618, 1593, 1493, 1464, 1383, 1294, 1234, 1205, 1159, 1097, 1041, 1016 cm^{-1}; HRMS(ES^+) *m/z*: [M+H] calcd for $C_{18}H_{11}NO_3Cl_2$ 360.0194; found 360.0197.

***N*-(3-(5-Chloro-2-methoxyphenyl)-1,4-dioxo-1,4-dihydronaphthalen-2-yl)acetamide (10c)**. A solution of **9** (20.0 mg, 0.068 mmol) and tetrakis(triphenylphosphine)palladium(0) (4 mol%, 3.17 mg, 2.74 μmol) in THF:2M K_2CO_3 (10:1, 4.4 mL) stirred at rt for 30 min. 5-Chloro-2-methoxyphenyl boronic acid (25.52 mg, 0.14 mmol) was added and the solution stirred for 30 min at rt, then heated to reflux for 15 hr. The solution was cooled, filtered through celite, and diluted with EtOAc (50 mL). The organic layer was washed with H_2O (50 mL) and saturated aqueous sodium chloride (50 mL), dried (Na_2SO_4), filtered, and concentrated. The residue was purified by column chromatography (SiO_2, 9:1 hexanes:EtOAc) to afford **10c** (22.1 mg, 91%) as a yellow–orange amorphous solid: ^{1}H NMR ($CDCl_3$, 500 MHz) δ 8.13 (d, *J* = 7.25 Hz, 2H), 7.82 (bs, N-H), 7.76 (m, 2H), 7.31 (dd, *J* = 8.9, 2.6 Hz, 1H), 7.05 (d, *J* = 2.6 Hz, 1H), 6.95 (d, *J* = 8.9 Hz, 1H), 3.84 (s, 3H), 2.05 (s, 3H); ^{13}C NMR

($CDCl_3$, 125 MHz) δ 182.2, 181.8, 166.9, 155.7, 138.5, 134.6, 133.4, 132.4, 132.0, 130.4, 129.9, 128.7, 127.0, 126.4, 125.2, 124.6, 112.6, 56.3, 24.0; IR (film) ν_{max} 3292, 3070, 2959, 2935, 2849, 1693, 1666, 1618, 1593, 1487, 1441, 1396, 1369, 1339, 1294, 1269, 1250, 1202, 1180, 1159, 1142, 1111, 1016 cm^{-1}; HRMS(ES^+) *m/z*: [M+H] calcd for $C_{19}H_{14}NO_4Cl$ 356.0690; found 356.0687.

***N*-(3-(2-Ethoxyphenyl)-1,4-dioxo-1,4-dihydronaphthalen-2-yl)acetamide (10d)**. A solution of **9** (20.0 mg, 0.068 mmol) and tetrakis(triphenylphosphine)palladium(0) (4 mol%, 3.17 mg, 2.74 μmol) in THF:2M K_2CO_3 (10:1, 4.4 mL) stirred at rt for 30 min. 2-Ethoxyphenyl boronic acid (22.72 mg, 0.14 mmol) was added and the solution stirred for 30 min at rt, then heated to reflux for 15 hr. The solution was cooled, filtered through celite, and diluted with EtOAc (50 mL). The organic layer was washed with H_2O (50 mL) and saturated aqueous sodium chloride (50 mL), dried (Na_2SO_4), filtered, and concentrated. The residue was purified by column chromatography (SiO_2, 9:1 hexanes:EtOAc) to afford **10d** (19.1 mg, 83%) as an orange amorphous solid: ^1H NMR ($CDCl_3$, 500 MHz) δ 8.15 (m, 2H), 7.75 (m, 2H), 7.65 (bs, N-H), 7.38 (dt, *J* = 7.9, 1.7 Hz, 1H), 7.16 (dd, *J* = 7.9, 1.8 Hz, 1H), 7.02 (t, *J* = 7.8 Hz, 2H), 4.17 (m, 1H), 4.05 (m, 1H), 2.02 (s, 3H), 1.31 (t, *J* = 7.0 Hz); ^{13}C NMR ($CDCl_3$, 125 MHz) δ 183.1, 181.4, 167.5, 156.0, 139.2, 134.2, 133.3, 132.5, 131.1, 130.5, 130.4, 126.8, 126.4, 122.0, 120.4, 112.5, 64.4, 23.7, 14.8; IR (film) ν_{max} 3323, 3304, 3285, 3246, 3186, 3067, 2978, 2928, 2361, 2343, 1664, 1616, 1597, 1578,

1491, 1475, 1448, 1420, 1387, 1367, 1344, 1327, 1296, 1286, 1269, 1246, 1202, 1159, 1122, 1109, 1088, 1043, 1013, 989, 970, 922, 905 cm^{-1}; HRMS(ES^+) *m/z*: [M+H] calcd for $C_{20}H_{17}NO_4$ 336.1236; found 336.1249.

***N*-(3-(2,3-Dimethoxyphenyl)-1,4-dioxo-1,4-dihydronaphthalen-2-yl)acetamide (10e)**. A solution of **9** (20.0 mg, 0.068 mmol) and tetrakis(triphenylphosphine)palladium(0) (6 mol%, 4.75 mg, 4.11 μmol) in THF:2M K_2CO_3 (10:1, 4.4 mL) stirred at rt for 30 min. 2,3-Dimethoxyphenyl boronic acid (37.38 mg, 0.21 mmol) was added and the solution stirred for 30 min at rt, then heated to reflux for 15 hr. The solution was cooled, filtered through celite, and diluted with EtOAc (50 mL). The organic layer was washed with H_2O (50 mL) and saturated aqueous sodium chloride (50 mL), dried (Na_2SO_4), filtered, and concentrated. The residue was purified by column chromatography (SiO_2, 20:1 hexanes:EtOAc) to afford **10e** (22.8 mg, 95%) as a yellow amorphous solid: ^{1}H NMR ($CDCl_3$, 500 MHz) δ 8.16 (m, 2H), 7.77 (m, 2H), 7.71 (bs, N-H), 7.13 (t, *J* = 8.0 Hz, 1H), 7.00 (dd, *J* = 8.2, 1.4 Hz, 1H), 6.77 (dd, *J* = 7.8, 1.4 Hz, 1H), 3.92 (s, 3H), 3.79 (s, 3H), 2.05 (s, 3H); ^{13}C NMR ($CDCl_3$, 125 MHz) δ 183.6, 181.0, 167.9, 152.5, 146.3, 139.8, 134.21, 134.17, 133.6, 132.4, 131.3, 126.8, 126.6, 126.5, 123.8, 122.3, 113.2, 61.2, 55.7, 23.7; IR (film) ν_{max} 3292, 3285, 3258, 2930, 2853, 2837, 1666, 1647, 1618, 1595, 1578, 1474, 1425, 1400, 1367, 1346, 1325, 1290, 1265, 1236, 1223, 1169, 1161, 1124, 1084, 1065, 1041, 1003,

920, 906 cm^{-1}; HRMS(ES^+) *m/z*: [M+H] calcd for $C_{20}H_{17}NO_5$ 352.1185; found 352.1192.

***N*-(3-(2,4-Dimethoxyphenyl)-1,4-dioxo-1,4-dihydronaphthalen-2-yl)acetamide (10f)**. A solution of **9** (20.0 mg, 0.068 mmol) and tetrakis(triphenylphosphine)palladium(0) (4 mol%, 3.17 mg, 2.74 μmol) in THF:2M K_2CO_3 (10:1, 4.4 mL) stirred at rt for 30 min. 2,4-Dimethoxyphenyl boronic acid (24.91 mg, 0.14 mmol) was added and the solution stirred for 30 min at rt, then heated to reflux for 15 hr. The solution was cooled, filtered through celite, and diluted with EtOAc (50 mL). The organic layer was washed with H_2O (50 mL) and saturated aqueous sodium chloride (50 mL), dried (Na_2SO_4), filtered, and concentrated. The residue was purified by column chromatography (SiO_2, 5:1 hexanes:EtOAc) to afford **10f** (23.4 mg, 97%) as a red amorphous solid: ^{1}H NMR ($CDCl_3$, 500 MHz) δ 8.12 (dd, *J* = 7.0, 1.9 Hz), 7.73 (m, 2H), 7.61 (bs, N-H), 7.06 (d, *J* = 8.4 Hz), 6.56 (m, 2H), 3.84 (s, 3H), 3.83 (s, 3H), 2.02 (s, 3H); ^{13}C NMR ($CDCl_3$, 125 MHz) δ 183.2, 181.6, 161.7, 157.8, 139.0, 134.2, 134.1, 133.3, 132.5, 130.97, 130.91, 126.8, 126.3, 114.4, 104.9, 98.9, 55.9, 55.3, 23.7; IR (film) ν_{max} 3304, 3294, 3188, 3067, 3001, 2959, 2935, 2839, 1664, 1604, 1605, 1578, 1504, 1491, 1466, 1458, 1439, 1416, 1367, 1342, 1296, 1275, 1261, 1209, 1184, 1159, 1140, 1132, 1105, 1084, 1034, 1014, 989, 935, 921 cm^{-1}; HRMS(ES^+) *m/z*: [M+H] calcd for $C_{20}H_{17}NO_5$ 352.1185; found 352.1181.

***N*-(3-(2,5-Dimethoxyphenyl)-1,4-dioxo-1,4-dihydronaphthalen-2-yl)acetamide (10g)**. A solution of **9** (20.0 mg, 0.068 mmol) and tetrakis(triphenylphosphine)palladium(0) (4 mol%, 3.17 mg, 2.74 μmol) in THF:2M K_2CO_3 (10:1, 4.4 mL) stirred at rt for 30 min. 2,5-Dimethoxyphenyl boronic acid (24.91 mg, 0.14 mmol) was added and the solution stirred for 30 min at rt, then heated to reflux for 15 hr. The solution was cooled, filtered through celite, and diluted with EtOAc (50 mL). The organic layer was washed with H_2O (50 mL) and saturated aqueous sodium chloride (50 mL), dried (Na_2SO_4), filtered, and concentrated. The residue was purified by column chromatography (SiO_2, 3:1 hexanes:EtOAc) to afford **10g** (22.5 mg, 94%) as a red amorphous solid: ^{1}H NMR ($CDCl_3$, 500 MHz) δ 8.13 (m, 2H), 7.75 (m, 2H), 7.66 (bs, N-H), 6.97 (d, J = 9.0 Hz, 1H), 6.93 (dd, J = 9.0, 2.95 Hz, 1H), 6.69 (d, J = 2.95 Hz, 1H), 3.81 (s, 3H), 3.77 (s, 3H), 2.04 (s, 3H); ^{13}C NMR ($CDCl_3$, 125 MHz) δ 182.8, 181.5, 167.4, 153.3, 151.0, 139.1, 134.4, 133.8, 133.4, 132.5, 130.9, 126.9, 126.4, 122.9, 115.5, 115.3, 112.6, 56.6, 55.7, 23.8; IR (film) ν_{max} 3292, 2997, 2941, 2833, 1666, 1595, 1580, 1499, 1468, 1421, 1369, 1342, 1327, 1283, 1269, 1252, 1225, 1200, 1180, 1159, 1099, 1082, 1043, 1018, 949, 920 cm^{-1}; HRMS(ES$^+$) *m/z*: [M+H] calcd for $C_{20}H_{17}NO_5$ 352.1185; found 352.1179.

***N*-(1,4-Dioxo-3-(2-(trifluoromethyl)phenyl)-1,4-dihydronaphthalen-2-yl)acetamide (10h)**. A solution of **9** (20.0 mg, 0.068 mmol) and tetrakis(triphenylphosphine)palladium(0) (4 mol%, 3.17 mg, 2.74 μmol) in

THF:2M K_2CO_3 (10:1, 4.4 mL) stirred at rt for 30 min. 2-Trifluoromethylphenyl boronic acid (39.01 mg, 0.21 mmol) was added and the solution stirred for 30 min at rt, then heated to reflux for 15 hr. The solution was cooled, filtered through celite, and diluted with EtOAc (50 mL). The organic layer was washed with H_2O (50 mL) and saturated aqueous sodium chloride (50 mL), dried (Na_2SO_4), filtered, and concentrated. The residue was purified by column chromatography (SiO_2, 9:1 hexanes:EtOAc) to afford **10h** (15.2 mg, 62%) as a yellow amorphous solid: ^{1}H NMR ($CDCl_3$, 500 MHz) δ 8.87 (m, 2H), 7.78 (m, 2H), 7.75 (d, *J* = 7.8 Hz, 1H), 7.71 (bs, N-H), 7.59 (t, *J* = 7.6 Hz, 1H), 7.52 (t, *J* = 7.6 Hz, 1H), 7.28 (d, *J* = 7.7 Hz, 1H), 2.01 (s, 3H); ^{13}C NMR ($CDCl_3$, 125 MHz) δ 183.2, 181.8, 166.6, 137.7, 134.9, 133.9, 133.7, 132.0, 131.5, 131.1, 130.4, 128.7, 127.2, 126.6, 126.5, 125.3, 123.1, 24.0; IR (film) ν_{max} 3308, 3069, 1695, 1670, 1616, 1595, 1491, 1481, 1447, 1369, 1317, 1292, 1263, 1240, 1205, 1171, 1119, 1059, 1036, 1014, 989 cm^{-1}; HRMS(ES^+) *m/z*: [M+H] calcd for $C_{19}H_{12}NOF_3$ 360.0847; found 360.0860.

***N*-(1,4-dioxo-3-(3-(trifluoromethyl)phenyl)-1,4-dihydronaphthalen-2-yl)acetamide (10i).** A solution of **9** (20.0 mg, 0.068 mmol) and tetrakis(triphenylphosphine)palladium(0) (4 mol%, 3.17 mg, 2.74 μmol) in 4.4 mL THF:2M K_2CO_3 (10:1) stirred at rt for 30 min. 3-Trifluoromethylphenyl boronic acid (39.01 mg, 0.21 mmol) was added and the solution stirred for 30 min at rt. The solution was heated to reflux and stirred for 15 hr. The solution was cooled, filtered through celite, and diluted with EtOAc (50 mL). The EtOAc was

washed with H_2O (50 mL) and saturated aqeous sodium chloride (50 mL), dried (Na_2SO_4), filtered, and concentrated. The residue was purified by column chromatography (SiO_2, 20:1 hexanes:EtOAc) to afford **10i** (23.7 mg, 96%) as a yellow amorphous solid: ^{1}H NMR ($CDCl_3$, 500 MHz) δ 8.16 (m, 2H), 7.92 (bs, N-H), 7.79 (m, 2H), 7.60 (m, 4H) 2.01 (s, 3H); ^{13}C NMR ($CDCl_3$, 125 MHz) δ 182.9, 182.2, 166.2, 137.3, 135.0, 134.4, 133.7, 133.3, 132.5, 132.1, 130.3, 130.1, 128.4, 127.1, 126.4, 126.4, 125.2, 125.0, 24.0; IR (film) ν_{max} 3000, 1695, 1666, 1595, 1477, 1458, 1431, 1371, 1342, 1325, 1294, 1269, 1236, 1205, 1167, 1124, 1097, 1072, 1045, 1018 cm^{-1}; HRMS(ES$^+$) *m/z*: [M+H] calcd for $C_{19}H_{12}NOF_3$ 360.0847; found 360.0848.

1-(2-Hydroxy-5-(methoxymethoxy)phenyl)ethanone (11). 2',5'-Dihydroxyacetophenone (5.000 g, 32.86 mmol) and triethylamine (5.50 mL, 39.43 mmol) were dissolved in THF (100 mL) and stirred at rt. Methoxymethyl chloride (6.26M in MeOH, 10.50 mL, 65.72 mmol) was added dropwise, and the solution subsequently stirred at reflux for 48 h. The solution was quenched with H_2O (100 mL), and the aqueous layer was then extracted with EtOAc (3 x 50 mL). The combined organic layers were washed with saturated aqueous $NaHCO_3$ and saturated aqueous NaCl, dried (Na_2SO_4), filtered, and concentrated. The residue was purified by flash chromatography (SiO_2,9:1Hexanes:EtOAc) to afford **11** (6.447 g, 80%) as a yellow oil: ^{1}H NMR ($CDCl_3$, 500 MHz) δ 11.92 (s, 1H), 7.38 (d, *J* = 2.95 Hz, 1H), 7.21 (dd, *J* = 9.05 Hz, 2.95 Hz, 1H), 6.90 (d, *J* = 9.05

Hz, 1H), 5.12 (s, 2H), 3.49 (s, 3H), 2.61 (s, 3H); ^{13}C NMR ($CDCl_3$, 125 MHz) δ 204.1, 157.5, 149.2, 126.3, 119.2, 119.1, 117.0, 95.4, 55.9, 26.7; IR (film) ν_{max} 3254, 3045, 2997, 2955, 2903, 2847, 2827, 2789, 1645, 1620, 1585, 1485, 1427, 1404, 1367, 1321, 1288, 1248, 1211, 1192, 1153, 1080, 1011, 962, 922 cm^{-1}; HRMS(ES$^+$) *m/z*: [M+H] calcd for $C_{10}H_{12}O_4$ 196.0736; found 197.0781.

2-Acetyl-4-(methoxymethoxy)phenyl 2,4-dichlorobenzoate (12a). Compound **11** (1.000 g, 5.10 mmol) was dissolved in pyridine (1.5 mL) and stirred at rt. 2,4-Dichlorobenzoyl chloride (0.78 mL, 5.61 mmol) was added dropwise, and the solution stirred for 10 min at 75ºC. The solution was poured into 3M HCl (6 mL) at 0ºC, and the aqueous layer was extracted with EtOAc. The combined organic layers were dried (Na_2SO_4), filtered, and concentrated. The residue was purified by flash chromatography (SiO_2, 17:3 Hexanes:EtOAc to 1:1 Hexanes:EtOAc) to afford **12a** (1.78 g, 94%) as a pale yellow amorphous solid: ^{1}H NMR ($CDCl_3$, 500 MHz) δ 8.13 (d, *J* = 8.4 Hz, 1H), 7.54 (d, *J* = 2.0 Hz, 1H), 7.51 (d, *J* = 2.95 Hz, 1H), 7.40 (dd, *J* = 8.4, 2.0 Hz, 1H), 7.27 (dd, *J* = 8.8, 2.95 Hz, 1H), 7.16 (d, *J* = 8.8 Hz, 1H), 5.22 (s, 2H), 3.50 (s, 3H), 2.54 (s, 3H); ^{13}C NMR ($CDCl_3$, 125 MHz) δ 197.1, 163.3, 155.0, 142.8, 139.0, 135.5, 133.2, 131.1 (2C), 127.3, 127.2, 124.7, 120.9, 117.9, 94.6, 56.1, 29.1; IR (film) ν_{max} 3094, 2957, 2934, 2905, 2827, 1751, 1690, 1583, 1556, 1489, 1472, 1441, 1418, 1404, 1377, 1358, 1315, 1273, 1238, 1204, 1184, 1153, 1088, 1034, 1003, 922 cm^{-1}; HRMS(ES$^+$) *m/z*: [M+H] calcd for $C_{17}H_{14}Cl_2O_5$ 369.0297; found 369.0284.

2-Acetyl-4-(methoxymethoxy)phenyl 5-chloro-2-methoxybenzoate (12b). Compound **11** (1.000 g, 5.10 mmol) was dissolved in pyridine (1.5 mL) and stirred at rt. 5-Chloro-2-Methoxybenzoyl chloride (0.77 mL, 5.61 mmol) was added dropwise, and the solution stirred for 10 min at 75ºC. The solution was poured into 3M HCl (6 mL) at 0ºC, and the aqueous layer was extracted with EtOAc. The combined organic layers were dried (Na_2SO_4), filtered, and concentrated. The residue was purified by flash chromatography (SiO_2, 4:1 Hexanes:EtOAc to 3:2 Hexanes:EtOAc) to afford **12b** (1.36 g, 73%) as a pale yellow amorphous solid: ^{1}H NMR ($CDCl_3$, 500 MHz) δ 8.06 (d, *J* = 2.75 Hz, 1H), 7.51 (dd, *J* = 8.9, 2.75 Hz, 1H), 7.49 (d, *J* = 3.0 Hz, 1H), 7.24 (dd, *J* = 8.8, 3.0 Hz, 1H), 7.13 (d, *J* = 8.8 Hz, 1H), 6.98 (d, *J* = 8.9 Hz, 1H), 5.22 (s, 2H), 3.92 (s, 3H), 3.51 (s, 3H), 2.55 (s, 3H); ^{13}C NMR ($CDCl_3$, 125 MHz) δ 197.3, 163.3, 158.5, 154.9, 143.3, 134.1, 132.0, 131.7, 125.3, 124.8, 120.9, 119.8, 117.4, 113.5, 94.67, 56.3, 56.1, 29.5; IR (film) ν_{max} 3111, 3080, 3001, 2943, 2905, 2845, 2341, 1751, 1718, 1690, 1599, 1576, 1489, 1464, 1441, 1400, 1358, 1296, 1275, 1259, 1223, 1204, 1180, 1153, 1111, 1080, 1040, 1003, 922 cm^{-1}; HRMS(ES$^+$) *m/z*: [M+Na] calcd for $C_{18}H_{17}ClO_6$ 387.0611; found 387.0602.

2-Acetyl-4-(methoxymethoxy)phenyl 2-(trifluoromethyl)benzoate (12c). Compound **11** (0.486, 2.48 mmol) was dissolved in pyridine (0.75 mL) and stirred at rt. 2-Trifluoromethylbenzoyl chloride (0.40 mL, 2.72 mmol) was added dropwise, and the solution stirred for 10 min at 75ºC. The solution was poured

into 3M HCl (6 mL) at 0ºC, and the aqueous layer was extracted with EtOAc. The combined organic layers were dried (Na_2SO_4), filtered, and concentrated. The residue was purified by flash chromatography (SiO_2, 9:1 Hexanes:EtOAc to 1:1 Hexanes:EtOAc) to afford **12c** (0.91 g, 100%) as a pale yellow amorphous solid: ^{1}H NMR ($CDCl_3$, 500 MHz) δ 8.16 (d, *J* = 7.35 Hz, 1H), 7.81 (d, *J* = 7.50 Hz, 1H), 7.72 (t, *J* = 7.35 Hz, 1H), 7.67 (t, *J* = 7.50 Hz, 1H), 7.51 (d, *J* = 2.9 Hz, 1H), 7.28 (dd, *J* = 8.8, 3.0 Hz, 1H), 7.18 (d, *J* = 8.8 Hz, 1H), 5.22 (s, 2H), 3.50 (s, 3H), 2.55 (s, 3H); ^{13}C NMR ($CDCl_3$, 125 MHz) δ 197.2, 165.2, 155.1, 142.9, 132.0, 131.6, 131.4, 130.7, 126.74, 126.70, 126.65, 126.61, 124.4, 121.1, 117.8, 94.7, 56.1, 29.2; IR (film) ν_{max} 3498, 3366, 3080, 3051, 3001, 2959, 2937, 2907, 2851, 2829, 2791, 2073, 1998, 1961, 1890, 1846, 1809, 1755, 1693, 1605, 1578, 1487, 1450, 1418, 1404, 1358, 1315, 1277, 1258, 1219, 1204, 1169, 1153, 1084, 1043, 1032, 1003, 924 cm^{-1}; HRMS(ES$^+$) *m/z*: [M+Na] calcd for $C_{18}H_{15}F_3O_5$ 391.0769; found 391.0767.

2-Acetyl-4-(methoxymethoxy)phenyl 3-(trifluoromethyl)benzoate (12d). Compound **11** (4.5 g, 22.94 mmol) was dissolved in pyridine (6.75 mL) and stirred at rt. 3-Trifluorobenzoyl chloride (3.73 mL, 25.23 mmol) was added dropwise, and the solution stirred for 10 min at 75ºC. The solution was poured into 3M HCl (12 mL) at 0ºC, and the aqueous layer was extracted with EtOAc. The combined organic layers were dried (Na_2SO_4), filtered, and concentrated. The residue was purified by flash chromatography (SiO_2, 9:1 Hexanes:EtOAc) to

afford **12d** (8.45 g, 99%) as a pale yellow oil: ^{1}H NMR ($CDCl_3$, 500 MHz) δ 8.47 (s, 1H), 8.39 (d, *J* = 7.85 Hz, 1H), 7.90 (d, *J* = 7.85 Hz, 1H), 7.68 (t, *J* = 7.85 Hz, 1H), 7.53 (d, *J* = 3.0 Hz, 1H), 7.28 (dd, *J* = 8.8, 3.0 Hz, 1H), 7.15 (d, *J* = 8.8 Hz, 1H); ^{13}C NMR ($CDCl_3$, 125 MHz) δ 197.0, 164.3, 155.1, 143.1, 133.4, 131.2, 130.19, 130.14, 130.12, 129.3, 127.1, 127.08, 124.7, 121.0, 117.8, 94.7, 56.1, 29.3; IR (film) ν_{max} 3472, 3363, 3078, 2959, 2939, 2907, 2829, 2789, 2359, 2341, 2332, 1747, 1732, 1693, 1682, 1614, 1576, 1495, 1487, 1443, 1418, 1404, 1360, 1337, 1317, 1296, 1242, 1205, 1173, 1153, 1126, 1070, 1001, 922 cm^{-1}; HRMS(ES^{+}) *m/z*: [M+H] calcd for $C_{18}H_{15}F_3O_5$ 369.0950; found 369.0947.

1-(2,4-Dichlorophenyl)-3-(2-hydroxy-5-(methoxymethoxy)phenyl)propane-1,3-dione (13a). Compound **12a** (1.7 g, 4.50 mmol) was dissolved in THF (45 mL) and stirred at rt. Potassium *tert*-butoxide (0.61 g, 5.40 mmol) was added, and the solution stirred for 10 min at rt. The solution was poured into 3M HCl (90 mL) at 0ºC, and the aqueous layer was extracted with EtOAc. The combined organic layers were dried (Na_2SO_4), filtered, and concentrated. The residue was purified by flash chromatography (SiO_2, 9:1 Hexanes:EtOAc to 2:3 Hexanes:EtOAc) to afford **13a** (1.26 g, 76%) as a pale yellow amorphous solid: ^{1}H NMR ($CDCl_3$, 500 MHz) As the enol: δ 15.26 (s, 1H), 11.63 (s, 1H), 7.67 (d, *J* = 8.4 Hz, 1H), 7.53 (d, *J* = 2.0 Hz, 1H), 7.38 (dd, *J* = 8.4, 2.0 Hz, 1H), 7.35 (d, *J* = 2.9 Hz, 1H), 7.24 (dd, *J* = 9.05, 2.9 Hz, 1H), 6.95 (d, *J* = 9.05 Hz, 1H), 6.74 (s, 1H), 5.13 (s, 2H), 3.50 (s, 1H); ^{13}C NMR

($CDCl_3$, 125 MHz) As the enol: δ 195.6, 174.8, 157.9, 149.6, 137.4, 133.1, 131.9, 131.2, 130.8, 127.5, 126.2, 119.6, 118.4, 115.3, 98.1, 95.5, 56.0; IR (film) ν_{max} 3076, 2995, 2953, 2901, 2845, 2826, 1691, 1643, 1614, 1585, 1556, 1485, 1472, 1441, 1400, 1366, 1327, 1306, 1286, 1256, 1234, 1188, 1151, 1107, 1080, 1051, 1011, 922 cm^{-1}; HRMS(ES^-) *m/z*: [M-H] calcd for $C_{17}H_{14}Cl_2O_5$ 367.0140; found 367.0140.

1-(5-Chloro-2-methoxyphenyl)-3-(2-hydroxy-5-(methoxymethoxy)phenyl)propane-1,3-dione (13b). Compound **13b** was prepared following the same procedure used in the preparation of compound **13a**. The residue was purified by flash chromatography (SiO_2, 3:1 Hexanes:EtOAc) to afford **13b** (0.84 g, 65%) as a yellow amorphous solid: ^1H NMR ($CDCl_3$, 500 MHz) As a mixture of tautomers: δ 15.43 (s, 1H), 11.78 (s, 1H), 11.54 (s, 1H), 7.99 (d, *J* = 2.75 Hz, 1H), 7.92 (d, *J* = 2.75 Hz, 1H), 7.47 (d, *J* = 2.95 Hz, 1H), 7.47 (dd, *J* = 8.9, 2.7 Hz, 1H), 7.43 (dd, *J* = 8.9, 2.7 Hz, 1H), 7.36 (d, *J* = 2.8 Hz, 1H), 7.32 (s, 1H), 7.27 (dd, *J* = 9, 2.95 Hz, 1H), 7.20 (dd, *J* = 9, 2.95, 1H), 6.96 (d, *J* = 8.9 Hz, 1H), 6.95 (d, *J* = 8.9 Hz, 1H), 6.94 (d, *J* = 9 Hz, 1H), 6.89 (d, *J* = 8.9 Hz, 1H), 5.16 (s, 2H), 5.13 (s, 2H), 4.59 (s, 2H), 4.00 (s, 3H), 3.67 (s, 3H), 3.53 (s, 3H), 3.50 (s, 3H); ^{13}C NMR ($CDCl_3$, 125 MHz) As a mixture of tautomers: δ 195.8 (2C), 172.9 (2C), 157.7 (2C), 157.2 (2C), 149.7 (2C), 134.4, 132.6, 130.7, 129.6, 126.7, 126.2 (2C), 125.8, 123.4 (2C), 119.5, 119.4, 118.8 (2C), 116.4, 114.9, 113.2, 113.0, 97.9 (2C), 95.6 (2C), 56.0, 55.9, 55.7, 53.9; IR

(film) ν_{max} 2997, 2982, 2959, 2949, 2934, 2845, 2824, 1618, 1583, 1564, 1549, 1489, 1460, 1435, 1400, 1329, 1310, 1286, 1271, 1244, 1223, 1188, 1150, 1113, 1082, 1070, 1041, 1026, 1005, 922 cm^{-1}; HRMS(ES^+) *m/z*: [M+H] calcd for $C_{18}H_{17}O_6Cl$ 365.0792; found 365.0783.

1-(2-Hydroxy-5-(methoxymethoxy)phenyl)-3-(2-(trifluoromethyl)phenyl)propane-1,3-dione (13c). Compound **13c** was prepared following the same procedure used in the preparation of compound **13a**. The residue was purified by flash chromatography (SiO_2, 3:1 Hexanes:EtOAc) to afford **13c** (0.88 g, 80%) as a pale yellow amorphous solid: ^1H NMR ($CDCl_3$, 500 MHz) As the enol: δ 15.2 (s, 1H), 11.7 (s, 1H), 7.80 (d, *J* = 7.55 Hz, 1H), 7.64 (m, 3H), 7.32 (d, *J* = 2.8 Hz, 1H), 7.23 (dd, *J* = 9.05, 2.8 Hz, 1H), 6.95 (d, *J* = 9.05 Hz, 1H), 6.43 (s, 1H), 5.11 (s, 2H), 3.48 (s, 3H); ^{13}C NMR ($CDCl_3$, 125 MHz) As the enol: δ 195.6, 178.2, 157.9, 149.6, 131.9, 130.6, 130.0, 126.94, 126.90, 126.86, 126.3, 119.6, 118.3, 115.2, 97.3, 95.4, 55.9; IR (film) ν_{max} 2955, 2903, 2827, 1616, 1570, 1487, 1448, 1435, 1402, 1313, 1286, 1256, 1175, 1153, 1136, 1113, 1095, 1080, 1055, 1036, 1011, 922, 881 cm^{-1}; HRMS(ES^+) *m/z*: [M+H] calcd for $C_{18}H_{15}F_3O_5$ 369.0950; found 369.0934.

1-(2-Hydroxy-5-(methoxymethoxy)phenyl)-3-(3-(trifluoromethyl)phenyl)propane-1,3-dione (13d). Compound **13d** was prepared following the same procedure used in the preparation of compound **13a**. The residue was purified by flash chromatography (SiO_2, 4:1 Hexanes:EtOAc) to

afford **13d** (8.3 g, 94%) as a yellow amorphous solid: ^{1}H NMR ($CDCl_3$, 500 MHz) As a mixture of tautomers: δ 15.6 (s, 1H), 11.94 (s, 1H), 11.65 (s, 1H), 8.19 (s, 1H), 8.12 (d, *J* = 7.9 Hz, 1H), 7.82 (d, *J* = 7.7 Hz, 1H), 7.65 (t, *J* = 7.8 Hz, 1H), 7.44 (d, *J* = 2.95 Hz, 1H), 7.40 (d, *J* = 2.95 Hz, 1H), 7.27 (dd, *J* = 9, 2.95 Hz, 1H), 7.23 (dd, *J* = 9, 2.95 Hz, 1H), 6.97 (d, *J* = 9 Hz, 1H), 6.93 (d, *J* = 9 Hz, 1H), 6.80 (s, 1H), 5.18 (s, 2H), 5.14 (s, 2H), 3.53 (s, 3H), 3.51 (s, 3H), 2.63 (s, 2H); ^{13}C NMR ($CDCl_3$, 125 MHz) As a mixture of tautomers: δ 195.6 (2C), 175.4 (2C), 157.7 (2C), 149.6 (2C), 134.4 (2C), 129.9, 129.4, 128.8, 128.7, 126.4 (2C), 125.9 (2C), 123.7, 123.6, 119.6, 119.2, 118.5 (2C), 117.1 (2C), 115.4 (2C), 95.5 (2C), 92.9 (2C), 56.1 (2C), 26.8 (2C); IR (film) ν_{max} 3076, 2955, 2903, 2827, 1620, 1576, 1556, 1487, 1448, 1423, 1404, 1337, 1285, 1248, 1190, 1169, 1153, 1128, 1076, 1040, 1011, 920 cm^{-1}; HRMS(ES^{+}) *m/z*: [M+H] calcd for 369.0950; found 369.0945.

2-(2,4-Dichlorophenyl)-6-hydroxy-4*H*-chromen-4-one (14a). Compound **13a** (0.91 g, 2.46 mmol) and a catalytic amount of concentrated H_2SO_4 (120 μL) were dissolved in EtOH (19 mL) at rt. The solution was sealed under argon, and exposed to microwave irradiation (25 W, 100°C) for 30 min. The reaction mixture was concentrated *in vacuo*, washed with cold diethyl ether, and filtered to provide **14a** (0.52 g, 70%) as a white amorphous solid: ^{1}H NMR (DMSO-d_6, 500 MHz) δ 10.11 (s, 1H), 7.88 (d, *J* = 2.05 Hz, 1H), 7.82 (d, *J* = 8.35 Hz, 1H), 7.64 (dd, *J* = 8.35, 2.05 Hz, 1H), 7.56 (d, *J* = 9 Hz, 1H), 7.34 (d, *J* = 3

Hz, 1H), 7.27 (dd, *J* = 9, 3 Hz, 1H), 6.57 (s, 1H); ^{13}C NMR (DMSO-d_6, 125 MHz) δ 176.5, 160.9, 155.1, 149.7, 136.3, 132.8, 132.6, 130.5, 130.0, 128.0, 124.1, 119.9, 111.4, 107.4; IR (film) ν_{max} 3452, 1666, 1651, 1634, 1549, 1470, 1410, 1354, 1275, 1252, 1227, 1107, 1078, 1026, 916 cm^{-1}; HRMS(ES$^+$) *m/z*: [M+H] calcd for $C_{15}H_8Cl_2O_3$ 306.9929; found 306.9916.

2-(5-Chloro-2-methoxyphenyl)-6-hydroxy-4*H*-chromen-4-one (14b). Compound **14b** was isolated as a yellow amorphous solid (0.59 g, 87%) following the same procedure used in the preparation of compound **14a**: ^{1}H NMR (DMSO-d_6, 500 MHz) δ 10.03 (s, 1H), 7.92 (d, *J* = 2.75 Hz, 1H), 7.65 (d, *J* = 8.9 Hz, 1H), 7.61 (dd, *J* = 8.9, 2.75 Hz, 1H), 7.30 (d, *J* = 3 Hz, 1H), 7.28 (d, *J* = 9 Hz, 1H), 7.24 (dd, *J* = 9, 3 Hz, 1H), 6.86 (s, 1H), 3.92 (s, 3H); ^{13}C NMR (DMSO-d_6, 125 MHz) δ 177.0, 158.7, 156.4, 154.9, 149.6, 132.1, 128.4, 124.7, 124.0, 123.2, 121.7, 120.0, 114.5, 111.1, 107.3, 56.5; IR (film) ν_{max} 3258, 1647, 1626, 1597, 1566, 1479, 1375, 1358, 1283, 1250, 1236, 1180, 1148, 1126, 1111, 1041, 1014, 914 cm^{-1}; HRMS(ES$^+$) *m/z*: [M+H] calcd for $C_{16}H_{11}ClO_4$ 303.0424; found 303.0411.

6-Hydroxy-2-(2-(trifluoromethyl)phenyl)-4*H*-chromen-4-one (14c). The β-ethoxy Michael adduct of compound **14c** was isolated as a yellow amorphous solid (0.897 mg) following the same procedure used in the preparation of compound **14a**. Stirring at rt in 2:1 THF: 0.5M aqueous NaOH afforded **14c** (0.53 g, 65%) as a pale yellow amorpohous solid: ^{1}H NMR (DMSO-d_6, 500 MHz)

δ 10.1 (s, 1H), 7.97 (d, *J* = 7.6 Hz, 1H), 7.87 (m, 2H), 7.84 (m, 1H), 7.49 (d, *J* = 9.0 Hz, 1H), 7.35 (d, *J* = 3.0 Hz, 1H), 7.27 (dd, *J* = 9.0, 3.0 Hz, 1H); ^{13}C NMR (DMSO-d_6, 125 MHz) δ 176.5, 162.8, 155.1, 149.5, 133.0, 131.51, 131.47, 130.9, 130.8, 127.0, 126.9, 124.0, 119.6, 110.5, 107.4; IR (film) ν_{max} 3217, 2961, 2922, 2851, 1624, 1607, 1574, 1541, 1489, 1472, 1396, 1375, 1360, 1312, 1265, 1232, 1169, 1130, 1111, 1074, 1036, 968, 916 cm^{-1}; HRMS(ES$^+$) *m/z*: [M+H] calcd for $C_{16}H_9F_3O_3$ 307.0582; found 307.0602.

6-Hydroxy-2-(3-(trifluoromethyl)phenyl)-4*H*-chromen-4-one (14d). Compound **14d** was isolated as a white amorphous solid (0.35 g, 85%) following the same procedure used in the preparation of compound **14a**: ^{1}H NMR (DMSO-d_6, 500 MHz) δ 10.03 (s, 1H), 7.90 (dd, *J* = 7.8, 1.75 Hz, 1H), 7.60 (d, *J* = 9 Hz, 1H), 7.54 (dt, *J* = 7.8, 1.75 Hz, 1H), 7.30 (d, *J* = 3 Hz, 1H), 7.24 (dd, *J* = 9, 3 Hz, 1H), 7.22 (d, *J* = 7.3 Hz, 1H), 7.13 (dt, *J* = 7.3, 1 Hz, 1H), 6.90 (s, 1H), 4.19 (q, *J* = 6.9 Hz, 2H), 1.38 (t, *J* = 6.9 Hz, 3H); ^{13}C NMR (DMSO-d_6, 125 MHz) δ 177.1, 160.5, 156.9, 154.8, 149.7, 132.8, 129.2, 124.0, 123.2, 120.7, 120.1, 119.9, 113.4, 110.6, 107.4, 64.2, 14.6; IR (film) ν_{max} 3439, 3105, 3059, 2976, 2953, 2935, 2889, 2799, 2725, 2642, 2596, 2581, 1614, 1576, 1566, 1475, 1448, 1416, 1389, 1360, 1294, 1248, 1202, 1192, 1167, 1129, 1107, 1080, 1036, 928, 906 cm^{-1}; HRMS(ES$^+$) *m/z*: [M+H] calcd for $C_{17}H_{14}O_4$ 283.0970; found 283.0988.

***tert*-Butyl 2-(2,4-dichlorophenyl)-4-oxo-4*H*-chromen-6-yl carbonate (15a)**. Compound **14a** (0.52 g, 1.69 mmol) and di-*tert*-butyl dicarbonate (0.85 g,

3.88 mmol) were dissolved in DMF (10 mL) and stirred at rt. A catalytic amount of 4-Dimethylaminopyridine (22.67 mg, 0.19 mmol) was added, and the solution was stirred for 1 h. The reaction mixture was quenched with H_2O (10 mL), and extracted with EtOAc (3 x 10 mL). The combined organic layers were washed with H_2O, brine, dried (Na_2SO_4), filtered, and concentrated. The residue was purified by flash chromatography (SiO_2, 7:3 Hexanes:EtOAc) to afford **15a** (0.69 g, 100%) as a white amorphous solid: ^{1}H NMR ($CDCl_3$, 500 MHz) δ 8.03 (dd, *J* = 2.4, 0.9 Hz, 1H), 7.57 (m, 2H), 7.53 (m, 2H), 7.42 (dd, *J* = 8.3 Hz, 1H), 6.64 (s, 1H), 1.59 (s, 9H); ^{13}C NMR ($CDCl_3$, 125 MHz) δ 177.2, 161.7, 153.9, 151.5, 148.2, 137.5, 133.8, 131.4, 130.8, 130.2, 127.9, 127.6, 124.5, 119.5, 117.6, 112.6, 27.7 (3C); IR (film) ν_{max} 3084, 3051, 2982, 2934, 2359, 2341, 1755, 1657, 1626, 1587, 1551, 1481, 1450, 1391, 1371, 1352, 1271, 1250, 1148, 1130, 1109, 1070, 1047, 1028, 914 cm^{-1}; HRMS(ES$^+$) *m/z*: [M+H] calcd for $C_{20}H_{16}Cl_2O_5$ 407.0453; found 407.0439.

***tert*-Butyl 2-(5-chloro-2-methoxyphenyl)-4-oxo-4*H*-chromen-6-yl carbonate (15b)**. Compound **15b** was prepared following the same procedure used in the preparation of compound **15a**. The residue was purified by flash chromatography (SiO_2, 3:7 Hexanes:EtOAc) to afford **15b** (0.74 g, 98%) as a white amorphous solid: ^{1}H NMR ($CDCl_3$, 500 MHz) δ 8.11 (d, *J* = 2.85 Hz, 1H), 7.99 (d, *J* = 2.7 Hz, 1H), 7.68 (d, *J* = 8.9 Hz, 1H), 7.61 (dd, *J* = 9, 2.85 Hz, 1H), 7.54 (dd, *J* = 9, 2.7 Hz, 1H), 7.37 (s, 1H), 7.09 (d, *J* = 8.9 Hz, 1H), 4.05 (s, 3H),

1.69 (s, 9H); ^{13}C NMR ($CDCl_3$, 125 MHz) δ 178.0, 159.2, 156.6, 153.7, 151.6, 147.9, 132.0, 128.8, 127.6, 126.0, 124.4, 121.8, 119.4, 117.4, 113.1, 112.6, 84.2, 56.1, 27.7 (3C); IR (film) ν_{max} 3115, 3078, 2980, 2941, 2910, 2845, 1759, 1643, 1624, 1593, 1566, 1479, 1454, 1394, 1371, 1350, 1273, 1252, 1213, 1182, 1150, 1113, 1080, 1034, 1018, 928 cm^{-1}; HRMS(ES$^+$) *m/z*: [M+H] calcd for $C_{21}H_{19}ClO_6$ 403.0948; found 403.0959.

***tert*-Butyl 4-oxo-2-(2-(trifluoromethyl)phenyl)-4*H*-chromen-6-yl carbonate (15c)**. Compound **15c** was prepared following the same procedure used in the preparation of compound **15a**. The residue was purified by flash chromatography (SiO_2, 3:7 Hexanes:EtOAc) to afford **15c** (0.66 g, 95%) as a white amorphous solid: ^{1}H NMR ($CDCl_3$, 500 MHz) δ 8.03 (dd, *J* = 2.0, 1.4 Hz, 1H), 7.86 (dd, *J* = 9.0, 1.8 Hz, 1H), 7.67 (m, 3H), 7.51 (m, 2H), 6.51 (s, 1H), 1.59 (s, 9H); ^{13}C NMR ($CDCl_3$, 125 MHz) δ 177.3, 164.0, 153.8, 151.5, 148.2, 132.2, 131.0, 130.9 (2C), 127.9 (2C), 127.19, 127.16, 124.5, 119.6, 117.6, 111.6, 84.3, 27.6 (3C); IR (film) ν_{max} 3074, 2982, 2935, 1759, 1657, 1628, 1583, 1574, 1479, 1452, 1396, 1313, 1285, 1273, 1248, 1148, 1070, 1036, 962, 932, 914 cm^{-1}; HRMS(ES$^+$) *m/z*: [M+H] calcd for $C_{21}H_{17}F_3O_5$ 407.1106; found 407.1114.

***tert*-Butyl 4-oxo-2-(3-(trifluoromethyl)phenyl)-4*H*-chromen-6-yl carbonate (15d)**. Compound **15d** was prepared following the same procedure used in the preparation of compound **15a**. The residue was purified by flash chromatography (SiO_2, 3:7 Hexanes:EtOAc) to afford **15d** (1.33 g, 100%) as a

white amorphous solid: ^{1}H NMR ($CDCl_3$, 500 MHz) δ 8.20 (s, 1H), 8.09 (d, *J* = 8 Hz, 1H), 8.03 (d, *J* = 2.9 Hz, 1H), 7.82 (d, *J* = 7.8 Hz, 1H), 7.69 (t, *J* = 7.8 Hz, 1H), 7.64 (d, *J* = 9 Hz, 1H), 7.55 (dd, *J* = 9, 2.9 Hz, 1H), 6.87 (s, 1H), 1.59 (s, 9H); ^{13}C NMR ($CDCl_3$, 125 MHz) δ 177.4, 161.8, 153.5, 151.5, 148.2, 132.5, 129.8, 129.4, 128.20, 128.17, 127.9, 124.6, 123.2, 123.1, 119.5, 117.6, 107.9, 84.3, 27.7 (3C); IR (film) ν_{max} 3462, 3084, 3055, 2982, 2935, 1761, 1649, 1626, 1576, 1481, 1458, 1396, 1371, 1327, 1281, 1253, 1169, 1150, 1126, 1101, 1078, 1047, 1016, 924, 906 cm^{-1}; HRMS(ES^{+}) *m/z*: [M+H] calcd for $C_{21}H_{17}F_3O_5$ 407.1106; found 407.1092.

***tert*-Butyl 4-oxo-2-phenyl-4*H*-chromen-6-yl carbonate (15e)**. Commercially available 6-hydroxyflavone (0.55 g, 2.31 mmol) and di-*tert*-butyl dicarbonate (1.16 g, 5.31 mmol) were dissolved in DMF (10 mL) and stirred at rt. A catalytic amount of 4-Dimethylaminopyridine (31.0 mg, 0.25 mmol) was added, and the solution was stirred for 1 h. The reaction mixture was quenched with H_2O (10 mL), and extracted with EtOAc (3 x 10 mL). The combined organic layers were washed with H_2O, brine, dried (Na_2SO_4), filtered, and concentrated. The residue was purified by flash chromatography (SiO_2, 7:3 Hexanes:EtOAc) to afford **15e** (0.78 g, 100%) as a white amorphous solid: ^{1}H NMR ($CDCl_3$, 500 MHz) δ 8.02 (d, *J* = 2.85 Hz, 1H), 7.94 (d, *J* = 7.65, 1.45 Hz, 1H), 7.93 (d, *J* = 8.15, 1.95 Hz, 1H), 7.60 (d, *J* = 8.9 Hz, 1H), 7.54 (m, 4H), 6.83 (s, 1H), 1.59 (s, 9H); ^{13}C NMR ($CDCl_3$, 125 MHz) δ 177.7, 163.6, 153.6, 151.5, 148.0, 131.7,

131.6, 129.1 (2C), 127.6, 126.3 (2C), 124.6, 119.4, 117.5, 107.1, 84.2, 27.7 (3C); IR (film) ν_{max} 3069, 2982, 2937, 2878, 1807, 1759, 1651, 1626, 1572, 1543, 1497, 1479, 1454, 1396, 1371, 1358, 1310, 1259, 1213, 1148, 1122, 1070, 1026, 1001, 951, 932, 908 cm^{-1}; HRMS(ES^+) *m/z*: [M+H] calcd for $C_{20}H_{18}O_5$ 339.1233; found 339.1236.

3-Amino-2-(2,4-dichlorophenyl)-4-oxo-4*H*-chromen-6-yl *tert*-butyl carbonate (16a). Compound **15a** (0.20 g, 0.49 mmol) and ammonium nitrate (0.16 g, 2.0 mmol) were dissolved in anhydrous AcCN (10 mL), and stirred at rt. Freshly distilled trifluoroacetic anhydride (0.27 mL, 2.0 mmol) was added dropwise, and the reaction mixture stirred for 2 h at rt. The solution was quenched with saturated aqueous $NaHCO_3$ (10 mL), and the aqueous layer was then extracted with EtOAc (3 x 15 mL). The combined organic layers were washed with saturated aqueous NaCl, dried (Na_2SO_4), filtered, and concentrated. The residue was purified by flash chromatography (SiO_2, Toluene) to afford the nitro intermediate as a yellow solid. The solid was subsequently dissolved in EtOH (3.5 mL) and the solution was purged with argon for 15 min. 10% w/w Pd/C (5.5 mg, 0.052 mmol) was added, and hydrogen gas was bubbled through the solution for 30 min. This was followed by stirring under an H_2 blanket for 2 h. The reaction mixture was filtered through celite to remove catalyst, and rinsed with EtOAc (50 mL). Rotoevaporation of the filtrate afforded **16a** (47.7 mg, 23% over two steps) as a pale yellow amorphous solid: ^{1}H NMR ($CDCl_3$, 500 MHz) δ 8.05 (t, *J* = 1.65

Hz, 1H), 7.61 (d, *J* = 2.0 Hz, 1H), 7.57 (d, *J* = 8.3 Hz, 1H), 7.46 (d, *J* = 1.65 Hz, 2H), 7.44 (dd, *J* = 8.3, 2.0 Hz, 1H), 3.76 (bs, -N**H**$_2$, 2H); ^{13}C NMR ($CDCl_3$, 125 MHz) δ 172.6, 153.2, 151.7, 147.2, 141.7, 137.1, 134.7, 132.1, 130.5, 129.2, 129.1, 127.9, 127.2, 121.7, 119.5, 117.3, 84.1, 27.7 (3C); IR (film) ν_{max} 3439, 3333, 3084, 2980, 2930, 2854, 1759, 1643, 1626, 1589, 1566, 1556, 1483, 1394, 1371, 1319, 1286, 1269, 1244, 1219, 1192, 1144, 1107, 1051, 1024, 905 cm^{-1}; HRMS(ES$^+$) *m/z*: [M+H] calcd for $C_{20}H_{17}Cl_2NO_5$ 422.0562; found 422.0539.

3-Amino-2-(5-chloro-2-methoxyphenyl)-4-oxo-4*H*-chromen-6-yl *tert*-butyl carbonate (16b). The nitro intermediate for compound **16b** was prepared following the same procedure used in the preparation of compound **16a**, and was purified by flash chromatography (SiO_2, 9:1 Hexanes:EtOAc). The solid (100 mg, 0.22 mmol) was dissolved in THF (4 mL) and the solution was purged with argon for 15 min. Pt_2O (15 mg, 15% w/w) was added, and hydrogen gas was bubbled through the solution for 30 min. This was followed by stirring under an H_2 blanket for 3 h. The reaction mixture was filtered through celite to remove catalyst, and rinsed with EtOAc (100 mL). Purification by preparative TLC (7:3 Hexanes:EtOAc) afforded **16b** (51.5 mg, 63% over two steps) as a yellow amorphous solid: ^{1}H NMR ($CDCl_3$, 500 MHz) δ 8.05 (d, *J* = 3.0 Hz, 1H), 7.57 (d, *J* = 2.6 Hz, 1H), 7.48 (d, *J* = 9.1 Hz, 1H), 7.46 (t, *J* = 3.0 Hz, 1H), 7.45 (t, *J* = 2.7 Hz, 1H), 7.02 (d, *J* = 8.9 Hz, 1H), 4.01 (bs, -N**H**$_2$, 2H), 3.92 (s, 3H), 1.59 (s, 9H); ^{13}C NMR ($CDCl_3$, 125 MHz) δ 172.8, 154.9, 153.4, 151.7, 147.1, 142.1, 131.4,

130.4, 129.6, 127.0, 126.3, 122.7, 121.5, 119.4, 117.2, 113.2, 84.1, 56.4, 27.7 (3C); IR (film) ν_{max} 3435, 3348, 3107, 3072, 3065, 2980, 2934, 2851, 1759, 1622, 1589, 1566, 1485, 1464, 1410, 1394, 1371, 1283, 1269, 1254, 1242, 1182, 1146, 1070, 1047, 1024, 930, 901 cm^{-1}; HRMS(ES^+) *m/z*: [M+H] calcd for $C_{21}H_{20}ClNO_6$; found 418.1058.

3-Amino-4-oxo-2-(2-(trifluoromethyl)phenyl)-4*H*-chromen-6-yl *tert*-butyl carbonate (16c). Compound **16c** was prepared following the same procedure used in the preparation of compound **16a**. The nitro intermediate was purified by flash chromatography (SiO_2, 50:1 Toluene:EtOAc). **16c** (5.0 mg, 2.6% over two steps) was afforded as a yellow amorphous solid: ^1H NMR ($CDCl_3$, 500 MHz) δ 8.06 (dd, *J* = 2.2, 0.9 Hz, 1H), 7.90 (d, *J* = 7.8 Hz, 1H), 7.75 (d, *J* = 0.9 Hz, 1H), 7.74 (dd, *J* = 2.1, 0.9 Hz, 1H), 7.68 (m, 1H), 7.45 (m, 2H); ^{13}C NMR ($CDCl_3$, 125 MHz) δ 172.7, 153.0, 151.7, 147.2, 142.8, 132.5, 131.3, 130.6, 129.9, 129.6, 128.6, 127.5, 127.2, 121.7, 119.5, 117.2, 84.1, 27.7 (3C); IR (film) ν_{max} 3448, 3348, 3072, 2980, 2930, 2856, 1759, 1639, 1605, 1589, 1568, 1483, 1462, 1450, 1410, 1396, 1371, 1315, 1286, 1265, 1244, 1219, 1196, 1173, 1146, 1111, 1082, 1055, 1036, 1024, 1009, 962, 928, 903cm^{-1}; HRMS(ES^+) *m/z*: [M+H] calcd for $C_{21}H_{18}F_3NO_5$ 422.1215; found 422.1209.

3-Amino-4-oxo-2-(3-(trifluoromethyl)phenyl)-4*H*-chromen-6-yl *tert*-butyl carbonate (16d). Compound **16d** was prepared following the same procedure used in the preparation of compound **16a**. The nitro intermediate was

purified by flash chromatography (SiO_2, Toluene). **16d** (11.8 mg, 23% over two steps) was afforded as a pale yellow amorphous solid: ^{1}H NMR ($CDCl_3$, 500 MHz) δ 8.20 (s, 1H), 8.15 (d, *J* = 7.7 Hz, 1H), 8.05 (d, *J* = 2.8 Hz, 1H), 7.73 (d, *J* = 7.8 Hz, 1H), 7.69 (t, *J* = 7.75 Hz, 1H), 7.54 (d, *J* = 9.1 Hz, 1H), 7.49 (dd, *J* = 9.1, 2.8 Hz, 1H), 4.08 (-N**H**$_2$), 1.59 (s, 9H); ^{13}C NMR ($CDCl_3$, 125 MHz) δ 172.9, 152.9, 151.6, 147.3, 142.5, 133.5, 130.7, 129.6, 128.4, 127.3, 126.31, 126.28, 124.40, 124.37, 121.3, 119.4, 117.3, 84.2, 27.7 (3C); IR (film) ν_{max} 3337, 2982, 2930, 2853, 1759, 1717, 1684, 1636, 1622, 1589, 1568, 1541, 1506, 1485, 1458, 1396, 1371, 1331, 1285, 1269, 1242, 1167, 1148, 1099, 1074, 1028, 1013, 928, 903 cm^{-1}; HRMS(ES$^+$) *m/z*: [M+H] calcd for $C_{21}H_{18}F_3NO_5$ 422.1215; found 422.1233.

3-Amino-4-oxo-2-phenyl-4*H*-chromen-6-yl *tert*-butyl carbonate (16e). Compound **16e** was prepared following the same procedure used in the preparation of compound **16a**. The nitro intermediate was purified by flash chromatography (SiO_2, 8:2 Hexanes:EtOAc). **16e** (170.3 mg, 82% over two steps) was afforded as a pale yellow amorphous solid: ^{1}H NMR ($CDCl_3$, 500 MHz) δ 8.03 (d, *J* = 2.8 Hz, 1H), 7.92 (d, *J* = 1.4 Hz, 1H), 7.91 (d, *J* = 7.2 Hz, 1H), 7.55 (m, 3H), 7.51 (d, *J* = 9.1 Hz, 1H), 7.46 (dd, *J* = 9.1, 2.9 Hz, 1H), 4.07 (bs, -N**H$_2$**, 2H), 1.58 (s, 9H); ^{13}C NMR ($CDCl_3$, 125 MHz) δ 172.8, 152.9, 151.7, 147.1, 144.5, 133.0, 132.5, 129.8, 129.3, 129.0, 127.8, 127.6, 126.9, 121.4, 119.4, 117.1, 84.1, 27.6 (3C); IR (film) ν_{max} 3427, 3340, 3205, 3066, 2982, 2934, 1759, 1663,

1622, 1587, 1564, 1537, 1481, 1456, 1404, 1371, 1281, 1242, 1217, 1188, 1144, 1076, 1047, 1022, 924, 901 cm^{-1}; HRMS(ES^+) *m/z*: [M+H] calcd for $C_{20}H_{19}NO_5$ 354.1342; found 354.1358.

3-Amino-2-(2-methoxyphenyl)-4-oxo-4*H*-chromen-6-yl *tert*-butyl carbonate (16f). Utilizing compound **15b** as starting material, compound **16f** was prepared following the same procedure used in the preparation of compound **16a**. The nitro intermediate was purified by flash chromatography (SiO_2, 9:1 Hexanes:EtOAc). **16f** (31.7 mg, 17% over two steps) was afforded as a yellow amorphous solid: ^1H NMR ($CDCl_3$, 500 MHz) As a mixture of conformational isomers: δ 8.05 (t, *J* = 2.9 Hz, 1H), 7.57 (d, *J* = 2.65 Hz, 1H), 7.46 (m, 3H), 7.14 (t, *J* = 8.3 Hz, 1H), 7.08 (d, *J* = 8.4 Hz, 1H), 7.02 (d, *J* = 1H), 4.01 (bs, -N**H₂**, 2H), 3.92 (s, 3H), 3.91 (s, 3H), 1.59 (s, 9H); As a mixture of conformational isomers: ^{13}C NMR ($CDCl_3$, 125 MHz) δ 172.8, 172.7, 156.4, 154.9, 153.4, 153.3, 151.7, 151.6, 147.1, 147.0, 142.1, 131.8, 131.4, 130.7, 130.4, 129.6, 129.3, 127.0, 126.7, 126.3, 122.7, 121.6, 121.5, 121.4, 121.2, 121.1, 119.4, 117.2, 117.1, 113.2, 111.8, 84.0, 56.3, 55.9, 27.7 (3C); IR (film) ν_{max} 3435, 3348, 3070, 2980, 2935, 2872, 2851, 1759, 1622, 1566, 1483, 1462, 1433, 1408, 1396, 1371, 1254, 1242, 1182, 1146, 1070, 1047, 1022, 978, 930, 901 cm^{-1}; HRMS(ES^+) *m/z*: [M+H] calcd for $C_{21}H_{21}NO_6$ 384.1447; found 384.1463.

***N*-(2-(2,4-Dichlorophenyl)-6-hydroxy-4-oxo-4*H*-chromen-3-yl)acetamide (17a)**. Compound **16a** (7.7 mg, 0.018 mmol) was dissolved in

anhydrous AcCN (0.15 mL) and stirred at rt. N,N-Diisopropylethylamine (3.81 μL, 0.022 mmol) was added dropwise, followed by acetyl chloride (1.68 μL, 0.024 mmol), and stirred at rt for 1.5 h. The solution was brought up in EtOAc (5 mL), and washed with H_2O, saturated aqueous NaCl, dried, and concentrated. The residue was purified by flash chromatography (SiO_2, 8:2 Hexanes:EtOAc to 100% EtOAc) to afford the N-acylated intermediate as a pale yellow solid. The solid was subsequently dissolved in MeOH (0.15 mL), and stirred at rt. HCl gas was bubbled through solution for 10 seconds, and the solution stirred for 5 min, followed by rotoevaporation. The residue was purified by flash chromatography (SiO_2, 1:1 Hexanes:EtOAc) to afford **17a** (2.4 mg, 28% over two steps) as a pale yellow amorphous solid: ^{1}H NMR (MeOD, 500 MHz) δ 7.66 (d, *J* = 1.9 Hz, 1H), 7.53 (d, *J* = 8.3 Hz, 1H), 7.48 (m, 3H), 7.29 (dd, *J* = 9.1, 3.0 Hz, 1H), 1.94 (s, 3H); ^{13}C NMR (MeOD, 125 MHz) δ 176.7, 173.3, 161.7, 157.1, 151.7, 138.5, 135.4, 133.1, 131.1, 130.1, 128.7, 125.44, 125.35, 121.3, 121.0, 109.1, 22.5; IR (film) ν_{max} 3269, 2953, 2924, 2854, 1740, 1697, 1670, 1622, 1591, 1556, 1487, 1472, 1456, 1387, 1362, 1337, 1256, 1236, 1204, 1182, 1151, 1101, 1082, 1116, 970, 912 cm^{-1}; HRMS(ES$^+$) *m/z*: [M+Na] calcd for $C_{21}H_{11}Cl_2NO_4$ 385.9963; found 385.9943.

***N*-(2-(5-Chloro-2-methoxyphenyl)-6-hydroxy-4-oxo-4*H*-chromen-3-yl)acetamide (17b)**. Compound **17b** was prepared following the same procedure used in the preparation of compound **17a**. The N-acylated intermediate was

purified by flash chromatography (SiO_2, 7:3 Hexanes:EtOAc to 100% EtOAc). Purification in the final step by preparative TLC (SiO_2, 1:9 Hexanes:EtOAc) afforded **17b** (14.6 mg, 33% over two steps) as a pale yellow amorphous solid: ^{1}H NMR (MeOD, 500 MHz) As a mixture of conformational isomers: δ 7.48 (m, 4H), 7.27 (dd, *J* = 9.0, 3.0 Hz, 1H), 7.15 (d, *J* = 9.0 Hz, 1H), 3.84 (s, 3H), 1.95 (2s, 3H); ^{13}C NMR (MeOD, 125 MHz) δ 176.7, 173.3, 161.9, 157.4, 156.9, 151.8, 133.2, 130.9, 126.5, 125.4, 125.1, 123.6, 121.0, 114.5, 109.1, 56.9, 30.6, 22.5; IR (film) ν_{max} 2930, 2851, 1655, 1637, 1610, 1574, 1543, 1483, 1472, 1435, 1404, 1391, 1356, 1313, 1281, 1259, 1248, 1227, 1204, 1171, 1148, 1128, 1111, 1070, 1040, 1018, 984, 933 cm^{-1}; HRMS(ES^+) *m/z*: [M+H] calcd for $C_{18}H_{14}ClNO_5$ 360.0639; found 360.0621.

***N*-(6-Hydroxy-4-oxo-2-(2-(trifluoromethyl)phenyl)-4*H*-chromen-3-yl)acetamide (17c)**. Compound **17c** was prepared following the same procedure used in the preparation of compound **17a**. The N-acylated intermediate was purified by flash chromatography (SiO_2, 6:4 Hexanes:EtOAc to 100% EtOAc). Purification in the final step by preparative TLC (SiO_2, 3:7 Hexanes:EtOAc) afforded **17c** (2.1 mg, 49% over two steps) as a pale yellow amorphous solid: ^{1}H NMR (MeOD, 500 MHz) δ 7.91 (m, 1H), 7.75 (m, 1H), 7.66 (m, 1H), 7.48 (d, *J* = 3.0 Hz, 1H), 7.45 (d, *J* = 9.0 Hz, 1H), 7.30 (dd, *J* = 9.0, 3.0 Hz, 1H), 1.94 (s, 3H); ^{13}C NMR (MeOD, 125 MHz) δ 176.7, 173.7, 163.3, 157.1, 151.5, 133.3, 132.5, 131.9, 129.6, 128.24, 128.21, 126.7, 125.5, 125.3, 120.9, 109.2, 30.6, 22.4; IR

(film) ν_{max} 3402, 3256, 3043, 3011, 2955, 2924, 2853, 2359, 2341, 1624, 1576, 1558, 1522, 1474, 1404, 1369, 1315, 1294, 1277, 1238, 1207, 1173, 1132, 1113, 1063, 1036, 1005, 966, 939 cm^{-1}; HRMS(ES^+) *m/z*: [M+H] calcd for $C_{18}H_{12}F_3NO_4$ 364.0797; found 364.0789.

***N*-(6-hydroxy-4-oxo-2-(3-(trifluoromethyl)phenyl)-4*H*-chromen-3-yl)acetamide (17d)**. Compound **17d** was prepared following the same procedure used in the preparation of compound **17a**. The N-acylated intermediate was purified by flash chromatography (SiO_2, 7:3 Hexanes:EtOAc to 100% EtOAc). Purification in the final step by preparative TLC (SiO_2, 1:1 Hexanes:EtOAc) afforded **17d** (5.0 mg, 51% over two steps) as a pale yellow amorphous solid: ^{1}H NMR (MeOD, 500 MHz) δ 8.09 (s, 1H), 8.05 (d, *J* = 7.8 Hz), 7.86 (d, *J* = 7.8 Hz, 1H), 7.75 (t, *J* = 7.8 Hz, 1H), 7.59 (d, *J* = 9.1 Hz, 1H), 7.47 (d, *J* = 3.0 Hz, 1H), 7.31 (dd, *J* = 9.1, 3 Hz), 2.05 (s, 3H); ^{13}C NMR (MeOD, 125 MHz) δ 177.0, 173.7, 162.3, 157.1, 151.5, 134.4, 133.1, 130.9, 128.7, 126.30, 126.27, 125.4, 121.1, 119.7, 109.1, 78.3, 30.6, 22.7; IR (film) ν_{max} 3367, 3248, 2922, 2853, 1717, 1699, 1666, 1651, 1634, 1622, 1574, 1558, 1539, 1516, 1472, 1456, 1385, 1367, 1327, 1294, 1269, 1229, 1173, 1117, 1097, 1082, 1003, 912 cm^{-1}; HRMS(ES^+) *m/z*: [M+H] calcd for $C_{18}H_{12}F_3NO_4$ 364.0707; found 364.0769.

***N*-(6-hydroxy-4-oxo-2-phenyl-4*H*-chromen-3-yl)acetamide (17e)**. Compound **17e** was prepared following the same procedure used in the preparation of compound **17a**. The N-acylated intermediate was purified by flash

chromatography (SiO_2, 7:3 Hexanes:EtOAc to 100% EtOAc). Purification in the final step by preparative TLC (SiO_2, 7:3 Hexanes:EtOAc) afforded **17e** (29.7 mg, 60% over two steps) as an orange amorphous solid: ^{1}H NMR (MeOD, 500 MHz) δ 7.78 (d, *J* = 7.5 Hz, 1H), 7.77 (d, *J* = 8.05 Hz, 1H), 7.55 (m, 4H), 7.46 (d, *J* = 2.95 Hz, 1H), 7.29 (dd, *J* = 9.05, 3.0 Hz, 1H), 2.06 (s, 3H); ^{13}C NMR (MeOD, 125 MHz) δ 177.2, 173.9, 164.4, 156.9, 151.6, 133.3, 132.3, 129.8 (2C), 129.5 (2C), 125.2, 125.1, 121.0, 119.1, 109.1, 22.7; IR (film) ν_{max} 3418, 3192, 2928, 2853, 1661, 1616, 1568, 1556, 1539, 1520, 1495, 1472, 1447, 1404, 1367, 1312, 1294, 1269, 1236, 1204, 1178, 1146, 1111, 1076, 1026, 1001, 966, 924 cm^{-1}; HRMS(ES$^+$) *m/z*: [M+H] calcd for $C_{17}H_{13}NO_4$ 296.0923; found 296.918.

***N*-(6-Hydroxy-2-(2-methoxyphenyl)-4-oxo-4*H*-chromen-3-yl)acetamide (17f)**. Compound **17f** was prepared following the same procedure used in the preparation of compound **17a**. The N-acylated intermediate was purified by flash chromatography (SiO_2, 7:3 Hexanes:EtOAc to 100% EtOAc). Purification in the final step by preparative TLC (SiO_2, 2:8 Hexanes:EtOAc) afforded **17f** (55.8 mg, 55% over two steps) as a pale yellow amorphous solid: ^{1}H NMR (MeOD, 500 MHz) As a mixture of conformational isomers: δ 7.67 (d, *J* = 7.7 Hz, 1H), 7.50 (m, 1H), 7.45 (m, 3H), 7.24 (m, 1H), 7.13 (d, *J* = 8.3 Hz, 1H), 7.04 (t, *J* = 7.7 Hz, 1H), 3.87 (2s, 3H), 1.95 (bs, 3H); ^{13}C NMR (MeOD, 125 MHz) As a mixture of conformational isomers: δ 163.7, 161.7, 158.3, 156.4, 151.7, 151.6, 135.4, 133.5, 133.0, 131.7, 131.0, 130.6, 125.6, 124.7, 122.4, 121.8,

121.3, 121.1, 120.75, 120.69, 114.3, 113.3, 112.6, 108.9, 108.5, 56.7, 56.3, 30.3, 22.3; IR (film) ν_{max} 3493, 3246, 3084, 3011, 2945, 2841, 2565, 2419, 2351, 2243, 2135, 1651, 1614, 1574, 1479, 1454, 1435, 1416, 1371, 1285, 1254, 1211, 1180, 1165, 1150, 1117, 1105, 1082, 1049, 1020, 972, 935, 879 cm^{-1}; HRMS(ES^+) *m/z*: [M+H] calcd for $C_{18}H_{15}NO_5$ 326.1028; found 326.1021.

Anti-Proliferation Assays

MCF-7 and SKBr3 cells were maintained in a 1:1 mixture of Advanced DMEM/F12 (Gibco) supplemented with non-essential amino acids, L-glutamine (2 mM), streptomycin (500 μg/mL), penicillin (100 units/mL), and 10% FBS. Cells were grown to confluence in a humidified atmosphere (37 °C, 5% CO_2), seeded (2000/well, 100 μL) in 96-well plates, and allowed to attach overnight. Each compound or geldanamycin at varying concentrations in DMSO (1% DMSO final concentration) was added, and cells were returned to the incubator for 72 h. At 72 h, the number of viable cells was determined using an MTS/PMS cell proliferation kit (Promega) per the manufacturer's instructions. Cells incubated in 1% DMSO were used as 100% proliferation, and values were adjusted accordingly. IC_{50} values were calculated from separate experiments performed in triplicate using GraphPad Prism.

Western Blot Analysis

MCF-7 cells (1 x 10^6) were cultured in a Tissue Culture Dish (Becton Dickinson, Franklin Lakes, NJ) in 5 mL media and allowed to attach overnight at 37˚C in a humidified incubator under 5% CO_2. **10c**, **10d**, **17a**, **17b** or geldanamycin (positive control) was added in 50 μL DMSO for a final concentration of 0.1 to 100 μM of inhibitor. An additional vehicle (DMSO) sample was utilized as a negative control. After inoculation, the cells were allowed to incubate 24 hr before the cells were harvested via scraping the Tissue Culture Dish, washing with PBS (2 x 5 mL), and storing on ice. After pelleting the cells (1000 x rpm, 4°C), PBS and media were removed, and the pellets resuspended in lysis buffer (150 μL, 50 mM Tris-HCl pH 7.5, 1% NP-40, 150 mM NaCl, 0.1% SDS, 2.5 mM Na_3VO_4, 10 mM PMSF, 10 μM aprotinin, 10 μM leupeptin, and 10 μM soybean trypsin inhibitor) and transferred to 1.5 mL Eppendorf tubes. Samples were incubated for 1 hr at 4°C. Lysates were cleared by centrifugation at 14000 x rpm for 10 minutes at 4°C. The supernatants were collected and comprised the experimental samples. The protein concentration of each sample was determined by a BSA assay (Pierce, Rockford, IL). Equal amounts of protein were resolved on a 9% polyacrylamide gel (100V, 100 mA, 2 hr) and transferred to a nitrocellulose membrane (25 V, 100 mA, 12 hr). Bands were visualized with Ponceau to

confirm protein transfer. Blots were blocked with 5% nonfat milk in PBST (3 x 15 mL, 10 min), probed with primary antibody (1:1500, Her2 (c-*erb*B-2) rabbit polyclonal IgG, Zymed Laboratories, Paisley, UK; 1:1500, Hsp90 mouse polyclonal IgG, Stressgen, Ann Arbor, MI; 1:1500, Actin rabbit polyclonal IgG, Santa Cruz Biotechnology, Santa Cruz, CA; 1:1500 cRaf-1 rabbit polyclonal IgG, Stressgen, Ann Arbor, MI; 1:1500 Cdk4 rabbit polyclonal IgG, Stressgen, Ann Arbor, MI; 1:1500 Akt 1/2/3 rabbit polyclonal IgG, Santa Cruz Biotechnology, Santa Cruz, CA; 3 hr). The blots were washed with 5% milk/PBST (3 x 15 mL, 10 min), incubated with horseradish peroxidase-conjugated secondary antibody (1:2000 goat α-rabbit IgG, Amersham, Piscataway, NJ; 1:2000 goat α-mouse IgG, Santa Cruz Biotechnology, Santa Cruz, CA; 1.5 hr), then washed with 5% milk/PBST (1 x 15 mL, 10 min), followed by PBST (2 x 15 mL, 10 min). Protein bands were visualized by chemiluminescence using ECL detection reagents (Amersham, Piscataway, NJ).

V. References

(1) Hadden, M. K.; Hill, S. A.; Davenport, J.; Matts, R. L.; Blagg, B. S. J. *Bioorg. Med. Chem.* **2009**, *17(2)*, 634–640.

(2) Galam, L.; Hadden, M. K.; Ma, Z.; Ye, Q.; Yun, B.; Blagg, B. S. J.; Matts, R. L. *Bioorg. Med. Chem.* **2007**, *15*, 1939–1946.

(3) Donnelly, A. C.; Mays, J. R.; Burlison, J. A.; Nelson, J. T.; Vielhauer, G.; Holzbeierlein, J.; Blagg, B. S. J. *J. Org. Chem.* **2008**, *73(22)*, 8901–8920.

(4) de Brito, M. A.; Rodrigues, C. R.; Cirino, J. J. V.; de Alencastro, R. B.; Castro, H. C.; Albuquerque, M. G. *J. Chem. Inf. Model.* **2008**, *48*, 1706–1715.

(5) Lei, B.; Du, J.; Li, S.; Liu, H.; Ren, Y.; Yao, X. *J. Comput. Aided Mol. Des.* **2008**, *22*, 711–725.

(6) Guo, J.; Wu, J. J.; Wright, J. B.; Lushington, G. H. *Chem. Res. Toxicol.* **2006**, *19*, 209–216.

(7) Blagg, B. S. J.; Kerr, T. D. *Med. Res. Rev.* **2006**, *26*, 310–338.

(8) Chiosis, G.; Timaul, M. N.; Lucas, B.; Munster, P. N.; Zheng, F. F.; Sepp-Lorenzino, L.; Rosen, N. *Chem. Biol.* **2001**, *8*, 289–299.

(9) Hastings, J. M.; Hadden, M. K.; Blagg, B. S. J. *J. Org. Chem.* **2008**, *73*, 369–373.

(10) Shen, G.; Blagg, B. S. J. *Org. Lett.* **2005**, *7*.

(11) Shen, H. Y.; He, J. C.; Wang, Y.; Huang, Q. Y.; Chen, J. F. *J. Biol. Chem.* **2005**, *280*, 39962–39969.

(12) Waza, M.; Adachi, H.; Katsuno, M.; Minamiyama, M.; Sang, C.; Tanaka, F.; Inukai, A.; Doyu, M.; Sobue, G. *Nat. Med.* **2005**, *11*, 1088–1095.

(13) Dou, F.; Netzer, W. J.; Tanemura, K.; Li, F.; Hartl, F. U.; Takashima, A.; Gouras, G. K. *Proc. Natl. Acad. Sci. USA* **2003**, *100*, 721–726.

(14) Ansar, S.; Burlison, J. A.; Hadden, M. K.; Yu, X. M.; Desino, K. E.; Bean, J.; Neckers, L.; Audus, K. L.; Michaelis, M. L.; Blagg, B. S. J. *Bioorg. Med. Chem. Lett.* **2007**, *17*, 1984–1990.

(15) Lu, Y.; Ansar, S.; Michaelis, M. L.; Blagg, B. S. J. *Bioorg. Med. Chem.* **2009**, *17(4)*, 1709–1715.

(16) Amolins, M. W.; Blagg, B. S. J. *Mini Rev. Med. Chem.* **2009**, *9(2)*, 140–152.

(17) Burlison, J. A.; Avila, C.; Vielhauer, G.; Lubbers, D. J.; Holzbeierlein, J.; Blagg, B. S. J. *J. Org. Chem.* **2008**, *73*, 2130–2137.

(18) Rodriquez, C. E.; Shinyashiki, M.; Froines, J.; Yu, R. C.; Fukuto, J. M.; Cho, A. K. *Toxicology* **2004**, *201*, 185.

(19) Morris, G. M.; Goodsell, D. S.; Halliday, R. S.; Huey, R.; Hart, W. E.; Belew, R. K.; Olson, A. J. *J. Comput. Chem.* **1998**, *19*, 1639.

(20) Park, H.; Kim, Y.; Hahn, J. *Bioorg. Med. Chem.* **2007**, *17*, 6345–6349.

(21) Roe, S. M.; Prodromou, C.; O'Brien, R.; Ladbury, J. E.; Piper, P. W.; Pearl, L. H. *J. Med. Chem.* **1999**, *42*, 260–266.

(22) Jez, J. M.; Chen, C.; Rastelli, G.; Stroud, R. M.; Santi, D. V. *Chem. Biol.* **2003**, *10*, 361–368.

(23) Baker, W. *J. Chem. Soc.* **1933**, 1381–1388.

(24) Mahal, H. S.; Venkataraman, K. *J. Chem. Soc.* **1934**, 1767–1768.

(25) Ghani, S. B. A.; Weaver, L.; Zidan, Z. H.; Ali, H. M.; Keevil, C. W.; Brown, R. C. D. *Bioorg. Med. Chem. Lett.* **2008**, *18*, 518–522.

(26) Zhang, H.; Cai, Q.; Ma, D.; *J. Org. Chem.* **2005**, *70*, 5164–5173.

(27) Ikawa, T.; Barder, T. E.; Biscoe, M. R.; Buchwald, S. L. *J. Am. Chem. Soc.* **2007**, *18*, 13001–13007.

(28) Shen, G.; Wang, M.; Welch, T. R.; Blagg, B. S. J. *J. Org. Chem.* **2006**, *71*, 7618–7631.

(29) Clark, T.; Hennemann, M.; Murray, J. S.; Politzer, P. *J. Mol. Mod.* **2007**, *13*, 291–296.